CHARACTERISATION AND SUBSTITUTION KINETICS OF COBALT(III) - N-(2-CARBOXYETHYL)IMINODIACETATO COMPLEXES

A thesis submitted to meet the requirements for the degree of

MAGISTER SCIENTIAE

in the

Department of Chemistry

Faculty of Natural and Agricultural Sciences

at the

University of the Free State

by

Johannes Hendrik Wium Potgieter

Promotors

Dr. H.G. Visser

Prof. W. Purcell

Dankbetuigings

Hiermee wens ek my opregte dank te betuig:

My hemelse Vader en God wat my altyd bystaan in alles wat ek aanpak.

"Ek is tot alles in staat deur Hom wat my krag gee." Filipense 4:13

Dankie dat U altyd met my is in die donkerste en die beste van dae - ek sal U lof altyd bly besing.

Die wonderlikste ouers in die wereld, Daan en Linda, dankie dat pa altyd so trots is op my en my in al my besluite ondersteun en dankie dat ma altyd in my glo en vir al die liefdevolle drukkies - ek het julle baie lief.

Yolandè Lubbe, dankie dat jy die beste in my uitbring. Jou entosiasme oor die klein dingetjies in die lewe inspireer my tot nuwe hoogtes.

My promotor, Deon Visser, 'n uitstekende promotor en 'n baie goeie vriend. Dankie vir al die geduld, moeite en ondersteuning – dit was 'n plesier om saam met jou te werk.

My mede-promotor, Prof. Purcell, u ondervinding en insig spoor almal aan.

My boetie en sussies, Johan, Adele en Ilzè, vir al die belangstelling en aanmoediging.

Vir al my vriende, Christiaan, Christian, Chantal, Tobie, Knoes, Deon, Marcel, Gerhard, Simon, Leon, Dewald, Jaap, Michael, Ananda, Anelie, Inge, Susan, Elbè, Janette, Eleanor, Liesel, Elisia, Hennie, Jenine, Rika, Vicky, Deborah, Joan, Tanya, Roelof, Sanmarie, Anè, Carmen-Jane, Nadine en Nerina - julle maak die lewe een groot fees!

Al die Personeel by Departement Chemie vir julle wonderlike bydrae.
Die UVS en NRF vir finansiële steun.

Table of contents

Table of contents

List of abbreviations

acac	= pentane-2,3-dione
apda	= N-(2-carboxyethyl)iminodiacetic acid
dien	= diethylenetriamine
dmap	= dimethylaminopyridine
EBT	= Eriochrome Black T
edda	= ethylenediaminediacetic acid
edta	= ethylenediaminetetra-acetate
en	= ethylenediamine
gly	= glycine
GTF	= glucose tolerance factor
H_2vi	= dihydrogenviolurate
im	= imidazole
IR	= infrared
k_{obs}	= observed rate constant
l-ala	= *l*-alanine
Ida	= (S)-leucine-N,N-diacetate
l-leu	= *l*-leucin
N,*N*-Et_2en	= *N*,*N*-diethylethylenediamine
NMR	= nuclear magnetic resonance
nta	= nitrilotriacetic acid
pd	= 1,3-propanediamine
pda	= (S)-phenylalanine-N,N-diacetate
phen	= *o*-phenantroline
TPPS	= *meso*-tetra(*p*-sulphonatophenyl)porphyrin
trdta	= trimethylenediaminetetra-acetate
l-val	= *l*-valine

List of figures:

Chapter 1

Chapter 2

Chapter 3

Chapter 4

Chapter 5

List of tables:

Chapter 2

Chapter 4

Chapter 5

List of schemes:

Chapter 2

Chapter 3

Chapter 4

Chapter 5

1 Aim of the study

In this chapter…

The relevance and aims of this study of Co(III) complexes with N-(2-carboxyethyl)iminodiacetic acid (apda) and related ligands are discussed in this chapter. The history and significance of these complexes are discussed in the first part of the chapter while the specific aims of this study are discussed in the second part of the chapter.

1.1 Introduction

1.1.1 Cobalt chemistry – history

The use of cobalt dates back to as far as 2000 BC where the Egyptians used it as a colouring agent. The cobalt amines where first discovered by Werner in the early twentieth century and form the basis for the formulation of the coordination theory in inorganic chemistry. The uses of cobalt compounds are widespread and include catalysts, pigments, and electroplaters. It is also used in ceramics, as dryers for paints and varnishes, high temperature alloys and also in radiology (Planinsek & Newkirk, 1979:481 and Morral, 1979:495).

Cobalt salts and complexes are most commonly used in dyestuffs for polyamide fibres and leather because of its kinetic inertness and the stability towards acid. The importance of such metal complexes stems principally from their very high light-fastness, attributed to the protection of the azo group of the dye by the metal against attack by, for example, singlet oxygen (Gordon & Gregory, 1983).

The substitution reactions of octahedral complexes of cobalt(III) have been under investigation for many years. The reasons for this are that a great variety of these complexes can easily be prepared and the substitution reactions of these complexes are slow enough to be followed by conventional means (Purcell & Kotz, 1985:710). Hence it is not surprising that one finds so many publications and review articles on the substitution reactions of these metal complexes (Hay, 1984:1 and Moore, 1984).

1.1.2 The significance of Co-apda complexes

Complexes of cobalt(III) with ligands that simulate bindings sites on protein chains have many applications and are of significant scientific value. According to Cooper *et al.* (1984:23) the glucose tolerance factor (GTF), a fraction isolated from brewer's yeast, which displays biological activity in a number of assay systems, may have an important role to play in glucose metabolism. This has lead to several studies on this subject (Toepfer, *et al.*, 1977:162, Mertz, 1975:129 and Haylock *et al*., 1983:105). Other examples include the construction of molecular recognition models for enzyme-substrate complex formation through weak non-covalent interactions (Jitsukawa *et al*., 1994:249), as well as many biomedical applications, such as the removal of toxic metal ions from the human body by chelating agents like penicillamine (Helis *et al*., 1977:3309 and Santos *et al*., 1992:1687).

The selected model complex was a cobalt(III) complex with N-(2-carboxyethyl)iminodiacetic acid, which was first prepared by Tsuchiya *et al.* (1969:1886).

The bonding modes of nitrilotriacetic acid (nta) have been of interest for many years and N-(2-carboxyethyl)iminodiacetic acid (apda) (Figure 1.1) is its closest analogue and differs from nta by having a longer propionate chain in place of one of the acetate groups (see Figure 2.1). These tripod-type ligands function as tetradentate ligands in most metal chelation compounds and their structures are well characterised in both their zwitterionic

and chelated forms (Skrypczak-Jankun & Smith, 1994:1097, Withlow, S.H., 1972:1914 and Okamoto *et al.*, 1992:1025).

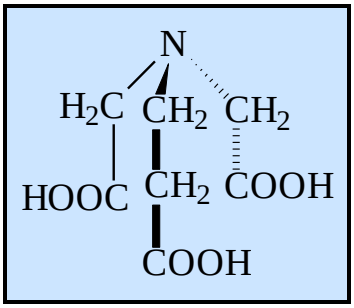

Figure 1.1 N-(2-carboxyethyl)iminodiacetic acid.

Substitution reactions at cobalt(III) centres are normally slow, but the rate of substitution can be significantly enhanced by having porphyrin, Schiff-base chelates or edta and related ligands (such as nta and apda) in the metal coordination sphere (Leipoldt & Meyer, 1987:1361 and Beswick *et al.*, 1996:991). It is believed that these ligands donate extra electron density to the inert central cobalt(III) ion, thereby changing its properties to react more like the labile cobalt(II) ion.

The above factor, as well as the fact that fully coordinated apda and nta leave two *cis* positions available on the metal centre, make these kinds of complexes very suitable to use as biological models (Visser *et al.*, 1994:1051, Bhattacharyya & Banerjee, 1997:849, Jitsukawa *et al.*, 1994:249 and Bocarsley & Barton, 1992:2827).

1.2 Aim of this study

Cobalt complexes with N-(2-carboxyethyl)iminodiacetic acid (apda) are rarely mentioned in the literature and not much information on its structures is available. Metal complexes with nitrilotriacetic acid (nta) have been of great interest for many years and many of these complexes have been isolated.

No kinetic studies on cobalt(III)-apda complexes have been published.

From this discussion it should be clear that there is a lot of uncertainty regarding the synthesis, characterisation and reactions of cobalt(III)-apda complexes.

The aim of this study was to:

a) synthesise suitable Co(III)-apda complexes that can be used as biological models in future studies;
b) develop alternative routes for the synthesis of Co(III)-apda complexes;
c) characterise these complexes with especially IR, single-crystal X-ray crystallography and ^{1}H NMR so that it could be used as starting material in kinetic studies;
d) investigate the bonding mode of the apda ligand in cobalt(III)-apda complexes;
e) investigate the ring strain in these complexes and the possible chemical effects it may have;
f) determine the mechanism of the substitution reactions of cobalt(III)-apda complexes with different ligands at different pH levels by means of a kinetic study.

2 Literature overview

In this chapter…

The first part of this chapter focuses on the synthesis and characterisation of metal complexes with N-(2-carboxyethyl)iminodiacetic acid (apda) whilst the second part focuses on the substitution reactions of these complexes. The shortcomings and possible future contributions are discussed at the end of this chapter (Paragraph 2.3).

2.1 Introduction.

The literature study will focus mainly on the synthesis and characterisation of cobalt(III) complexes with tripod-type ligands like N-(2-carboxyethyl)iminodiacetic acid (apda) as well as the substitution reactions of these complexes with various ligands. Some tripod-type ligands are shown in Figure 2.1.

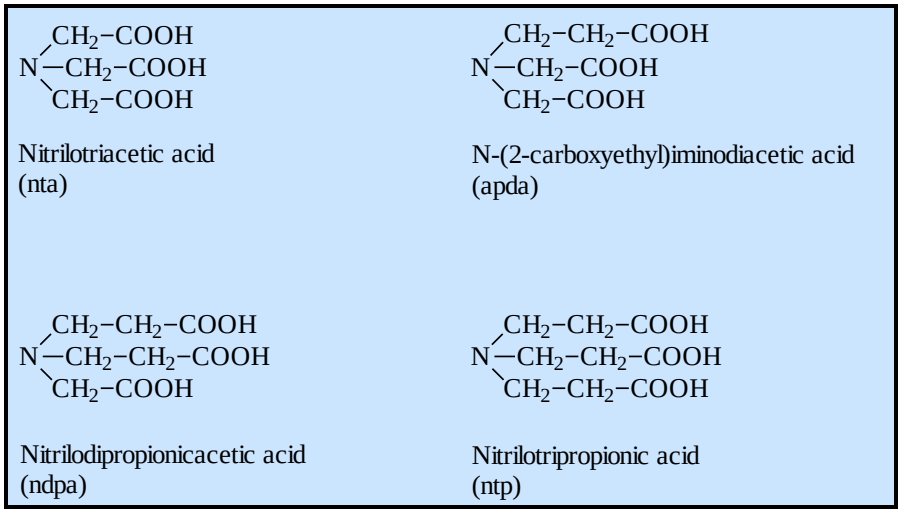

Figure 2.1 Tripod-type ligands.

2.2 Synthesis, characterisation and reactions of cobalt(III)-N-(2-carboxyethyl)iminodiacetic acetato (apda) complexes.

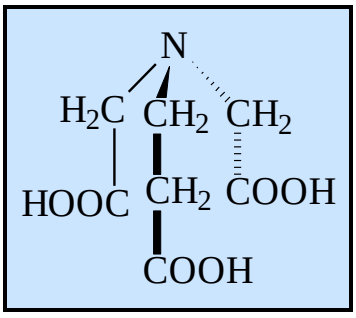

Figure 2.2 N-(2-carboxyethyl)iminodiacetic acid (apda).

2.2.1 Synthesis and characterisation

Cobalt(III)-apda complexes

The different bonding modes of apda were illustrated by Uehara *et al.* (1968:2385) in a study on Cr(III)-apda complexes. It was shown on the basis of chemical and thermal analysis, UV/VIS spectra, IR spectra and molar conductivities that apda acts as either a tridentate or tetradentate ligand (Figure 2.3).

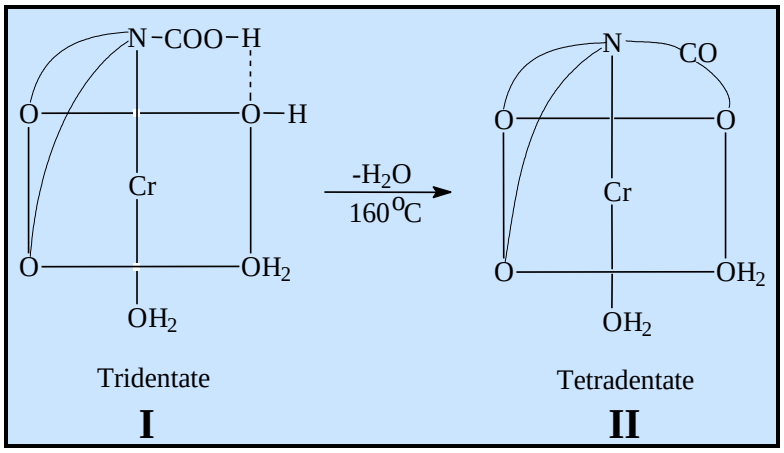

Figure 2.3 Coordinating modes of apda towards the Cr(III) ion as shown by Uehara *et al.* (1968:2385).

CHAPTER 2

Cobalt(III) – N-(2-carboxyethyl)iminodiacetic acetato (Co(III)–apda) complexes were first prepared by Tsuchiya and co-workers (1969:1886). According to their study a Co(III)-apda species with a tridentately coordinated apda could be isolated. The complex was formulated as $[Co(OH)(apda)(H_2O)_2]$ on the basis of chemical analysis and IR spectra. The coordination sphere contained a hydroxy group with apda acting as a tridentate ligand in which one of the carboxy groups is protonated and does not take part in the coordination. The structure of this complex is similar to that of the Cr(III)-apda complex proposed by Uehara *et al.* (1968:2385) (I in Figure 2.3). The complex was isolated by neutralising apda with potassium bicarbonate, adding $CoCl_26H_2O$ and H_2O_2 and then allowing the crystals to separate. The crystals were filtered and washed with ethanol and ether and re-crystallised from water.

Tsuchiya and co-workers had difficulty explaining some characteristics of the apda-coordinating mode of this Co(III) complex. The IR spectrum showed two bands near 1685 and 1630 cm^{-1}. The band at 1685 cm^{-1} was assigned to the non-coordinating, protonated COOH group, while the other band at 1630 cm^{-1} was assigned to the coordinated COO^- groups of apda. However, Nakamoto (1963:206) stated that COO^- groups have stretching frequencies between 1650 – 1620 cm^{-1} when coordinated to metals such as Co(III) and stretching frequencies between 1750 – 1700 cm^{-1} when uncoordinated. It can be seen that the band at 1685 cm^{-1} does not fall in either the coordinated nor the uncoordinated criteria specified by Nakamoto, which questions the structural assignments made by Tsuchiya and co-workers.

The Co(III)-apda complex synthesised by Tsuchiya *et al.* (1969:1886) was also prepared by Gladkikh and co-workers (1997:1346). They performed X – ray crystal structure determination studies on the cobalt(III)- and chromium(III)-apda complexes and an iron(III) analogue. These complexes were found to be iso-structural. The structure for the Co(III)-apda complex was determined as $[Co(apda)(H_2O)_2]$, with apda acting as a tetradentate ligand (Figure 2.4). The cobalt(III) coordination sphere was completed by the two oxygen atoms of coordinated water molecules. Unfortunately the IR spectrum of $[Co(apda)(H_2O)_2]$ was not recorded in the study.

The structural peculiarities regarding the $[Co(OH)(apda)(H_2O)_2]$ complex prepared by Tsuchiya and co-workers (1969:1886) were questioned by Gladkikh *et al.* (1997:1346). Gladkikh and co-workers stated that the carboxy group protonation due to the ionisation of the coordinated water molecule, that was observed in the case of germanium(IV) (Mizuta *et al*., 1989:65), is not likely to occur for the relatively weak hydrolysing Co(III)-(aqua) (aminocarboxylato) complexes. They also stated that the X-ray diffraction data for Cu(II) and Ni(II) complexes (Dung *et al*., 1987:2365 and Gladkikh *et al*., 1991:945) showed that the deprotonated apda anion can be tetradentate in the absence of competing ligands.

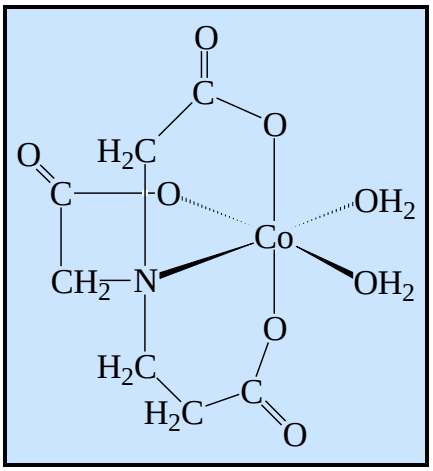

Figure 2.4 Structure of the $[Co(apda)(H_2O)_2]$ complex.

This structure determination confirmed that apda acts as a tetradentate ligand in this Co(III)-apda complex. The apda ligand forms three chelate rings with the Co atom: two five-membered glycinate and one six-membered alaninate rings. An interesting aspect of this coordination mode is that the coordinated oxygen atom of the propionato group is opposite to the coordinated oxygen atom of the acetato group on one of the octahedron axes. A similar arrangement was found for the rings in Ni(II) and Co(II) complexes containing a tetradentate apda ligand (Gladkikh *et al.*, 1991:945, Gonzales Perez *et al.*, 1991:243). These different coordinating positions of the apda oxygen atoms around the Co(III) centre were explained by the fact that the octahedron is significantly elongated due to the Jahn-Teller effect (Jahn & Teller, 1937:220), and it is energetically more favourable that the longer propionato group occupies the long axis of the octahedron.

The bond lengths and angles in the coordination polyhedron of the $[Co(apda)(H_2O)_2]$ complex were found to be similar to other known Co(III) aminopolycarboxylates with five and six - membered chelate rings (Visser *et al.*, 2001:175).

A cobalt(III)-apda complex in which apda acts as a tridentate ligand was synthesised by Obodovskaya *et al.* (1992:295). The complex was characterised on the basis of electronic adsorption, ^1H NMR spectra and X-ray crystallography as $[Co(dien)(Hapda)]ClO_4$ (Figure 2.5). The crystal structure revealed an octahedral complex in which the propionate group remained uncoordinated. The octahedral coordination of the Co(III) atom was completed by the three N atoms of the dien ligand. Unfortunately no IR data was published for this complex.

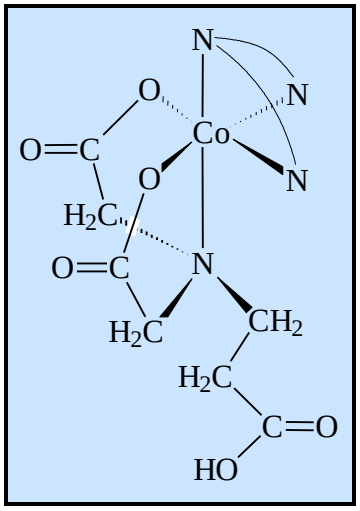

Figure 2.5 Structure of $[Co(dien)(Hapda)]ClO_4$.

The cobalt(III)-apda complex, $[Co(dien)(Hapda)]ClO_4$ (Figure 2.5), was used by Polyakova *et al.* (1997:1509) in the synthesis of a hexanuclear complex, $\{[Co(dien)(apda)]_2Cu(H_2O)\}_2(ClO_4)_4 8H_2O$, in which apda again acts as a tridentate ligand. The complex was characterised on the basis of magnetic properties and X-ray crystallography. The structure consists of centrosymmetric hexanuclear complex cations $\{[Co(dien)(apda)]_2Cu(H_2O)\}_2^{4+}$ (Figure 2.6), ClO_4^- anions and water molecules of crystallisation. In the cation, Cu atoms are linked together by four bidentate bridging

propionato groups. The cobalt(III) atoms are octahedrally surrounded by the N atom and two O atoms of apda acetato groups and three N atoms of the dien molecule.

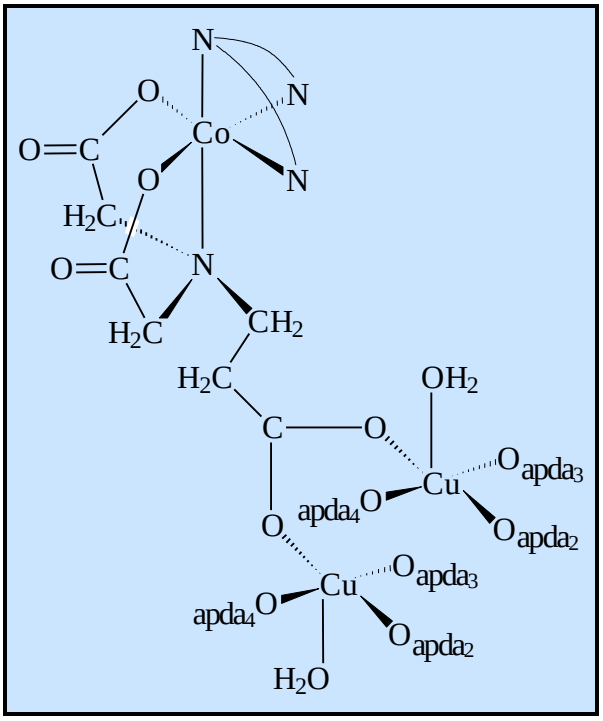

Figure 2.6 Structure of $\{[Co(dien)(apda)]_2Cu(H_2O)\}^{4+}$.

Since the isolation of the above-mentioned complexes no other cobalt(III) complexes with apda have been characterised by X–ray crystallography. The isolation and characterisation of cobalt(III)-apda complexes with apda acting either as a tridentate or tetradentate ligand will bring more light to the understanding of the structures of these complexes.

CHAPTER 2

Cobalt(III)-nta complexes

Nitrilotriacetic acid (nta) is another tripod-type ligand and one of the closest analogues to N-(2-carboxyethyl)iminodiacetic acid (apda). The nitrilotriacetato cation is shown in Figure 2.7.

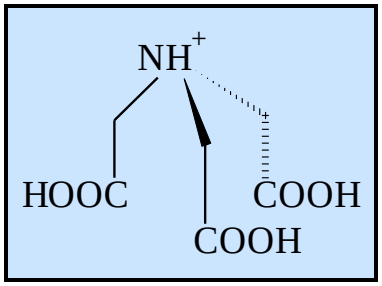

Figure 2.7 Nitrilotriacetato cation (nta).

Mori and co-workers (1958:940) were the first to prepare and identify different cobalt(III)-nitrilotriacetato complexes. According to their study two monomeric hydroxo-aqua cobalt(III)-nta isomers, the α- and β-isomers (Figure 2.8), as well as a dimeric μ-hydroxo bridged species, $K_2[Co(nta)(OH)]_2 3H_2O$, could be isolated.

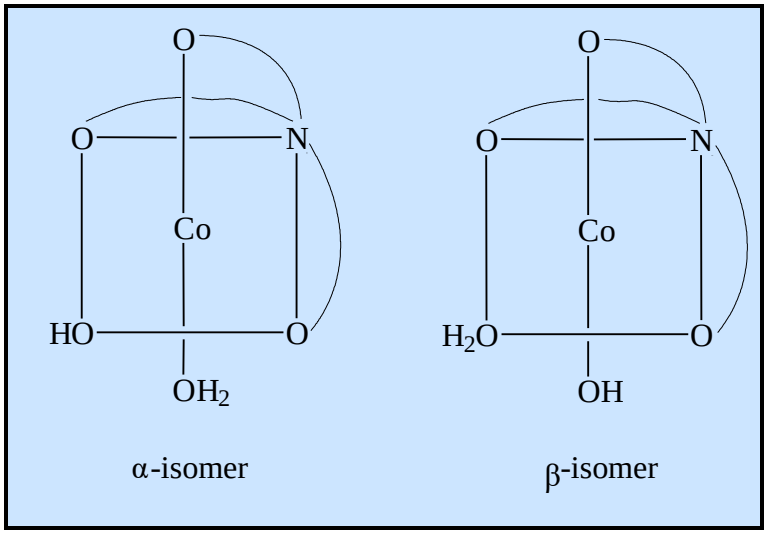

Figure 2.8 Isomers prepared by Mori *et al.* (1958:940).

The α-isomer was isolated by neutralising nta with potassium bicarbonate, adding $CoCl_2 6H_2O$ and H_2O_2 to this solution and then allowing the crystals to separate. The crystals were filtered and washed with ethanol and ether. The β-isomer was prepared by acidifying the filtrate obtained after isolation of the α-isomer with acetic acid, adding a large amount of ethanol and allowing the solution to stand overnight in a refrigerator. The dimeric complex was isolated by acidifying and boiling the above-mentioned filtrate on a water bath until the solution turned pink. On cooling a pink precipitate was collected. All the complexes were characterised by chemical analysis, thermal decomposition, coagulation studies and spectroscopic measurements.

Mori and his co-workers had difficulty in explaining several observations. Close inspection of the chemical analysis data revealed that the chemical composition of the three complexes were almost identical. They were also unable to explain the thermal decomposition and spectrochemical data with confidence.

The uncertainty regarding the formulation of the different Co(III)-nta complexes prepared by Mori and co-workers were solved by Smith and Sawyer (1968:923). They performed ^{1}H NMR and IR studies on 1:1 and 1:2 cobalt(III)- and rhodium(III)-nta complexes. It was argued that the identical chemical composition of the α- and β-isomers would relate into identical or nearly identical chemical properties.

Their results showed that the ^{1}H NMR spectra for both the α- and β-isomers displayed an AB pattern of two doublets and a singlet, but at different chemical shifts. {An AB pattern is the phenomenon which is observed when protons are in distinguishable environments yielding a doublet that is again split into a doublet by spin-spin interaction, for a total of four peaks of similar intensity}. As shown in Figure 2.9, the two doublets were assigned to the non-equivalent, coupled protons (H_{G1b}, H_{G2b} and H_{G1a}, H_{G1b}) in the two coplanar, five-membered, equatorial rings (G rings) and the singlet to the acetate CH_2 protons (H_{Ra} and H_{Rb}) on the third ring (R ring).

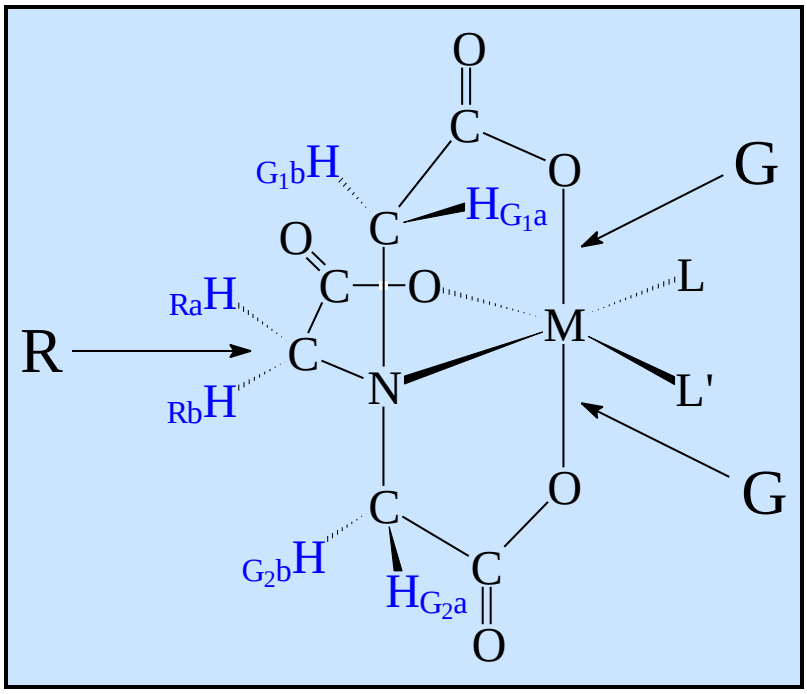

Figure 2.9 Glycinato rings in M(III)-nta complexes.

Smith and Sawyer predicted that if the two products isolated by Mori and co-workers (1958:940) were the α- and β-isomers (Figure 2.8), they would be expected to interconvert rapidly in solution at pH 6 due to proton exchange and therefore be expected to have the same spectrum. They assigned the difference in spectra points to the existence of a different Co(III)-nta species, possibly an oxo- or hydroxo-bridged dimer. This oxo- or hydroxo-bridged dimer would have a spectrum different from that of the isomers in Figure 2.8. They concluded that the α-isomer, according to the formulation of Mori *et al.* (1958:940), is actually the dimeric form because of its lower field AB proton positions. This would result from deshielding of the protons associated with the magnetic anisotropy of the metal-oxo or -hydroxo region.

Their results also indicated that the ^{1}H NMR spectra of the α- and β-forms were identical at pH 0.5. They attributed this observation to the formation of a diaqua Co(III)-nta species at this pH.

It was further observed by Smith & Sawyer that the IR spectra for the α- and β-forms were also different from each other. The α-form had COO-Co stretching frequencies at 1674 and 1615 cm^{-1} compared to the one stretching frequency at 1634 cm^{-1} for the β-form. The absence of any uncoordinated COOH stretching frequencies (1750 – 1700 cm^{-1}) points to the tetradentate coordination of the nta ligand in these complexes.

Koine and co-workers (1969:1583) continued the ^{1}H NMR study of Co(III)-nta complexes by investigating the spectra of $[Co(nta)(gly)]^-$ (gly = glycine) and $[Co(nta)(l\text{-ala})]^-$ (*l*-ala = *l*-alanine). The ^{1}H NMR spectrum of $[Co(nta)(gly)]^-$ was very similar to that found for the Co(III)-nta complexes studied by Smith & Sawyer (1968:923). These spectra consisted of two doublets in a simple AB pattern and a singlet. The singlet integrates for two protons. The AB pattern with centres at 4.41 and 3.99 ppm obtained for $[Co(nta)(gly)]^-$ was assigned to the non-equivalent, coupled G ring protons (H_{G1b}, H_{G1a} and H_{G2a}, H_{G2b} in Figure 2.9). The AB pattern is a result of the fact that the two equivalent protons (H_{G1a} and H_{G2a}) couple with the other equivalent proton pair (H_{G1b} and H_{G2b}). The singlet at 4.12 ppm was assigned to the equivalent acetate protons of the R ring.

The ^{1}H NMR spectra of $[Co(nta)(gly)]^-$ and $[Co(nta)(l\text{-ala})]^-$ resembled each other even though a more complex spectrum might have been expected for the *l*-alinato complex since all the acetate protons of nta in the $[Co(nta)(l\text{-ala})]^-$ complex have different chemical environments. The only difference between the ^{1}H NMR spectra of $[Co(nta)(gly)]^-$ and $[Co(nta)(l\text{-ala})]^-$ was that in the ^{1}H NMR spectra of the *l*-alaninato complex the lowest field peak of the AB pattern, which is overlapped by the HDO peak, shifted downfield. These results agree well with those reported by Buckingham and co-workers (1966:1649 and 1967:257) for several glycinato and *l*-alaninato complexes.

A study by Thacker and Higginson (1975:704) confirmed most of the results of the previous studies. Their results also added new insight to the knowledge regarding the structures of these complexes. They added that their preparations of the β-form always contained cobalt(II) as impurity and that the dimeric species that Mori prepared was in

fact a bis(nta) complex, $K[Co(Hnta)_2]2H_2O$ (Hnta represents the mono-protonated form of the tridentate coordinated nta). However, no formal structure of the $K[Co(Hnta)_2]2H_2O$ complex was proposed.

In the same study, Thacker and Higginson succeeded in the isolation and characterisation of the cis-aqua complex, $[Co(nta)(H_2O)_2]$, by acidifying the dimer or hydroxo-aqua complex. This was also confirmed in a study performed by Meloon and Harris (1977:434). It was also reported that there were still difficulties experienced to purify the starting material.

The first crystal structure of a cobalt-nta complex, $K[Co(nta)(H_2O)]2H_2O$, was published by Battaglia *et al*. (1975:1160). The structure determination revealed a distorted octahedral cobalt(II) species. The coordination sphere around the metal centre was occupied by one tetradentate nta ligand, a water molecule and the carboxylic oxygen of an adjacent anion (Figure 2.10).

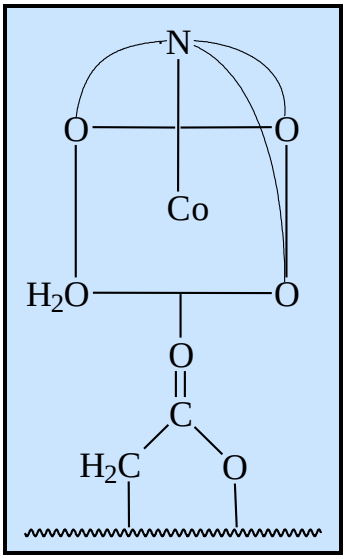

Figure 2.10 Structure of $K[Co(nta)(H_2O)]2H_2O$.

Visser and co-workers (1997:2851) prepared a cobalt(III)-nta complex similar to the method described by Mori *et al.* (1958:940) for the preparation of α-$K[Co(nta)(H_2O)(OH)]2H_2O$. The cobalt(III)-nta complex was characterised on the basis

of X-ray crystallography as $Cs_2[Co(nta)(\mu\text{-}OH)]_2 4H_2O$. They also obtained the UV/VIS spectrum of the $Cs_2[Co(nta)(\mu\text{-}OH)]_2 4H_2O$ complex and found that the spectrum was identical to that of the blue product obtained by Mori's method. These results confirmed the findings of Smith and Sawyer (1968:923) that the α-isomer was in fact the $[Co(nta)(\mu\text{-}OH)]_2^{2-}$ anion (Figure 2.11).

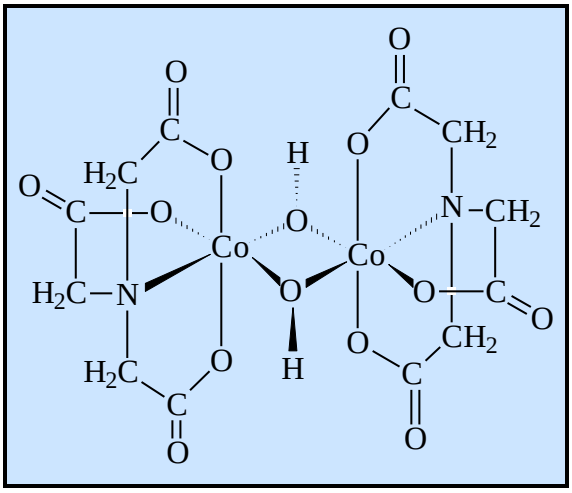

Figure 2.11 Structure of $[Co(nta)(\mu\text{-}OH)]_2^{2-}$.

Another cobalt(III)-nta complex, [Co(nta)(N,N-Et_2en)], was synthesised by Visser and co-workers (2001:175). They characterised this complex on the basis of IR spectra, ^1H NMR spectra and three-dimensional X-ray diffraction data. The cobalt centre has a distorted octahedral geometry and is surrounded by three oxygen atoms and the nitrogen atom of the nta ligand and the two nitrogen atoms of the ethylenediamine molecule. The substituted nitrogen of *N,N*-diethylethylenediamine is bonded *trans* to the nta nitrogen (Figure 2.12).

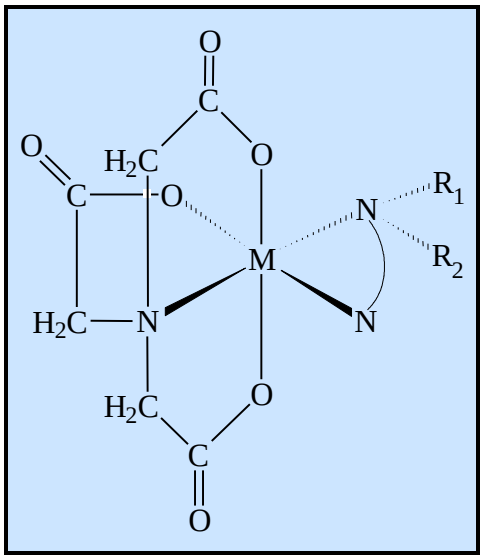

Figure 2.12 Structure of $[Co(nta)(enR_1R_2)]$ (enR_1R_2 = substituted ethylenediamines).

Visser and co-workers (2001:185) characterised another cobalt(III)-nta complex, $[Co(nta)(CO_3)]^{2-}$ (Figure 2.13), on basis of measurements in the UV/VIS region, IR spectra, ^1H NMR spectrometry and X-ray crystallography. The cobalt centre has a distorted octahedral geometry and is surrounded by three oxygen atoms and the nitrogen atom of the nta ligand and the two oxygen atoms of the carbonato ligand. The fact that $[Co(nta)(H_2O)_2]$ can be obtained by acidifying $[Co(nta)(CO_3)]^{2-}$ (Dasgupta & Harris, 1974:1275), provides an alternative route for the synthesis of different Co(III)-nta species.

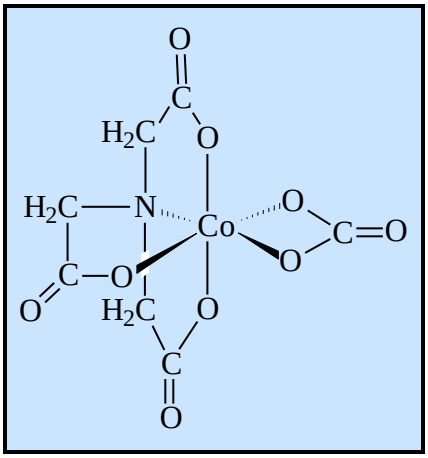

Figure 2.13 Structure of $[Co(nta)(CO_3)]^{2-}$.

The Co-N_{nta} bond lengths, O-Co-O and O-Co-N angles of different cobalt(III)-nta complexes, with nta acting as a tetradentate ligand, are shown in Table 2.1.

Table 2.1 Different bond lengths and angles in cobalt(III)–nta complexes.

Complex	Co-N (Å)	O-Co-O (º)	O-Co-N (º)	Reference
$K[Co(H_2Vi)(nta)]2H_2O$	1.942(7)	172.8(3)	86.3(3)	Almazan *et al.* (1990:2565)
$[Co(nta)(pd)]H_2O$	1.962(3)	170.5(1)	86.8(1)	Swaminathan & Sinha (1989:566)
$[Co(nta)(en)]H_2O$	1.946(3)	172.6(1)	87.6(1)	Gladkikh *et al.* (1992:1231)
$Ba[Co(nta)(gly)]ClO_43H_2O$	1.928(8)	172.5(3)	89.3(3)	Gladkikh *et al.* (1992:908)
$Cs_2[Co(nta)(\mu\text{-}OH)]_24H_2O$	1.922(6)	172.0(2)	88.1(2)	Visser *et al.* (1997:2851)
$[Co(nta)(N,N\text{-}Et_2en)]$	1.953(4)	170.6(2)	87.9(2)	Visser *et al.* (2001:175)
$Cs_2[Co(nta)(CO_3)]$	1.920(2)	173.62(9)	88.52(9)	Visser *et al.* (2001:185)

* Co-N bond refers to the bonding between Co and N of nta, O-Co-O refers to angle between *trans*-O atoms of the nta moiety, O-Co-N refers to the angle between the atoms in the same plane as the other chelating ligand e.g. en/pd etc.

These results show that the Co-N_{nta} bond distances vary between 1.962(3) and 1.920(2) Å for all the tabulated complexes. The O-Co-O angles vary between 170.5(3) and 173.62(9) º while the O-Co-N angles vary between 86.3(3) and 89.3(3) º for all the tabulated complexes.

All the tabulated bonds and angles are considered normal and agree well with those found in previous studies on $[Ca(nta)]2H_2O$ and Hnta (Hnta = monoprotonated form of nitrilotriacetic acid) (Whitlow S., 1972:1914 and Skrzypczak-Jankun *et al.*, 1994:1097).

Other cobalt(III)-nta complexes, $K_2[Co(nta)(ox)]xH_2O$, $Ba[Co(nta)(l\text{-leu})]_2xH_2O$, $Cs[Co(nta)(l\text{-val})]xH_2O$, $[Co(nta)(dmap)_2]6H_2O$ and $(NEt_4)_2[Co(nta)(NCS)_2]xH_2O$ (reason for x is that the number of water molecules per mole were not determined), was synthesised and characterised by Visser and co-workers (2001:175) using different analytical techniques.

Other metal(III)-apda complexes

Uehara *et al.* (1968:2385) prepared different chromium(III)-apda complexes, $[Cr(OH)(apdaH)(H_2O)_2]$, $NH_4[Cr(OH)(apda)(H_2O)]2H_2O$, $(NH_4)_3[Cr(apda)_2]2H_2O$, $[Cr(apda)(bipy)]3H_2O$, $[Cr(apda)(o\text{-phen})]3H_2O$, $[Cr(apda)(py)_2]$. These complexes were characterised on the basis of chemical and thermal analysis, UV/VIS spectra, molar conductivities and IR spectra. It was concluded from these studies that apda acts either as a tri- or tetradentate ligand in these complexes.

A copper(II)-apda complex was synthesised by Dung and co-workers (1987:2365) in which apda also acts as a tetradentate ligand. They characterised the Cu(II)-apda complex, $[Cu(II)(apda)(H_2O)]$ (Figure 2.14), on the basis of X-ray crystallography. The alaninate ring (R ring) is puckered in a boat-type conformation. The tetragonally elongated octahedral coordination sphere of the copper(II) ion was completed by an equatorial short bond, Cu-OH_2, and a *trans*-apical long bond, Cu-O_i (O_i = O donor atom of the bidentate-bridged acetate arm of a neighboring apda ligand).

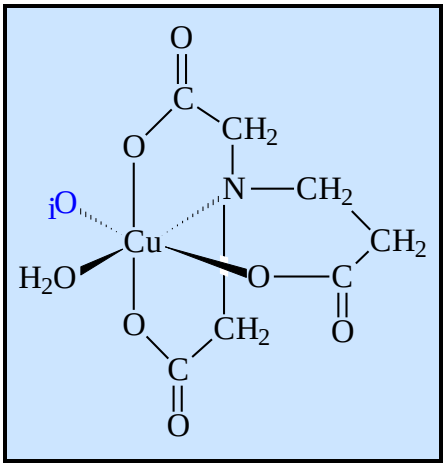

Figure 2.14 Structure of $[Cu(II)(apda)(H_2O)]$.

Other metal(II)-apda complexes in which apda acts as a tetradentate ligand, $M(H_2O)_6[M_2(apda)_2(H_2O)_2]4H_2O$ (M(II) = Co(II) or Zn(II)) were synthesised by Gonzàlez Pèrez *et al.* (1991:243). These homonuclear compounds were characterised on the basis of chemical analysis, magnetic susceptibility and/or IR spectra, thermal analysis

and X-ray diffraction methods. The crystal structure was determined for the cobalt(II) dimer (Figure 2.15). In the homodinuclear chelate anions, each cobalt(II) atom is bonded to one water molecule and one tetradentate chelating ligand. The dimer has an imposed C_i symmetry. One carboxylate oxygen atom from the propionate group acts as a bridge ligand between the two cobalt atoms, so completing the octahedral coordination sphere of the cobalt(II) ion.

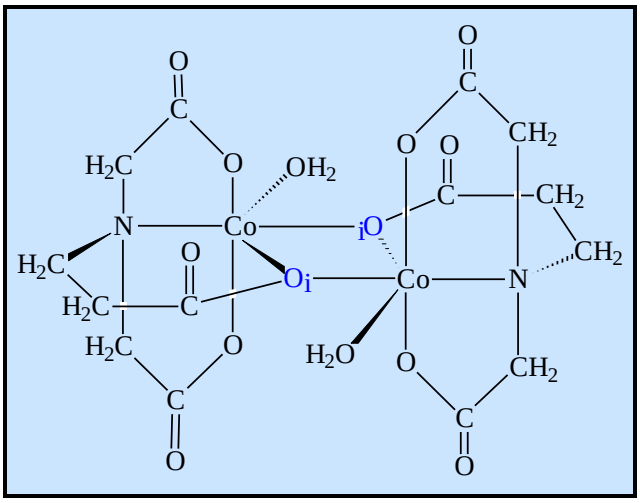

Figure 2.15 Structure of $[Co(II)_2(apda)_2(H_2O)_2]^-$.

A molybdenum(VI) complex in which apda acts as a tridentate ligand was synthesised by Obodovskaya *et al.* (1992:295). This complex was characterised on the basis of electronic adsorption, ^1H NMR spectra and X-ray crystallography as $Na_3[MoO_3(apda)]3H_2O$ (Figure 2.16). The crystal structure revealed an octahedral complex in which the propionate group (unprotonated) remained uncoordinated. The octahedral coordination of central the Mo(IV) atom was completed by three oxygen atoms. Unfortunately no IR data was published for this complex.

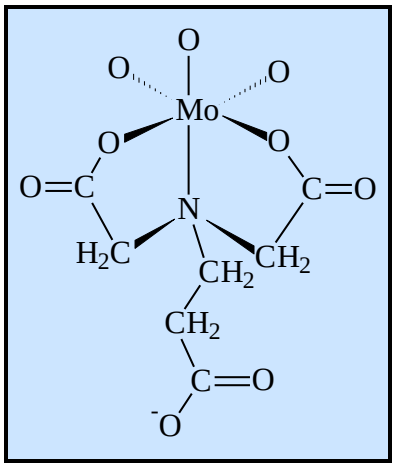

Figure 2.16 Structure of $Na_3[MoO_3(apda)]3H_2O$.

A vanadium(III)-apda complex was synthesised by Kanamori *et al.* (1995:3445). The complex was characterised on the basis of X-ray crystallography as $[V(III)(apda)(H_2O)_2]$ (Figure 2.17), in which apda acts as a tetradentate ligand. The complex adopts a hexa-coordinated structure in which the alaninato ring is situated in the G position (coaxial position). It was also found that the above-mentioned complex yields an oxo-bridged dinuclear complex upon hydrolysis.

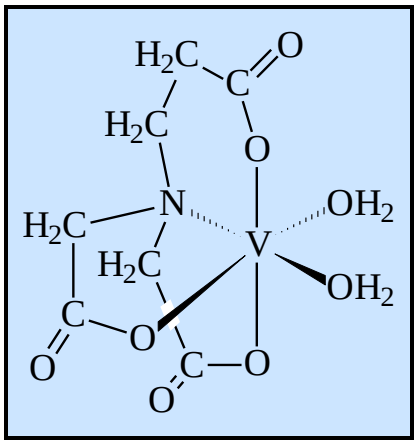

Figure 2.17 Structure of $[V(III)(apda)(H_2O)_2]$.

The M-N_{apda} bond lengths of different metal–apda complexes are shown in Table 2.2. The O-Co-O and O-Co-N angles for the metal-apda complexes with apda acting as a tetradentate ligand are also tabulated in Table 2.2.

Table 2.2 Different bond lengths and angles in metal–apda complexes.

Complex	M-N (Å)	O-Co-O (º)	O-Co-N (º)	apda Coordination mode	Reference
$[Co(III)(apda)(H_2O)_2]$	1.928(7)	176.1(4)	88.0(3)	Tetradentate	Gladkikh *et al.* (1997:1346)
$[Cu(II)(apda)(H_2O)]$	1.997(3)	167.5(1)	91.2(1)	Tetradentate	Dung *et al.* (1987:2365)
$Co(II)(H_2O)_6[Co(II)_2(apda)_2(H_2O)_2]4H_2O$	2.134(2)	155.93(8)	93.51(8)	Tetradentate	Gonzàlez Pèrez *et al.* (1991:243)
$[Co(III)(dien)(Hapda)]ClO_4$	2.019(3)	-	-	Tridentate	Obodovskaya *et al.* (1992:295)
$Na_3[MoO_3(apda)]3H_2O$	2.400(2)	-	-	Tridentate	Obodovskaya *et al.* (1992:295)
$\{[Co(III)(dien)(apda)]_2 Cu(H_2O)\}_2(ClO_4)_4 8H_2O$	2.020(8)	-	-	Tridentate	Polyakova *et al.* (1997:1509)
$[V(III)(apda)(H_2O)_2]$	2.156(7)	163.4(3)	81.4(3)	Tetradentate	Kanamori *et al.* (1995:3445)

* Co-N bond refers to the bonding between Co and N of apda, O-Co-O refers to angle between *trans*-O atoms of the apda moiety, O-Co-N refers to the angle between the atoms in the same plane as the other chelating ligand e.g. dien/H_2O etc.

For the cobalt(III)-apda complex in which apda acts as a tetradentate ligand the M-N_{apda} bond length has a value of 1.928(7) Å (Gladkikh *et al.,* 1997:1346), while the M-N_{apda} bond length for the cobalt(III)-apda complexes in which apda acts as a tridentate ligand vary between 2.019(3) and 2.020 Å (Obodovskaya *et al.,* 1992:295, Polyakova *et al.,* 1997:1509). The same lengthening of the M-N_{ligand} bond is observed in cobalt(III) complexes of ethylenediaminepolycarboxylates with uncoordinated carboxylates (Porai-Koshits *et al.,* 1984:725) and complexes with *N*-alkylated dien (Kushi *et al.,* 1983:2845).

The M-N_{apda} bond length for the cobalt(II)-apda complex in which apda acts as a tetradentate ligand has a value of 2.134(2) Å (Gonzàlez Pèrez *et al.,* 1991:243) compared to the cobalt(III)-apda complex in which apda acts as a tetradentate ligand which has a value of 1.928(7) Å (Gladkikh *et al.,* 1997:1346).

It seems as if the M-N_{apda} bond distance vary significantly with the coordination mode of apda and the oxidation state of the metal, although more evidence is needed to make any definite conclusions.

The O-Co-O angles for the metal-apda complexes with apda acting as a tetradentate ligand vary between 155.93(8) and 176.1(4) º while the O-Co-N angles for these complexes vary between 81.4(3) and 93.51(8) º. For the Co(III)-apda complex containing a tetradentate apda the O-Co-O and O-Co-N angles have values of 176.1(4) and 88.03(3) º, respectively (Gladkikh *et al.,* 1997:1346), compared to the Co(II)-apda complex containing a tetradentate apda which has values of 155.93(8) and 93.51(8) º, respectively (Gonzàlez Pèrez *et al.,* 1991:243). Although a somewhat large deviation is observed regarding the O-Co-O and the O-Co-N angles, no ratiocination can be made regarding these values since the observed deviation can be due to the combination of different factors and more evidence is needed to make any definite conclusions.

The tabulated lengths and angles found for the Co(III)-apda complexes in which apda acts as a tetradentate ligand compares very well to the values found for the Co(III)-nta complexes with nta acting as a tetradentate ligand (refer to Table 2.1).

Ring strain in metal(III)-apda complexes

The strain in the acetate-metal rings of complexes containing polyamino polycarboxylate ligands like $edta^-$, $trdta^-$, nta and of course apda brought about very interesting, yet conflicting results. Weakliem and Hoard (1959:549) observed that the two coplanar carboxylate-containing, five-membered, equatorial rings (denoted G, or girdling rings) for $[Co(III)(edta)]^-$ exhibit substantially more strain than the out-of-plane rings (termed R,

or relaxed rings). It was suggested that the sum of the bond angles of the rings could be used to determine the ring strain. The ideal value for the sum of the bond angles is 538.4˚, which would allow the rings to be nearly planar (Visser *et al.*, 2001:185).

Weakliem and Hoard attributed the strain in the G rings primarily to angular strain around the coordinated nitrogen atoms. They argued that each ring attempts to impose their own stereochemical requirements on the nitrogen atom, while the nitrogen is also constrained to tetrahedral geometry. These results not only manifest itself to angle and bond abnormalities in the G rings, but also to significant distortions of the nitrogen tetrahedron.

In a similar study on $[Co(trdta)]^-$ (trdta = trimethylenediaminetetra-acetate) it was also found that the R rings experienced less strain than the G rings (Nagao *et al.*, 1972:1852). The least square calculations on the deviations of the non-bonded carboxylate atoms from the Co-N-O-C-C planes, showed that the R ring was nearly planar. Furthermore, the Co-O_R distance was slightly shorter than the C-O_G bonding distance (1.861 Å compared to 1.904 Å). These results also suggested that the G ring is more strained than the R ring.

A study by Halloran and co-workers (1975:1762) on $[Co(edda)(pn)]^+$ (edda = ethylenediaminediacetic acid) further supported the results of the previous two studies although it was observed that the total strain was more evenly distributed over the entire chelate in this case (Figure 2.18).

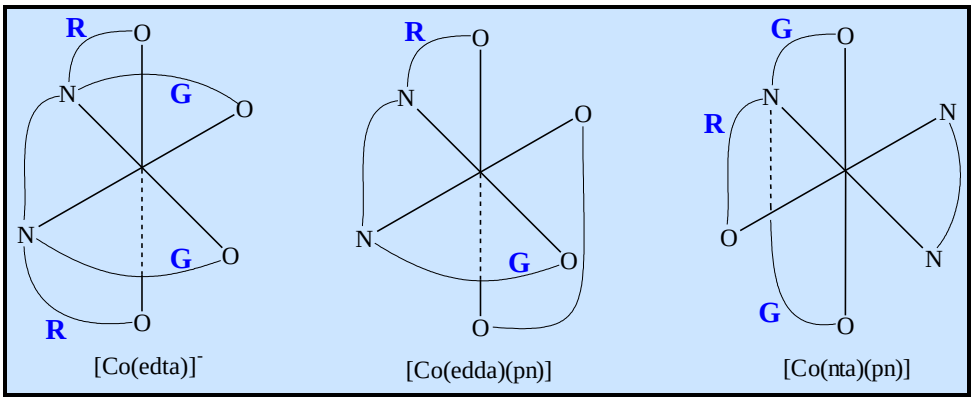

Figure 2.18 Illustration of R and G acetato rings of different Co(III) complexes.

In a study by Smith & Hoard (1959:556) it was demonstrated that the ring strain could influence the coordinating mode of ligands in these types of complexes. In a Ni(II)-edta complex, [Ni(edta)(H_2O)], in which edta act as a pentadentate ligand as a result of the larger Ni(II) cation, one of the glycinato rings in the G position fail to coordinate due to ring strain. It was also found that the glycinato rings of the isomer that was isolated had less strain than the glycinato rings in sexadentate $[Co(edta)]^-$.

The effect of the strain in glycinate rings on the chemical behaviour was illustrated by isotopic exchange studies on $[Co(edta)]^-$. Sudmeier and Occupati (1968:2524) as well as Terril and Reilly (1966:1988) showed that the α-carbon protons of the R rings of $[Co(edta)]^-$ exhibit a much more rapid rate of exchange in comparison with G ring protons. It was concluded that the strained nature of the G rings prevents the attainment of an enolate intermediate needed for proton exchange.

The ring strain was measured in the glycinate rings of two complexes with nta derivatives, [Cr(pda)$(im)_2$] and [Cr(Ida)$(im)_2$] (im = imidazole, pda = (S)-phenylalanine-N,N-diacetate, Ida = (S)-leucine-N,N-diacetate), by comparing the ring torsion angles (O-C-CH_2-N), the angles subtended by the atoms on the mutually perpendicular axes of the octahedron, and the octahedral angles about the Cr(III) centres (Bocarsley *et al.*, 1990:4898). It was found that the observed angles followed the anticipated order of the ring strain. Furthermore, the substituted G rings were more strained than its unsubstituted counterparts in each case.

The ring strain in [Co(nta)(pd)]H_2O was also investigated by Swaminathan and co-workers (1989:566). This study suggested that the R rings, contrary to previous studies, were more strained than the G ring. Unfortunately they misunderstood the method first used by Weakliem & Hoard (1959:549) to distinguish between the glycinato rings. Tetra-coordinated nta has two co-planar glycinato rings (G rings) and one R ring (see Figure 2.9 for correct representation of G and R rings in nta complexes). Therefore it can be concluded that the same sequence for strain was found for nta complexes with G rings being more strained than R rings.

In a study by Visser and co-workers the ring strain in different Co(III)-nta complexes has also been investigated. The study indicated that the sums of the endocyclic angles in $[Co(nta)(CO_3)]_2^{2-}$ (Figure 2.13) were 526.97(9) and 532.29(9) º for the G rings and 538.7(5) º for the R ring (Visser *et al.*, 2001:185). These values indicated that the R ring once again experienced less strain than the G rings. They also stated that the nitrogen tetrahedron was slightly distorted from the tetrahedral geometry with C-N-C angles varying between 112.0(3) º and 114.3(2) º, which were different from the uncoordinated H_3nta where the C-N-C angles were between 112.3(1) º and 113.6(1) º.

Visser and co-workers also investigated the ring strain in [Co(nta)(N,N-Et_2en)] (Figure 2.12). They stated that the sums of the endocyclic angles were 530.26 º for the G rings and 540.3 º for the R ring, which is once again indicative of a lesser-strained R ring (Visser *et al.*, 2001:175). The nitrogen tetrahedron was again significantly distorted from the tetrahedral geometry with C-N-C angles reaching values of 116.8(4) º.

The reasons for ring strain in the glycinato and alaninato rings of Co(III)-apda complexes have not yet been fully explained. The study by Gladkikh *et al.* (1997:1346) indicated that the glycinate ring (G ring in Figure 2.19) in the [Co(III)(apda)$(H_2O)_2$] complex, situated nearly in the same plane as the alaninante ring (G ring in Figure 2.19), is the most distorted.

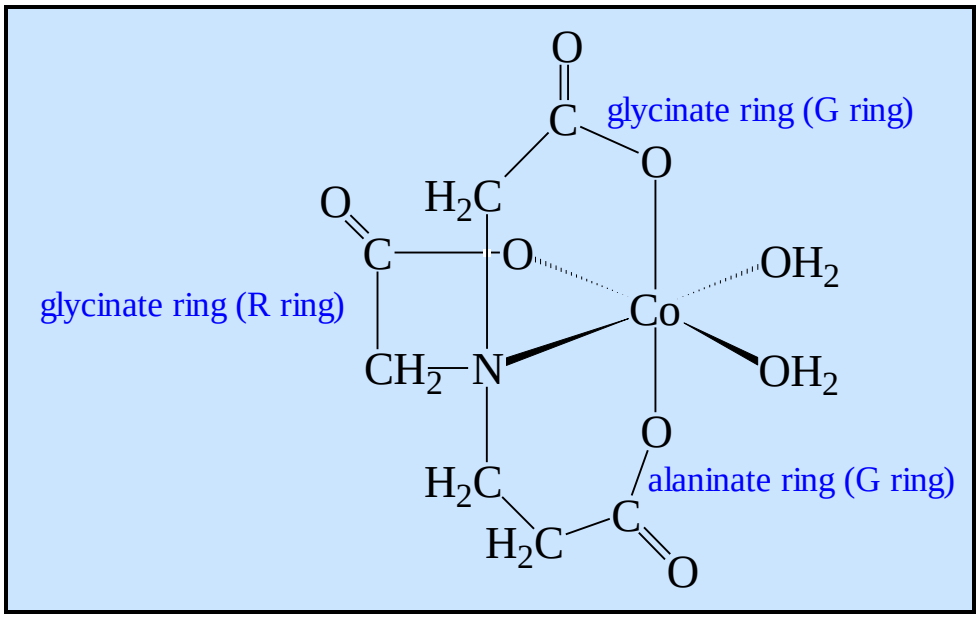

Figure 2.19 Glycinato and alaninato ring strain in Co(III)-apda complexes.

The distortion parameter for the glycinate ring in the G position was found to be q = 0.432 Å and the O-Co-N-C torsion angle 33.8 º. {q, according to Cremer *et al.*, 1975:1354, is a distortion parameter that is calculated from the specification of an appropriate mean plane given only the coordinates of the nuclear positions of the atoms in the ring}. For the glycinate ring in the R position the distortion parameter was found to be q = 0.171 Å and the O-Co-N-C torsion angle 11.0 º. A smaller degree of distortion was found for these glycinate rings than found to be characteristic of the glycinate rings in previously studied Co(III) complexes with nta acting as a tetradentate ligand (Gladkikh *et al.*, 1992:1156, Gladkikh *et al.*, 1992:1125, Gladkikh *et al.*, 1992:1131). Gladkikh and co-workers (1997:1346) indicated that the alaninate ring had a nearly semi-bath form with the apex at the carbon bonded to the nitrogen. The O-Co-N-C torsion angle in the alaninate ring was 23.3 º, which is characteristic of complexes with bi-, tri-, and tetradentate ligands containing a propionate group (Ilyukhin *et al.*, 1990:1597).

The distortion parameters and torsion angles for the glycinate rings in the G and R positions in [Co(apda)(H_2O)$_2$] also indicated that the glycinate ring situated in the G position is more strained than the glycinate ring in the R position. Unfortunately, no mention was made of the angular distortion around the apda nitrogen.

In the study by Obodovskaya *et al.* (1992:295) the ring strain in the [Co(dien)(Hapda)]ClO_4 complex (Figure 2.5) was also investigated. It was observed that the sums of the endocyclic angles for the glycinate ring in the G and R position were 535.2 and 536.9 º, respectively. These values indicated that the G ring is more strained than the R ring. The same was found by Polyakova *et al.* (1997:1509) for the glycinate rings in $\{[Co(dien)(apda)]_2Cu(H_2O)\}_2(ClO_4)_4 8H_2O$ (Figure 2.6). The sums of the endocyclic angles for the glycinate ring in the G and R position were 533.2 and 537.7 º, respectively. These values are also indicative of a less strained glycinate ring in the G position. The apda nitrogen was significantly distorted from the tetrahedral geometry with values for C-N-C angles varying between 108.6(7) and 111.5(7) º.

2.2.2 Reactions of cobalt(III)-apda and similar complexes

Very few metal complexes containing apda as ligand is cited and little or no kinetic studies have been published on these types of complexes. It was therefore decided to focus this part of the discussion on the substitution reactions of cobalt(III)-nta and similar complexes.

The mechanisms of the substitution reactions of Cr(III)- and Co(III)-nta complexes are complicated as will be discussed in the following paragraphs.

Anation reactions

The fact that nta and apda act mainly as tetradentate ligands implies that the remainder of the coordination sites of the octahedral coordination sphere is completed by two ligands bonded *cis* with respect to each other. It has already been postulated (refer to Paragraph 2.2.1) that *cis*-aquacobalt(III)-nta complexes can be obtained by merely acidifying either the μ–hydroxo dimeric species or the carbonato species. The *cis*-aquacobalt(III)-nta complex proved to be very useful in the investigation of substitution reactions (Thacker & Higginson, 1975:704 and Visser *et al.*, 2002:461).

CHAPTER 2

Cr(III)-nta complexes

The kinetics of the formation and dissociation of $[Cr(nta)(acac)]^-$ (acac = pentane-2,4-dione) have been fully investigated, but the complexity of the rate law prevented a full understanding of the mechanism. The results are presented in Scheme 2.1 and the value of K_1 was determined as 1.35(5) (Bhattcharyya & Banjeree, 1997:4217).

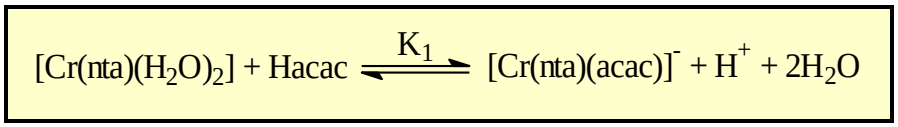

Scheme 2.1 Formation and dissociation of $[Cr(nta)(acac)]^-$.

Two different studies investigated the kinetic behaviour of $[Cr(nta)(H_2O)_2]$/ $[Cr(nta)(H_2O)(OH)]^-$ with different synthetic dyes, Solochrome Yellow 2G (Haulin & Xu, 1990:137) and Eriochrome Black T (EBT^-) (Visser *et al.*, 1994:1051). The second study also included the reactions with thiocyanate and H^+ ions. Both these studies were complicated by the fact that the dyes have very large extinction coefficients and the reactions were rather performed with the concentration of the metal in excess (pseudo first-order kinetics). The reaction scheme for the second study is represented in Scheme 2.2.

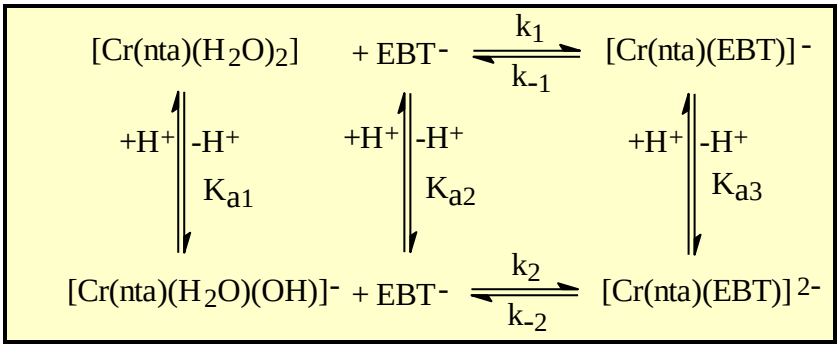

Scheme 2.2 Reaction scheme for the reaction of $[Cr(nta)(H_2O)_2]$ with Eriochrome Black T (EBT^-).

The study of Visser *et al.* (1994:1051) was further complicated by the fact that EBT^- has an acid dissociation constant of 6.3 (Vogel, 1989), close to that of $[Cr(nta)(H_2O)(OH)]^-$ which has a pK_a value of 5.47. At pH 6 and higher elucidation of the mechanism was even further complicated by precipitation reactions.

In spite of these limitations, very useful information was obtained from this study. The reaction between $[Cr(nta)(H_2O)_2]$ and EBT^- is about 16 times faster (9.5×10^{-2} M^{-1} s^{-1} at 30 ºC) than the corresponding reaction with NCS^- (5.8×10^{-3} M^{-1} s^{-1} at 25 ºC). This was attributed to the chelation effect of the EBT^- ligand during the reaction.

Haulin & Xu proposed a different mechanism for the reaction of $[Cr(nta)(H_2O)_2]$ with Solochrome Yellow 2G. They suggested a two-step mechanism (ion pair formation) that involved a rapid formation of the monodentate coordinated dye intermediate, followed by the rate determining ring-closure (Scheme 2.3). The rate constants, k_1 and k_2, for the ring-closure steps of the reaction of $[Cr(nta)(H_2O)_2]$ with this dye were determined as 2.3×10^{-2} s^{-1} and 1.7×10^{-2} s^{-1}, respectively.

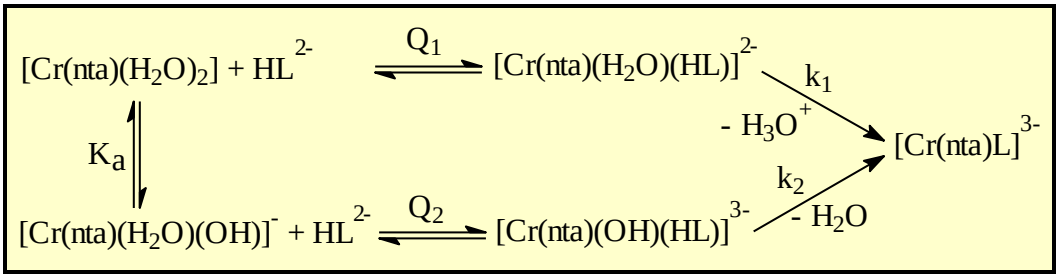

Scheme 2.3 Reaction scheme for the reaction of $[Cr(nta)(H_2O)_2]$ with Solochrome Yellow 2G (HL^{2-}).

Both studies found that the electron donating ability of nta improved the reactivity of the chromium(III) complex by several orders of magnitude. The second-order rate constant ($k_1 = 5.8 \times 10^{-3}$ M^{-1} s^{-1}) for the reaction of $[Cr(nta)(H_2O)_2]$ with NCS^- compares well with the k_1 value of 4.7×10^{-3} M^{-1} s^{-1} that was obtained for the reaction between $[Cr(TPPS)(H_2O)_2]^{3-}$ and NCS^- (Ashley *et al.*, 1980:1608). Porphyrins like TPPS are well known to increase the rate of substitution of inert metal(III) complexes by several orders of magnitude. The main reason for this is believed to be the electron donating ability of

the porphyrin, which increases the electron density on the central metal ion, making it react more like the labile metal(II) species (Ashley *et al.*, 1980:1608).

The reaction of $[Cr(nta)(H_2O)_2]$ with H^+ ions (Visser *et al.*, 1994:1051) was also investigated. It was proposed that the mechanism for the reaction involved the formation of an ion pair. Protonation of one of the carboxylate groups of the nta then occurs, which results in the dissociation of this bond to give the aquated tridentate nta complex, $[Cr(\eta^3\text{-nta})(H_2O)_3]^+$. A possible reaction scheme is presented in Scheme 2.4.

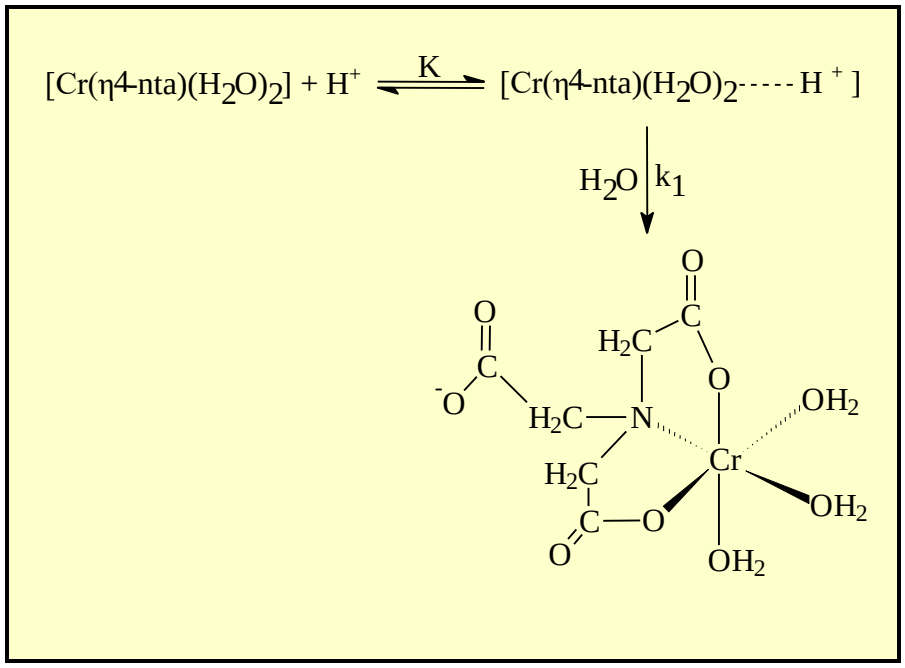

Scheme 2.4 Proposed mechanism for the formation of $[Cr(\eta 3\text{-nta})(H_2O)_3]^+$.

Co(III)-nta complexes

The first study on the anation reactions of *cis*-$[Co(nta)(H_2O)_2]$ was performed by Thacker & Higginson (1975:704). They studied the redox and substitution reactions of *cis*-$[Co(nta)(H_2O)_2]$ with various ligands. They found that, of all the ligands investigated only NCS^- did not show redox properties in the pH 3 – 5 region. They proposed Scheme 2.5 for this reaction (K_1 = 17 mol^{-1}). Unfortunately their experimental results were not good due to, among other things, interference of their buffer solutions.

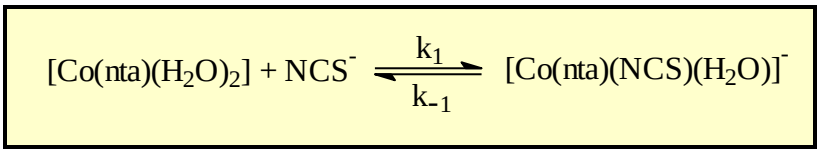

Scheme 2.5 Proposed mechanism for the reaction between $[Co(nta)(H_2O)_2]$ and NCS^-.

Visser *et al.* (2002:461) studied the influence of H^+ ions on the Co(III)-nta system. It was observed that the aqua-hydroxo complex, $[Co(nta)(H_2O)(OH)]^-$, reverts back to the dimer at pH 6 – 7 upon standing for several days (Scheme 2.6). They therefore studied the pH dependence of the $[Co(nta)(H_2O)_2]$ complex between pH 2 and 7 to avoid complication by competing reactions. The acid dissociation constant of $[Co(nta)(H_2O)_2]$, pK_{a2}, was determined as 6.52(2), which compares well to the value of 6.71(1) determined by Thacker & Higginson (1975:704) for the β-form of the Co(III)-nta used in their study, but is higher than the value obtained (pK_a = 5.43) for the same reaction by Haulin & Xu (1990:137).

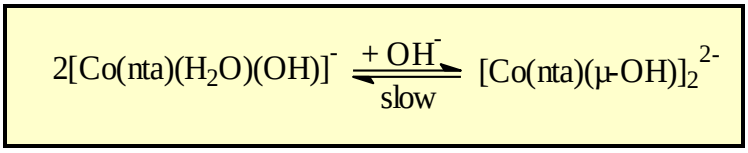

Scheme 2.6 $[Co(nta)(H_2O)(OH)]^-$ reverting back to the dimer at pH 6 – 7.

The reactions of $[Co(nta)(H_2O)_2]$/$[Co(nta)(H_2O)(OH)]^-$ with NCS^- ions were studied at pH values between 2 and 7, which allow both Co(III)-nta species to react with NCS^-. They proposed the following scheme:

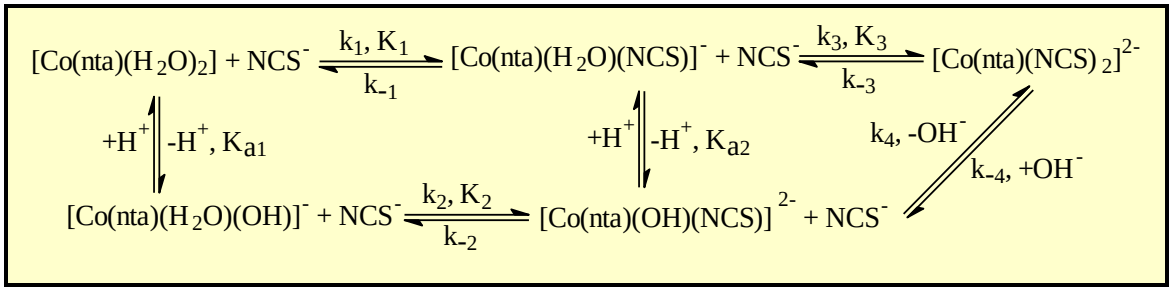

Scheme 2.7 Reactions of $[Co(nta)(H_2O)_2]$/$[Co(nta)(H_2O)(OH)]^-$ with NCS^- ions.

The final products in Scheme 2.7 were substantiated by the synthesis and successful characterisation of $[Co(nta)(NCS)_2]^{2-}$.

The different rate constants were obtained by the careful manipulation of the experimental conditions. The subsequent simplification of the rate law at pH 2 (K_{a1} and K_{a2} becomes negligible) is presented in Equation 2.1.

$$\mathbf{k_{obs} = k_1[NCS^-] + k_{-1} + k_3[NCS^-] + k_{-3}} \qquad \mathbf{(2.1)}$$

The $[Co(nta)(H_2O)(OH)]^-$ complex reacts about 70 times faster at 24.7 ºC with NCS^- than $[Co(nta)(H_2O)_2]$ with NCS^- (k_2 = 1.68(5) M^{-1} s^{-1} *vs.* 2.4(1) x 10^{-2} M^{-1} s^{-1} for k_1 at 24.7 ºC). This increase in substitution rate is attributed to the hydroxo ligand which labilises the *cis*-aqua bond so that an increase in rate is observed. The *cis*-labilising effect for the hydroxo ligand was also observed for the similar reaction of $[Cr(nta)(H_2O)(OH)]^-$ /$[Cr(nta)(H_2O)_2]$ with NCS^- where an increase of about 8 times was observed (Visser *et al.*, 1994:1051). Visser and co-workers also observed that the rate of substitution of the first aqua ligand (k_1 = 2.4(1) x 10^{-2} M^{-1} s^{-1} at 24.7 ºC) at low pH is about 120 times faster than the rate of substitution of the second aqua ligand (k_3 = 1.98(6) x 10^{-4} M^{-1} s^{-1} at 24.7 ºC), which indicated that the NCS^- ligand does not have a high *cis*-labilising effect on the remaining aqua ligand.

For the similar reaction of the chromium complex (Visser *et al.*, 1994:1051) the k_1 value, k_1 = 5.8 x 10^{-3} M^{-1} s^{-1}, was a factor of 4 times slower than the k_1 value obtained for cobalt complex in the previous paragraph. The value of k_2 at 24.7 ºC (1.68(5) M^{-1} s^{-1}) was approximately 70 times faster than the value obtained for the similar reaction of $[Cr(nta)(H_2O)(OH)]^-$/$[Cr(nta)(H_2O)_2]$ with NCS^- at 25.0 ºC. This clearly indicates that Co(III) complexes are more labile than Cr(III) complexes, as was observed for several M(III)-porphydrin (M = Co/Cr) complexes (Ashley *et al.*, 1980:1608).

Other similar Co(III) complexes

There are a few papers available in the literature on the anation and aquation reactions of *cis*-[Co(edda)$(X)_2$] complexes (X = Cl^-, H_2O) (Weyh *et al.*, 1973:2374; 1976:2298 and Garnett & Watts, 1974:307). There are also very few reports on the substitution reactions of mono-aqua complexes of chromium(III) where the other five coordination positions are occupied by five-coordinate, edta-type ligands (Ogino *et al.*, 1975:2093 and Sulfab *et al.*, 1976:2388). All these studies illustrated that these types of ligands (multidentate N, O donors) labilise the metal centre and enhance the rate of substitution by several orders of magnitude.

Bridge cleavage reactions by hydrogen ions

Sykes and Weil (1970) wrote a comprehensive review on the acidic bridge cleavage reactions of binuclear cobalt complexes. Bridging ligands can vary from peroxo, amido, superoxo, phosphato, nitrito, halido, acetato and hydroxo ligands.

It has been suggested that complexes of cobalt and aminopolycarboxylic acids like nta and edta do not appear to combine with O_2 to form peroxo- or superoxo-bridged species (Fallab, 1967:496). The reason given is that these ligands contain too many oxygenic groups attached to the cobalt, which reduce the readiness with which these complexes form stable adducts with molecular oxygen. On the other hand, there are countless examples of hydroxo-bridged species of cobalt complexes like $[Co(nta)(\mu\text{-}OH)]_2^{2-}$, prepared by Visser *et al.* (2003:235).

The stability of di- and tri-μ-hydroxo complexes in aqueous solutions is very much dependant on the hydrogen ion concentration. Hoffman and Taube (1968:903) studied the kinetics of the reaction of hydrogen ions with $[Co(NH_3)_4(\mu\text{-}OH)]_2^{4+}$. The assigned rate law is shown in Equation 2.2 and the reaction scheme is shown in Scheme 2.8. The value of k_1 was determined as 1.2×10^{-3} M^{-1} s^{-1} at 25.0 ºC and μ = 1.0 M.

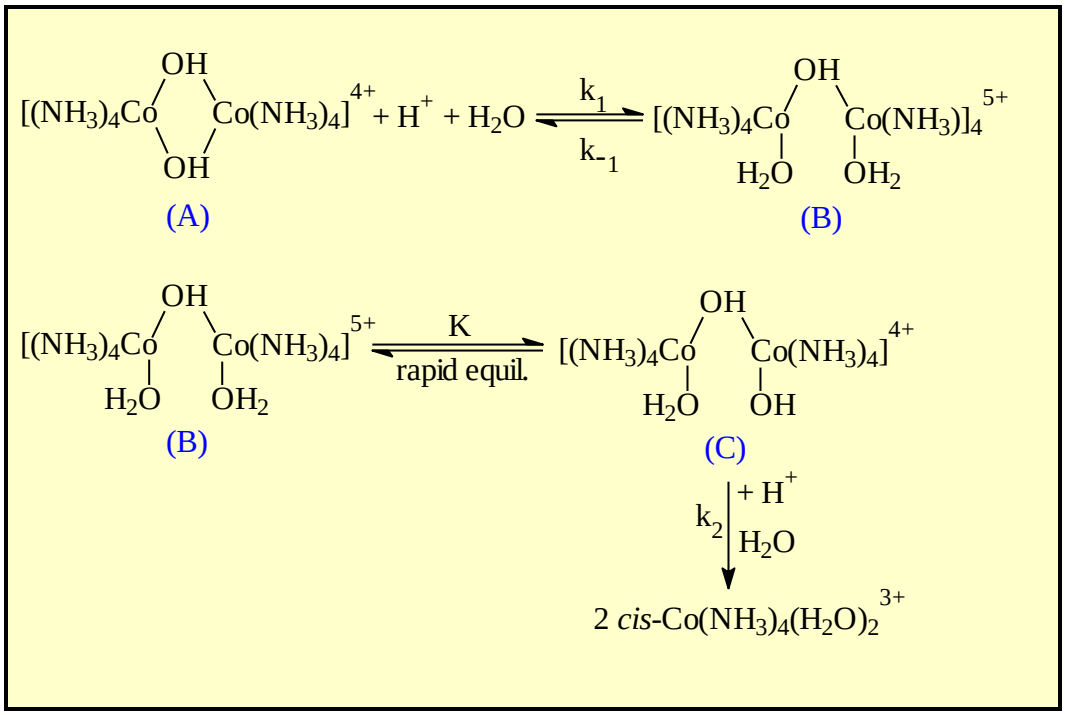

Scheme 2.8 Acidic cleavage of $[Co(NH_3)_4(\mu\text{-}OH)_2]^{4+}$.

$$\mathbf{R = (k_2k_1K[H^+])/(k_2K + k_{-1})} \qquad \mathbf{(2.2)}$$

Lee Hin-Fat and Higginson (1971:2589) investigated the hydroxo bridge cleavage of $[Co(C_2O_4)_2(OH)]_2^{4-}$ at pH 3.5 – 4.5. They also found a first-order $[H^+]$ dependence for this reaction.

The acid assisted cleavage of the di-μ-hydroxo bonds in $[Co(en)_2(OH)]_2^{4+}$ was also studied by different research groups (El-Awady & Hugus, 1971:1415 and DeMaine & Hunt, 1971:2106). The study of DeMaine and Hunt (1971:2106) suggested the same mechanism as the one that was proposed for $[Co(NH_3)_4(\mu\text{-}OH)]_2^{4+}$ (as indicated in Scheme 2.8).

The study of El-Awady and Hugus (1971:1415) proposed two possible mechanisms for the acid assisted cleavage of the di-μ-hydroxo bridges in $[Co(en)_2(OH)]_2^{4+}$. Both mechanisms included the formation of a single hydroxo-bridged dimeric species as an intermediate. One of the proposed mechanisms involves the protonation of the dimer and

the intermediate in a fast reversible step (Scheme 2.9). The second mechanism is very similar to that proposed by Hoffman and Taube (1968:903) (Scheme 2.8). The rate law (Equation 2.3) included a $[H^+]^2$ dependence in the numerator, which was not evident in the other studies.

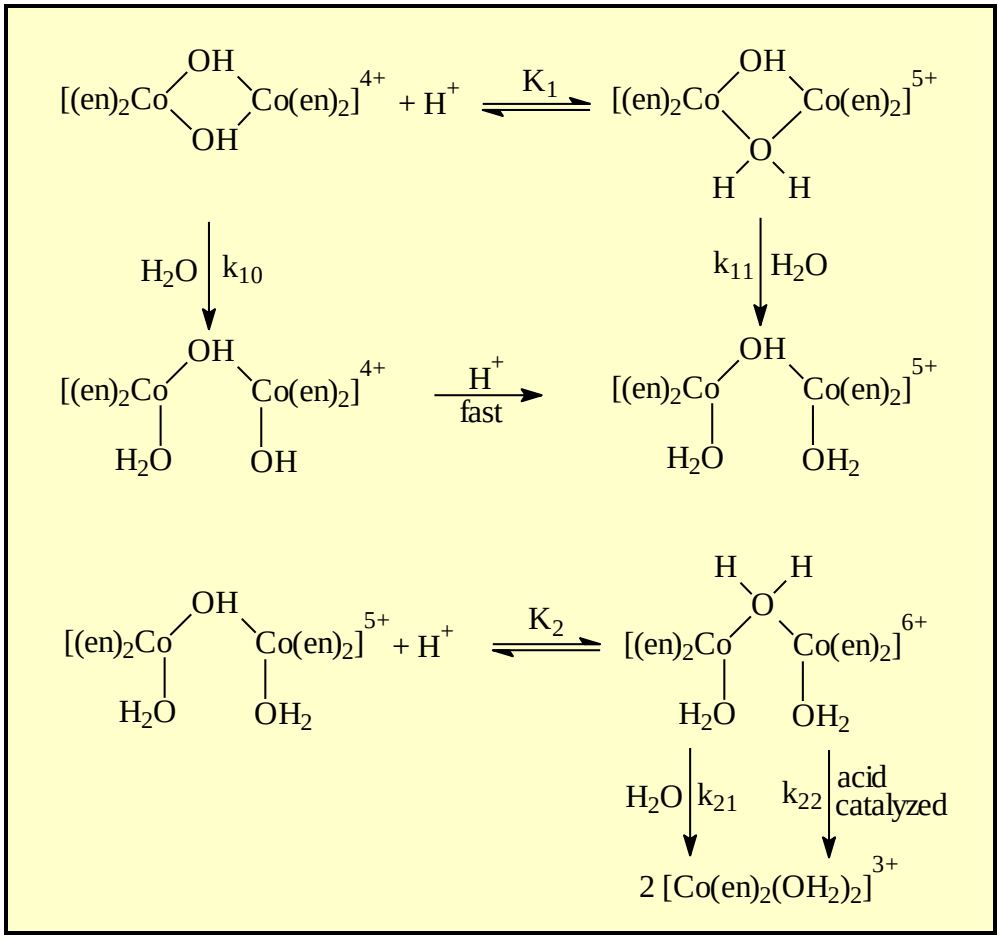

Scheme 2.9 Acid assisted cleavage of the di-μ-hydroxo bridges in $[Co(en)_2(OH)]_2^{4+}$.

$$\mathbf{R = (K_{21}K_2[H^+] + k_{22}K_2[H^+]^2)/(1 + K_2[H^+])} \qquad \mathbf{(2.3)}$$

Ellis and co-workers (1972:2565) provided a possible solution for the differences in the observed hydrogen ion concentration dependence in the above-mentioned studies. The rate laws for the acid cleavage of μ-hydroxo-cobalt(III) complexes sometimes involve an acid-independent term and invariably show an acid dependence for the reaction, which varies from simple first-order to a combination of first- and second-order terms.

Complexes with a single hydroxo bridge yield a linear dependence between the observed rate constant and the hydrogen ion concentration. Any deviation from such dependence in di-μ-hydroxo bridged complexes must be a function of the second hydroxo bridge. The mechanism they predicted for the acidic cleavage of a μ-hydroxo cobalt(III) complex is shown in Scheme 2.10.

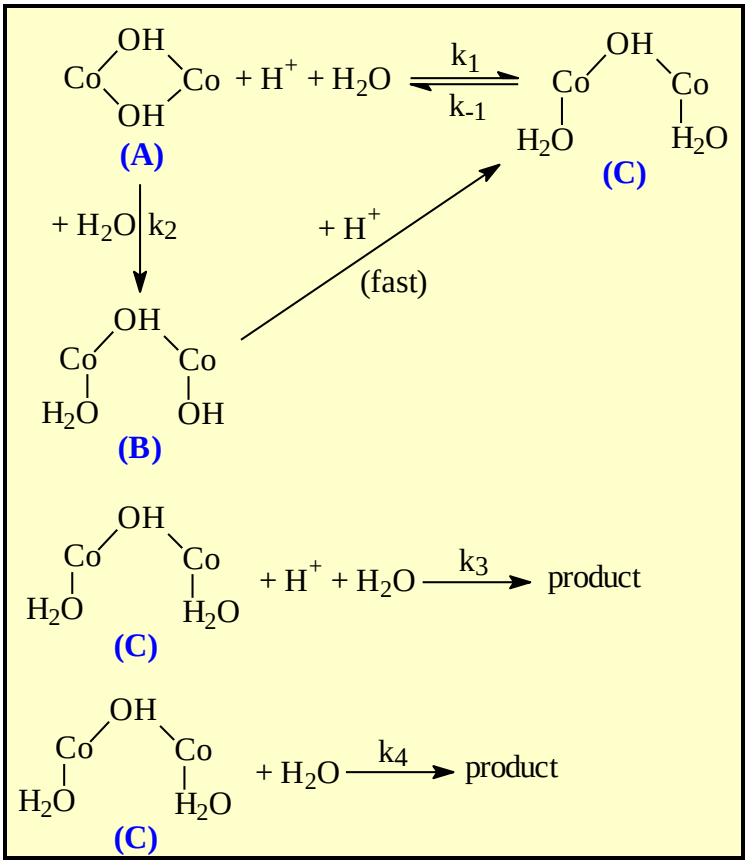

Scheme 2.10 Acidic cleavage of a μ-hydroxo cobalt(III) complex.

The pseudo first-order rate constant, k_{obs}, is given in Equation 2.4.

$$\mathbf{K_{obs} = (k_2k_4 + k_2k_3 + k_1k_4[H^+] + k_1k_3[H^+]^2)/(k_{-1} + k_4 + k_3[H^+])} \qquad \mathbf{(2.4)}$$

It can be seen from Equation 2.4 that a k_{-2} pathway was ignored. The reason given for this is that the intermediate, (B) (Scheme 2.10), can partially rotate and form hydrogen bonds with another intermediate complex or the dimer, especially through the OH^- ligand.

It was further concluded that k_{-2} will only make a contribution at very small hydrogen ion concentrations.

The acidic cleavage of the hydroxo bridges of $[Co(nta)(\mu\text{-}OH)]_2^{2-}$ has been investigated by other workers (Thacker & Higginson, 1975:704 and Meloon & Harris, 1977:434). Both these studies observed a fast initial reaction followed by a second slower reaction upon allowing $[Co(nta)(\mu\text{-}OH)]_2^{2-}$ to stand in moderately acidic solutions (*ca.* pH 4) for 20 – 30 minutes. It was observed that the aqueous solutions of $[Co(nta)(\mu\text{-}OH)]_2^{2-}$ did not show any evidence of normal acidic or basic properties when titrated rapidly with dilute acid and back-titrated with a base. It was postulated that these two reactions involved the formation of a mono-hydroxo-bridged species that dissociates to form *cis*-$[Co(nta)(H_2O)_2]$ in the second, slower step (Scheme 2.11).

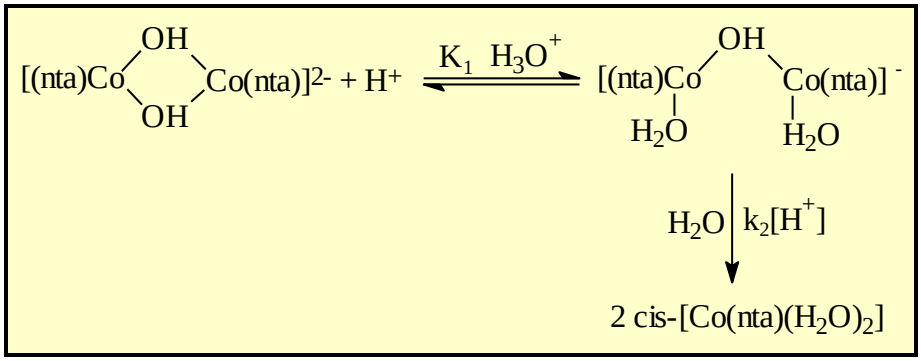

Scheme 2.11 Acidic cleavage of $[Co(nta)(\mu\text{-}OH)]_2^{2-}$.

The rate law that was proposed for this reaction is illustrated in Equation 2.5.

$$\mathbf{k_{obs} = (k_2K[H^+]^2])/(1 + K[H^+])} \qquad \mathbf{(2.5)}$$

The values for K and k_2 at 25 ºC in Equation 2.5 were determined as 43(3) M^{-1} and 17(1) M^{-1} s^{-1}, respectively (Meloon & Harris, 1977:434).

Thacker & Higginson also calculated the acid dissociation constant (pK_a = 6.71(1)) for the formation of *cis*-$[Co(nta)(H_2O)(OH)]^-$ from *cis*-$[Co(nta)(H_2O)_2]$. It was mentioned that *cis*-$[Co(nta)(H_2O)(OH)]^-$ was not very stable in solution.

Research by Koine *et al.* (1986:2835) showed with ^2H NMR that an intermediate species is formed upon acidification of $[Cr(nta)(OH)]_2^{2-}$. They concluded that the intermediate might also be a mono-hydroxo-bridged species. Other observers also support this assumption (Toftlund & Springborg, 1976:1017 and Grant & Hamm, 1958:4166).

The acidic cleavage of $[Co(nta)(\mu\text{-}OH)]_2^{2-}$ (1 in Scheme 2.12) by the slow acidification at pH 6 – 2 was investigated by Visser *et al.* (2002:461). Their results did not exhibit the expected diprotic behaviour for the protonation of $[Co(nta)(\mu\text{-}OH)]_2^{2-}$, instead only one protonation step was observed under the experimental conditions. Previous studies proved that the cobalt(III)-nta species present in solution at pH 6 – 7 is in fact the di-μ-hydroxo complex and that the main complex present at pH 2 is $[Co(nta)(H_2O)_2]$ (Visser *et al.*, 1997:2851). Furthermore, the results presented in previous studies (Hoffman & Taube, 1968:903, Demaine & Hunt, 1971:2106, Linhart & Siebert, 1969:24) for the stepwise bridge cleavage of di-μ-hydroxo complex ions support this type of protonation. Reactions 2 and 3 (Scheme 2.12) were proposed for the protonation of $[Co(nta)(\mu\text{-}OH)]_2^{2-}$.

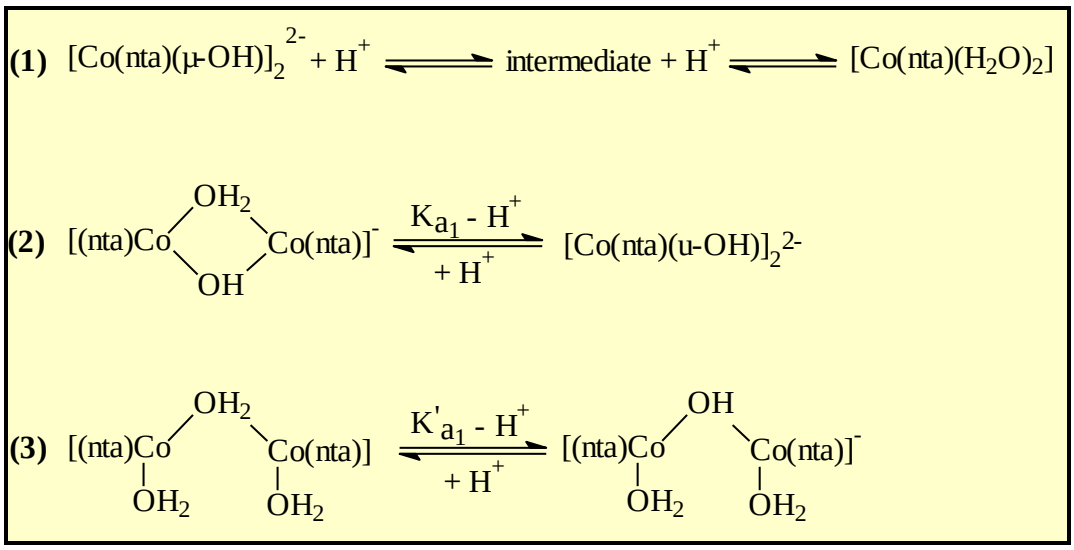

Scheme 2.12 Proposed protonation reactions of $[Co(nta)(\mu\text{-}OH)]_2^{2-}$.

In Reactions 1 and 2 (Scheme 2.12), K_{a1} and K'_{a1} represent the acid dissociation constants of the di-μ-hydroxo complex ion and singly bridged μ-hydroxo species, respectively. Due to the fact that only one protonation step was observed, Equation 2.6 was found to be applicable.

$$\mathbf{A = (A_h + A_0(K_{a1}/[H^+]))/(1 + (K_{a1}/[H^+]))} \qquad \mathbf{(2.6)}$$

The acid dissociation constant, K_{a1}, of $[Co(nta)(\mu\text{-}OH)]_2^{2-}$ was determined spectrophotometrically as 3.09(3). According to their study, a possible reason for only one protonation step and not two, as expected, was due to the fact that the UV/VIS spectra of the intermediate species (Reactions 1 – 3 in Scheme 2.12) were very similar under their experimental conditions. Therefore, it was impossible to decide on the basis of available information which of K_{a1} or K'_{a1} (Scheme 2.12) was actually detected in this study.

The study of kinetics of the acid cleavage of $[(phen)_2Cr(\mu\text{-}OH)]_2^{4+}$ (Wolcott & Hunt, 1968:755) showed different mechanistic results than the previous mentioned studies. It was proposed that proton-transfer reactions in aqueous solutions are far too rapid for the acid dependence of the cleavage rate to be explained in terms of rate-determining addition of a proton to the dimer (Scheme 2.13).

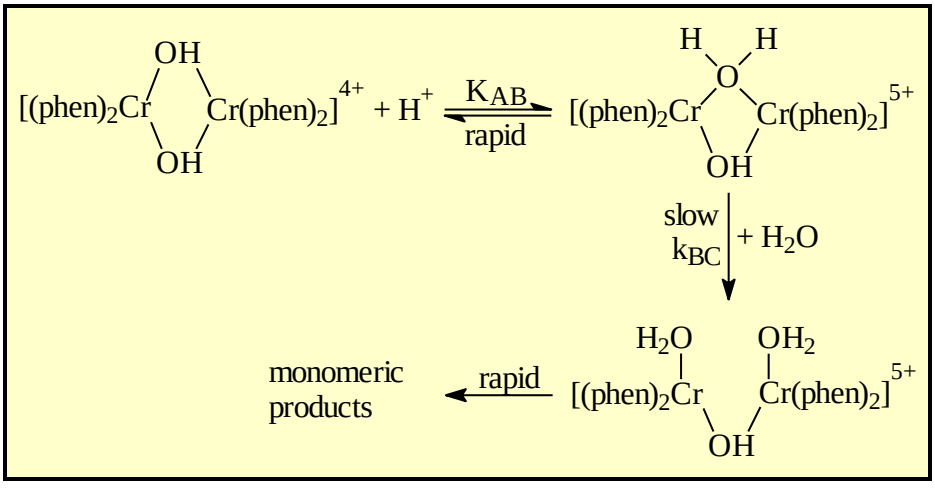

Scheme 2.13 Acidic cleavage of $[(phen)_2Cr(\mu\text{-}OH)]_2^{4+}$.

They suggested that the first-order dependence of the rate law (Equation 2.7) on $[H^+]$ is due to a rapid acid-base reaction preceding the rate-determining step. This rapid acid-base reaction involved the addition of a proton to the dimer.

$$\mathbf{R = k_{BC}K_{AB}[H^+][dimer]} \qquad \mathbf{(2.7)}$$

It can be seen from the previous paragraphs that by making the appropriate assumptions concerning the magnitude of the various constants, one can readily derive an expression corresponding to any of the observed mechanisms for related cobalt(III) complexes. It is also observed that different workers suggest different types of mechanisms for bridge cleavage reactions. The above discussion represents a fairly complete set of results on these types of reactions, making the investigation of these reactions very interesting due to the limited data available on these complex reactions.

Bridge cleavage reactions by hydroxide ions

Very little work has been done on bridge cleavage reactions of di-μ-hydroxo-bridged cobalt(III) and chromium(III) complexes. El-Awady & Hugus (1971:1415) investigated the reaction between $[Co(en)_2(OH)]_2^{4+}$ and OH^- ions and predicted a mechanism similar to those discussed for the acidic cleavage of this complex. It was also mentioned that they were not very satisfied with their experimental data.

The carbon dioxide uptake of different tri-μ-hydroxo bridged cobalt(III) complexes in basic medium was investigated by Sadler and Dasgupta (1987:3254 & 1987:185). They observed that OH^- ions first split one of the hydroxo bridges, forming the intermediate (A) in Scheme 2.14. One of the non-bridging hydroxide ions in intermediate (A) reacts with CO_2 in the rate-determining step to form intermediate (B), which quickly undergoes ring-closure to form the final product, (C).

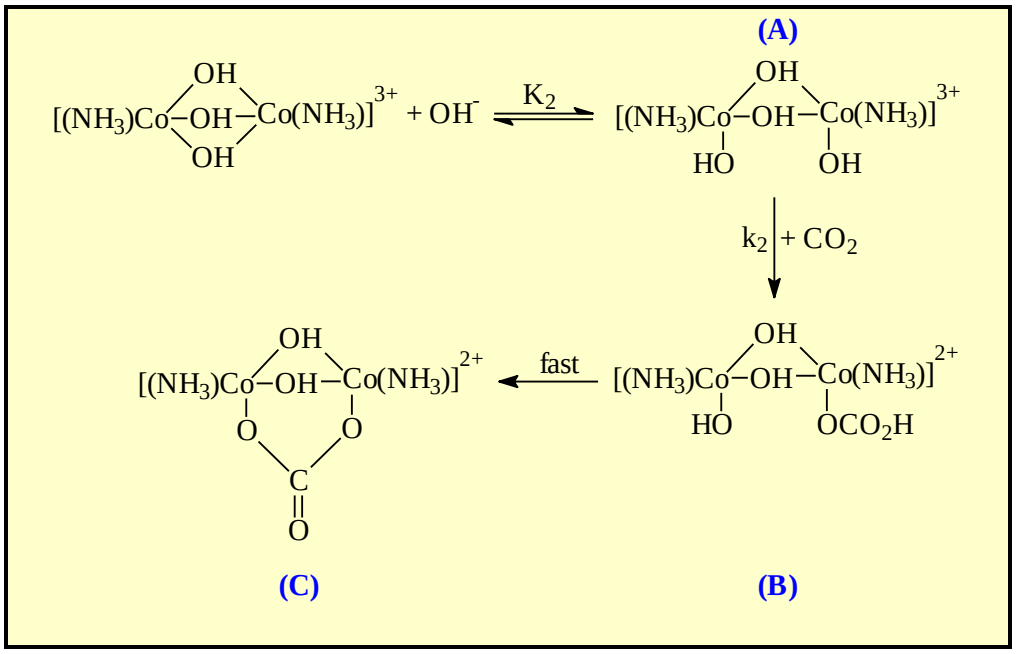

Scheme 2.14 Different intermediates and final product in CO_2 uptake reactions.

The di-μ-hydroxo bridge-cleavage reactions between $[Co(nta)(\mu\text{-}OH)]_2^{2-}$ and different monodentate ligands were investigated by Visser and co-workers (2003:235). Scheme 2.15 was proposed for these reactions.

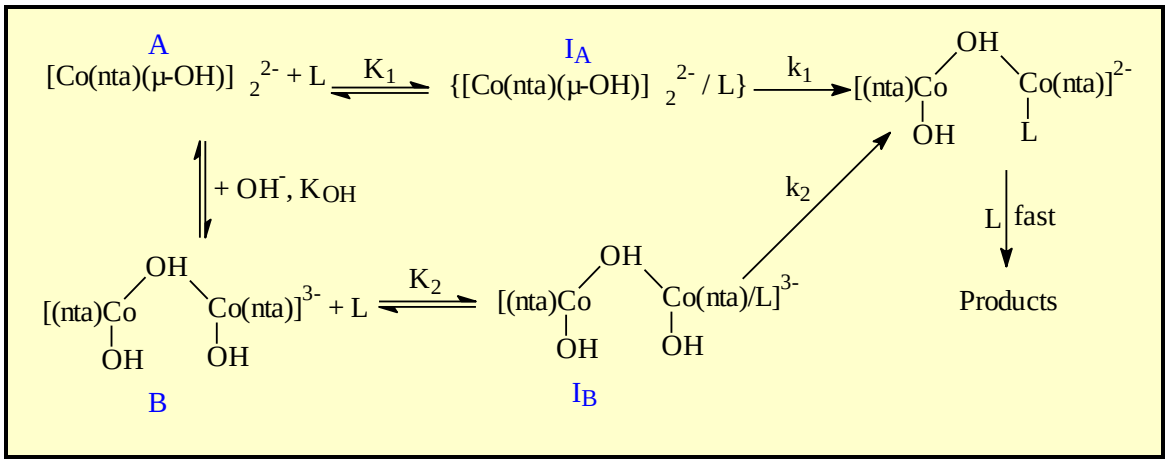

Scheme 2.15 The di-μ-hydroxo bridge-cleavage reactions between $[Co(nta)(\mu\text{-}OH)]_2^{2-}$ and different monodentate ligands.

They found that $[Co(nta)(\mu\text{-}OH)]_2^{2-}$ equilibrates rapidly in aqueous basic solutions with a mono-μ-hydroxo bridged Co(III) species (B in Scheme 2.15) [pK_{OH} = 3.26(2)]. Both these species react with the incoming ligand to form different ion associated species (I_A and I_B in Scheme 2.15), which react in the subsequent rate-determining steps (k_1 and k_2) to form presumably a ligand-substituted, mono-bridged species [(nta)(OH)Co-μ-OH-Co(nta)(L)]$^{2-}$. Values for k_2, the preferred mono-μ-hydroxy bridged substitution pathway for these reactions, vary between 6.8(2) x 10^{-4} s^{-1} (py) and 8.5(4) x 10^{-2} s^{-1} (dmap).

2.3 Conclusion

It can be seen from this chapter that there are many possibilities in the investigation of cobalt(III)-apda complexes. The isolation and characterisation of new cobalt(III)-apda complexes, with apda acting as a tri- or tetradentate ligand, by way of especially IR, ^{1}H NMR and X-ray crystallography will bring more light to the understanding of the strain in these complexes.

No kinetic studies have been undertaken on the cobalt(III)-apda complexes and very few starting complexes, intermediates and final products have been isolated. The kinetic study and isolation of these complexes would provide a lot of information on the mechanism of the substitution reactions of these complexes.

Further studies on these complexes could provide important information on the behaviour of living systems in the presence of transition metals.

3 Synthesis and identification of Co(III)-apda complexes

In this chapter…

The different water soluble cobalt(III)-apda complexes that were investigated in this study are discussed in Paragraph 3.1. The rest of this chapter focuses on the experimental approach followed in this study as well as the synthesis and characterisation of N-(2-carboxyethyl)iminodiacetic acid (apda) and different Co(III)-apda complexes by means of IR, ^{1}H NMR and UV/VIS spectral studies. An overview of the results is presented at the end of this chapter.

3.1 Introduction

It were shown in the previous chapters that the synthesis and identification of cobalt(III)-apda complexes have not yet been conclusively documented. The identification of the starting complexes and final products in this study was also vitally important to the determination of the mechanism of substitution reactions, which will be discussed in Chapter 5.

Most of the studies on apda and nta complexes (Chapter 2) relied heavily on identification with IR and UV/VIS spectroscopy. The identification of these types of complexes by IR is complicated and not always conclusive. It has been shown that the oxygen atoms of the carboxyl groups which are not bonded to the metal are hydrogen-bonded, either to the amino group of the neighbouring molecule, or to the water of crystallisation, or weakly bonded to the metal of a neighbouring complex (Nakamoto, 1963:206).

The COO–M stretching frequencies of complexes containing apda, nta and related compounds are therefore affected by coordination as well as by intermolecular interaction, making the assignment of IR stretching frequencies complicated. However, according to Nakamoto (1963:206) COO^- groups have stretching frequencies of 1650 – 1620 cm^{-1} when coordinated to metals such as cobalt(III) and stretching frequencies of 1750 – 1700 cm^{-1} when un-ionised or uncoordinated.

^1H NMR can provide important structural information, especially by investigating the signals of the acetate ring protons of apda and nta (refer to Paragraph 2.2.1). This chapter includes very informative results with regards to the identification of the different Co(III)-apda complexes by means of ^1H NMR spectra.

Previous studies (Visser *et al.*, 2002:461 and Thacker & Higginson 1975:704) have shown that Co(III)-nta complexes are soluble in water. These studies also showed that different species are formed in solution at different pH values, for example $[Co(nta)(H_2O)(OH)]^-$ and $[Co(nta)(H_2O)_2]$ at pH 7 and 2, respectively (Visser *et al.*, 2002:461). During this study, Co(III)-apda complexes were synthesised and the formation of different species in solution were investigated by all physical techniques available.

This chapter deals mainly with the synthesis of different Co(III)-apda complexes. The characterisation of these complexes with IR-, UV/VIS-, and ^1H NMR spectroscopy is also discussed in this chapter while the identification of $[Co(H_2O)_6][Co(Hapda)_2]_2H_2O$ with X-ray crystallography will be discussed in detail in Chapter 4.

Scheme 3.1 provides a schematic presentation of the formation of different cobalt(III)-apda complexes investigated in this study.

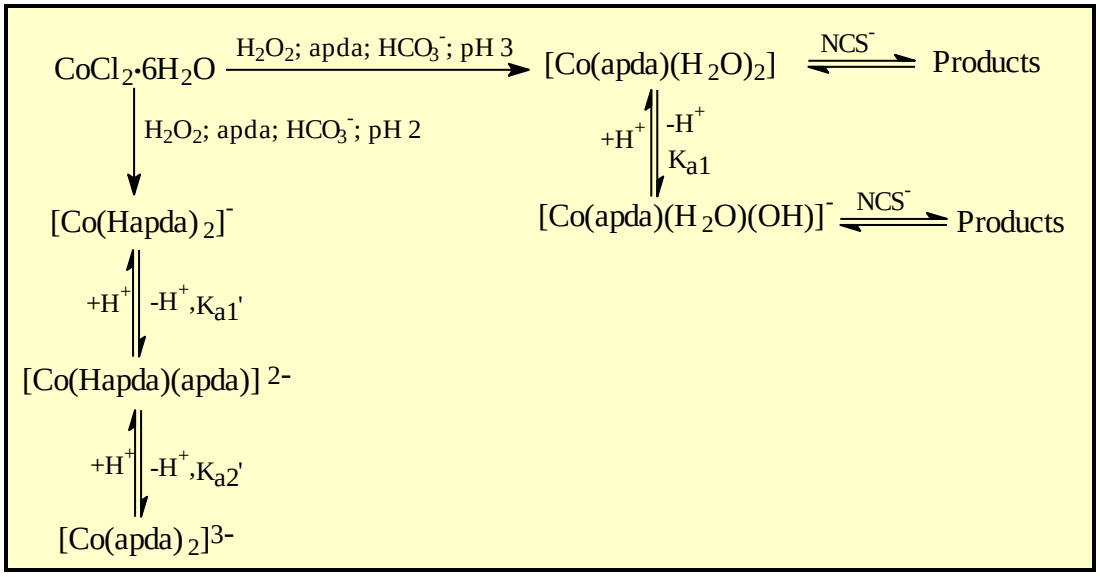

Scheme 3.1 Synthesis and reactions of cobalt(III)-apda complexes.

3.2 Apparatus and chemicals

Unless otherwise stated, all reagents were of reagent grade. All pH measurements were performed on a pH 211 microprocessor pH meter, calibrated with pH 7.01 (HI7007) and pH 4.01 (HI7004) buffer solutions, all obtained from Hanna instruments. A custom made column (25mm x 300mm) filled with Amberlite IRA 402 CL anion-exchange resin (Rohm & Haas) was used for ion-exchange chromatography. UV/VIS measurements were performed on a Cary 50 (Conc.) spectrophotometer equipped with a constant temperature cell holder (accuracy within 0.1 ºC), while infrared spectra were recorded on a Digilab FTS2000 f.t.i.r. spectrometer in the range of 4900 – 670 cm^{-1} (s = strong, sh = shoulder, w = weak). ^{1}H NMR spectra were recorded on a 300 MHz Bruker spectrometer (s = singlet, d = doublet, m = multiplet, t = triplet), using Norell 507-HP high precision NMR tubes.

3.3 N-(2-carboxyethyl)iminodiacetic acid (apda).

3.3.1 Synthesis of N-(2-carboxyethyl)iminodiacetic acid (apda).

N-(2-carboxyethyl)iminodiacetic acid (apda) was synthesised according to a method obtained from Niclós Gutiérrez (University of Granada, personal communication). Chloroacetic acid (10.84g, 115 mmol) was neutralised by adding potassium hydroxide (6.42g, 119 mmol) in a N_2 atmosphere over a period of 20 minutes at 5 ºC. β-alanin (5.0 g, 56 mmol), neutralised with potassium hydroxide (3.14 g, 56 mmol), was added to the chloroacetic acid solution. The solution was refluxed on a water bath for 5 hours under N_2 while potassium hydroxide (6.42 g, 115 mmol) was added during the first 30 minutes of heating (*ca.* 90 ºC). The solution was cooled to room temperature and the pH was adjusted to ~ 6.5 with hydrochloric acid (6 M). The solution was concentrated under vacuum (60 ºC) until potassium hydroxide crystallised. The resulting solution was then cooled to room temperature and the potassium hydroxide crystals were filtered off. The pH was adjusted to 2.5 with the aid of hydrochloric acid (6 M) and the solution was allowed to stand overnight while the N-(2-carboxyethyl)iminodiacetic acid (apda) precipitated. The precipitate was filtered and re-crystallised from water (60 ºC).

Yield: 7.69 g (67 %).
IR (υ-$_{COOH}$(cm^{-1})): 1706 (s).
^{1}H NMR (D_2O) δ: 3.08 (2 H *s*), 3.61 (2 H *d*), 3.78 (2 H *s*), 4.17 (2 H *d*).

3.3.2 IR spectrum of N-(2-carboxyethyl)iminodiacetic acid (apda).

Nakamoto (1963:206) stated that un-ionised and uncoordinated COO^- groups have stretching frequencies of 1750 – 1700 cm^{-1}. The IR spectra of the free N-(2-carboxyethyl)iminodiacetic acid (apda) (*ca.* pH 3) show a stretching frequency of 1706 cm^{-1}. This is indicative of un-ionised or uncoordinated COO^- groups as expected. The IR spectrum for the free N-(2-carboxyethyl)iminodiacetic acid (apda) is shown in Figure 3.1.

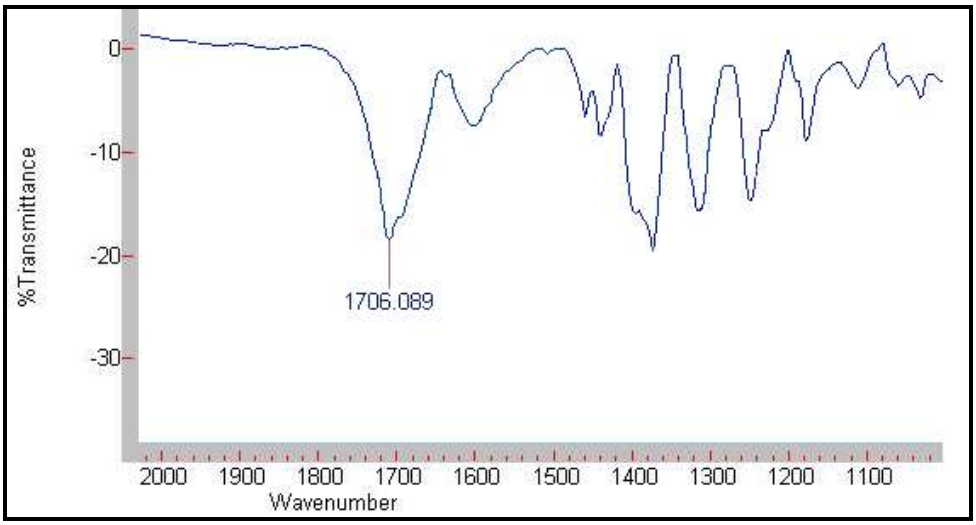

Figure 3.1 IR spectrum of the free N-(2-carboxyethyl)iminodiacetic acid (apda).

3.3.3 ^{1}H NMR spectrum of N-(2-carboxyethyl)iminodiacetic acid (apda).

The ^{1}H NMR spectrum of N-(2-carboxyethyl)iminodiacetic acid (apda) integrates for 8 protons and show two doublets and two singulets. The two doubles at 3.61 and 4.17 ppm each integrates for two protons and are assigned to the four hydrogen atoms of the propionate group. The two singulets at 3.08 and 3.78 ppm each integrates for two protons that are assigned to the two hydrogen atoms on the acetate groups of apda.

The ^{1}H NMR spectrum of N-(2-carboxyethyl)iminodiacetic acid (apda) is presented in Figure 3.2.

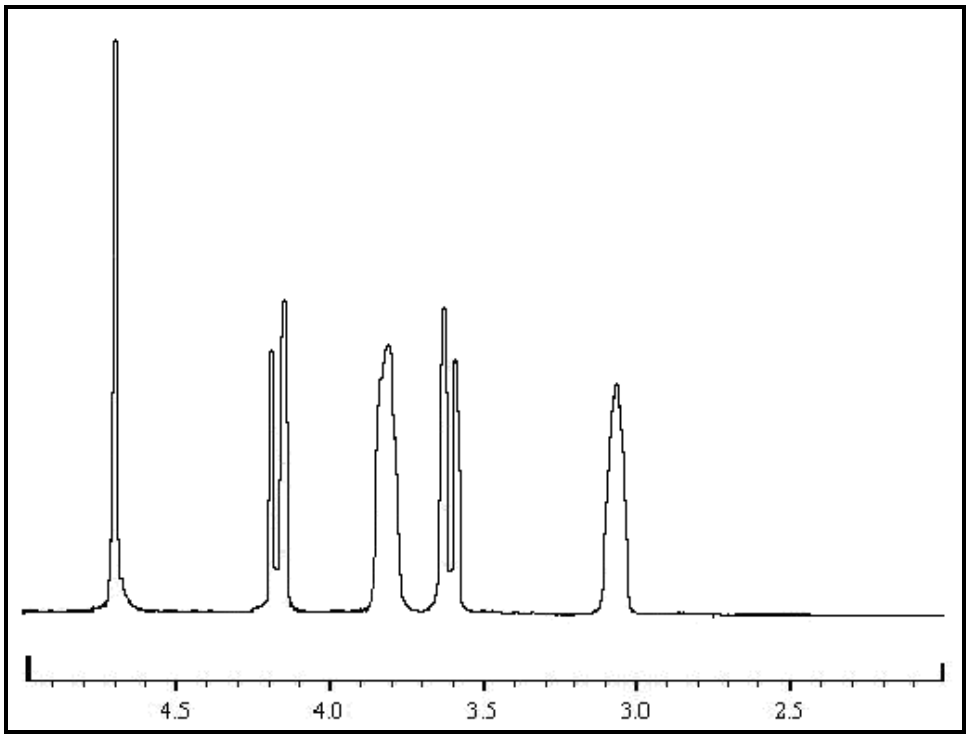

Figure 3.2 ^{1}H NMR spectrum of N-(2-carboxyethyl)iminodiacetic acid (apda).

Both the IR and ^{1}H NMR spectra, Figures 3.1 and 3.2 respectively, confirm the successful synthesis of N-(2-carboxyethyl)iminodiacetic acid (apda).

3.4 [Co(III)(apda)$(H_2O)_2$].

3.4.1 Synthesis of [Co(apda)$(H_2O)_2$].

[Co(apda)$(H_2O)_2$] was prepared similar to the method described by Tsuchiya and co-workers (1969:1886). $CoCl_26H_2O$ (5.7 g, 24.3 mmol) was added to a 25 cm^3 solution containing apda (5 g, 24.3 mmol) and $KHCO_3$ (5 g, 50 mmol). The mixture was heated on a water bath for about 1 hour. The solution was then placed on an ice bath and H_2O_2 (1 cm^3, 30 %) was added after which it was stirred for 30 minutes. The pH of the resultant solution was adjusted to 3 with perchloric acid (6 M) and stirred for another 2 hours. Ethanol (200 cm^3) was added to the mixture until precipitation occurred. The precipitate was re-dissolved in the minimum amount of water. Purple crystals separated out after 24 hours.

Yield: 3.14 g (44 %).

IR (υ-COOH(cm^{-1})): 1670 (s), 1580 (m).

^{1}H NMR (D_2O) δ: 2.57 (1 H *d*), 2.80 (2 H *m*), 3.47 (2 H *m*), 3.78 (1 H *d*), 3.97 (1 H *d*), 4.18 (1 H *d*).

UV/VIS (λ_{max} (nm)(ε, M^{-1} cm^{-1})): 209.9 (1.48 x 10^4), 240.0 (1.29 x 10^4), 400.0 (1.07 x 10^2), 559.9 (1.63 x 10^2).

3.4.2 IR spectrum of [Co(apda)(H_2O)$_2$].

It was mentioned earlier (Paragraph 3.1) that the use of IR techniques as identification tool for these types of complexes are complicated and not always conclusive, but it is possible to derive some structural properties from the spectra.

In the case of [Co(apda)(H_2O)$_2$], the spectrum shows stretching frequencies of 1670 and 1580 cm^{-1}. The stretching frequency at 1670 cm^{-1} appears as a shoulder with the strongest peak at 1580 cm^{-1}. Both these values are indicative of COO^- groups coordinated to a metal centre such as Co(III). The stretching frequencies at 1670 and 1580 cm^{-1} obtained for [Co(apda)(H_2O)$_2$] correlate very well to the values, 1679 and 1584 cm^{-1}, observed by Tsuchiya and co-workers (1969:1886) for their Co(III) – apda complex. The Co(III) – apda complex prepared by Tsuchiya and co-workers was later conclusively characterised by Gladkikh *et al.* (1997:1346). Their X-ray crystallographic study indicated that the complex is in fact the *cis* – diaqua [Co(apda)(H_2O)$_2$] complex.

The same results were observed by Gonzalez Perez *et al.* (1991:243) in their cobalt(II)-apda dimer, [Co(H_2O)$_6$][Co$_2$(apda)$_2$(H_2O)$_2$]4H_2O, in which apda acts as a tetradentate ligand. They observed a stretching frequency of 1680 cm^{-1}, appearing as a shoulder with the strongest peak at a stretching frequency of 1580 cm^{-1}. Gonzalez Perez and co-workers stated that both these stretching frequencies were due to the anti-symmetric stretching mode of the coordinated carboxylate groups.

The IR spectrum obtained for the [Co(apda)(H_2O)$_2$] complex is given in Figure 3.3.

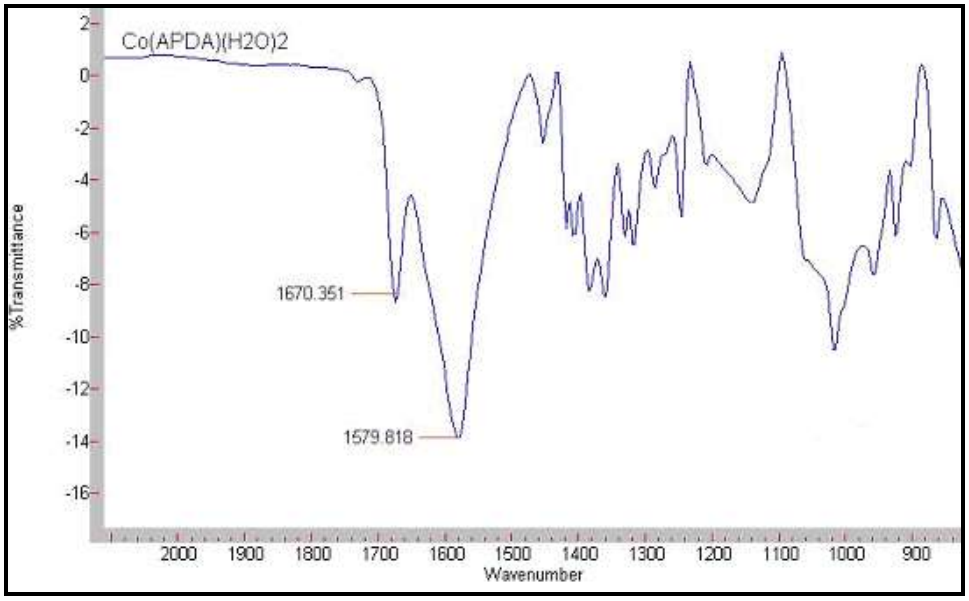

Figure 3.3 IR spectrum of [Co(apda)(H_2O)$_2$].

3.4.3 UV/VIS spectral studies of [Co(apda)(H_2O)$_2$].

The [Co(apda)(H_2O)$_2$] crystals were dissolved in water (pH *ca.* 4) and the UV/VIS spectrum was recorded (209.9 (w), 240.0 (w), 400.0 (s), 559.9 (s)). Unfortunately, no UV/VIS spectrum for the [Co(apda)(H_2O)$_2$] complex was published by either Tsuchiya *et al.* (1969:1886) or Gladkikh *et al.* (1997:1346). [Co(apda)(H_2O)$_2$] crystals were again dissolved in water (pH *ca.* 4) and the UV/VIS spectrum was recorded (Figure 3.4) in order to determine the influence of H^+ ions on the Co(III)-apda system. A few drops of HCl (1.0 M) were added to this solution (pH *ca.* 1) and the spectrum was again recorded (Figure 3.4). No change in absorption maxima at 400 or 560 nm was observed.

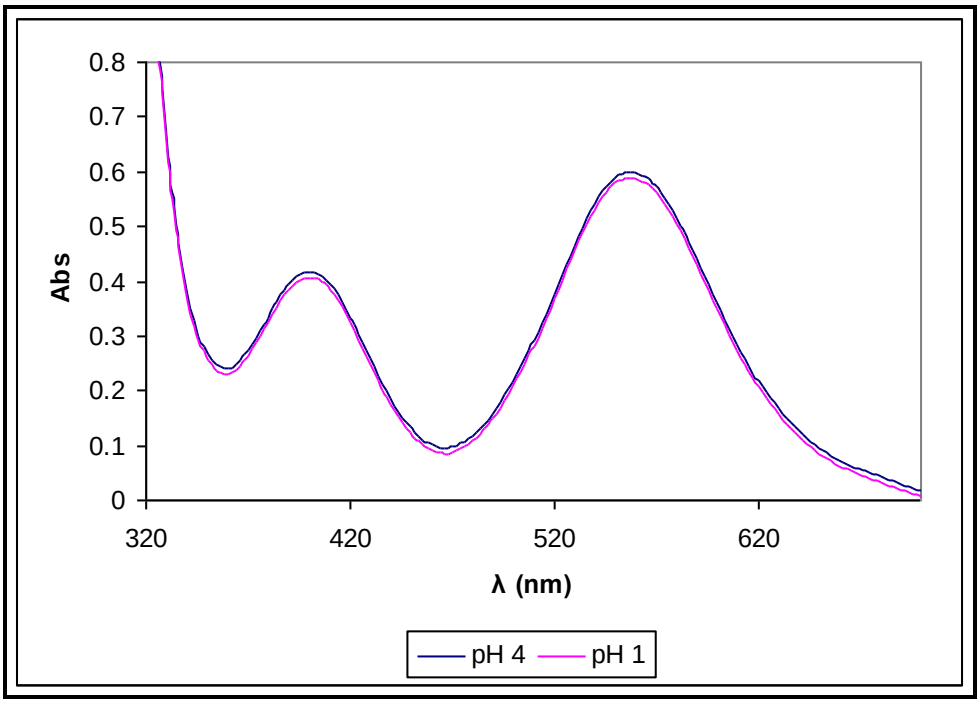

Figure 3.4 UV/VIS spectra of [Co(apda)(H_2O)$_2$] at pH 4 and pH 1.

A fresh solution of [Co(apda)(H_2O)$_2$] was again prepared and its spectrum recorded (Figure 3.5). KOH (1.0 M) was used to adjust the pH to 5 and the spectrum was recorded. This procedure was repeated 3 times and the spectrum was recorded at each pH unit until the pH reached a value of 7 (Figure 3.5). The absorption maximum at 559 nm decreased and the maximum shifted to 563 nm. These results clearly indicate the formation of a new species in solution, presumably [Co(apda)(H_2O)(OH)]$^-$.

At a pH > 7, a continuous change in spectrum was observed, possibly due to dimer formation, it was therefore decided to keep the reaction conditions between pH 2 – 7 in order to avoid complication by competitive reactions. Visser and co-workers (2002:461) also observed a continuous change in spectrum for their [Co(nta)(H_2O)$_2$] complex at a pH > 7. They attributed these changes to the formation of the Co(III)-nta dimer.

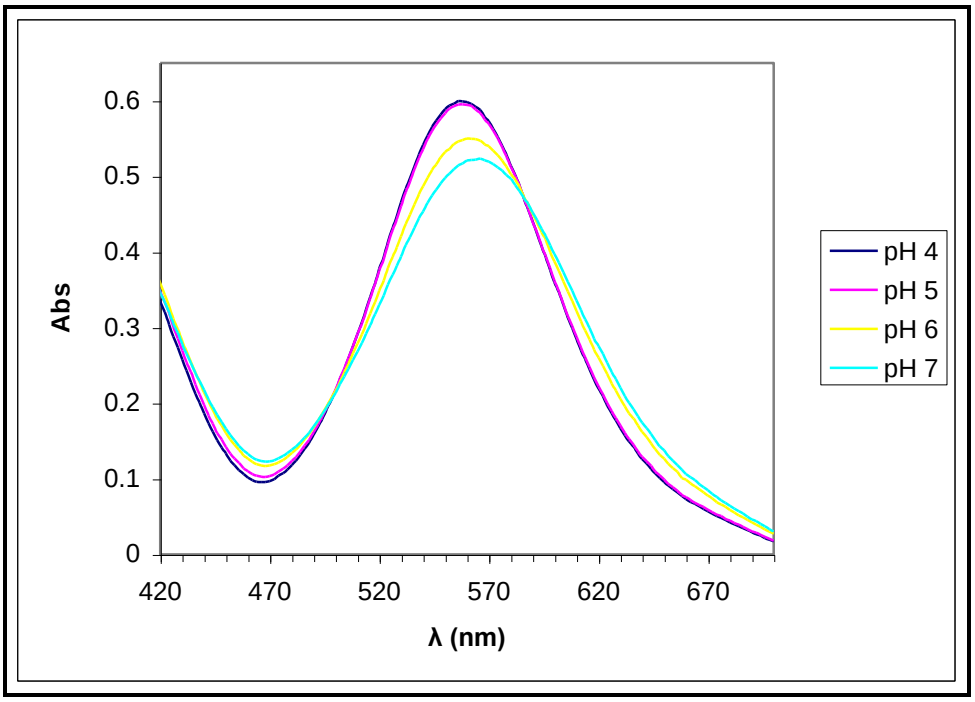

Figure 3.5 UV/VIS spectral change of [Co(apda)(H_2O)$_2$] on addition of KOH.

A fresh solution of [Co(apda)(H_2O)$_2$] was prepared and its spectrum recorded (Figure 3.6). KOH (1.0 M) was added to this solution until the pH reached 7.5 and the spectrum was recorded (Figure 3.6). This resulted in the immediate shift in the absorption maximum at 559 nm to 563 nm with a decrease in absorption. HCl (1.0 M) was used to change the pH (*ca.* 4) and the spectrum was again recorded (pH 4 (2) in Figure 3.6). This resulted in the immediate change in absorption maximum at 563 nm back to the original spectrum at low pH (*ca.* 4) (see Figure 3.6). These results indicate a reversible protonation/deprotonation equilibrium between pH 4 and 7.

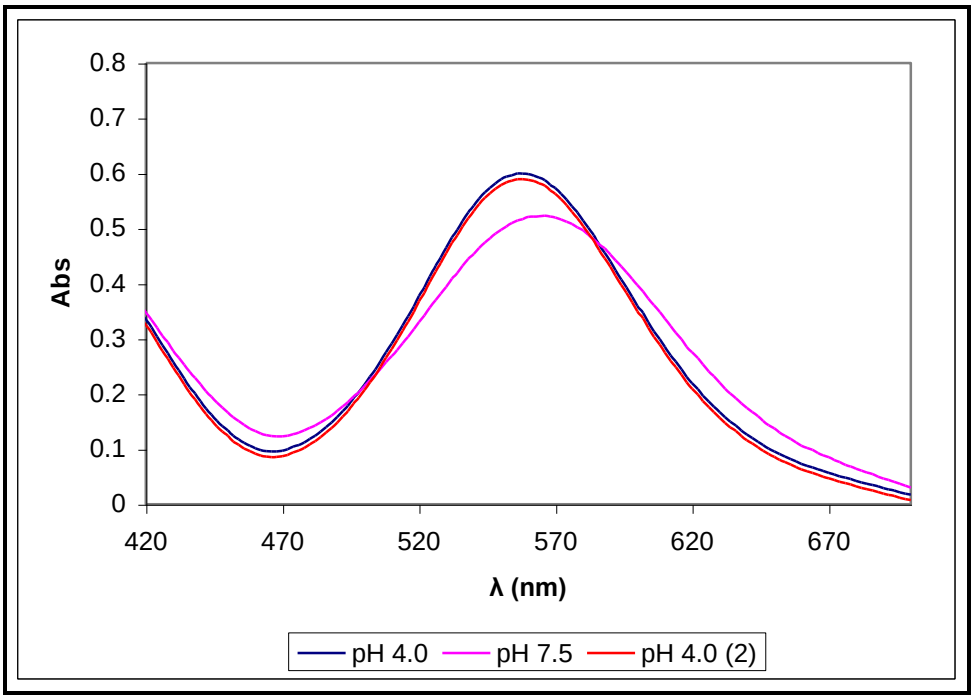

Figure 3.6 UV/VIS spectra of different Co(III)-apda species in solution.

A possible explanation for these observed changes in UV/VIS spectra is an acid dissociation reaction presented in Scheme 3.2. The determination of the acid dissociation constant, K_{a1}, is discussed in Chapter 5.

$$[Co(apda)(H_2O)_2] \underset{+\,H^+}{\overset{K_{a_1},\,-\,H^+}{\rightleftharpoons}} [Co(apda)(OH_2)(OH)]^-$$

Scheme 3.2 Acid dissociation reaction of $[Co(apda)(H_2O)_2]$.

Similar results were found by Visser and co-workers (2002:461) for the pH dependence of $[Co(nta)(H_2O)_2]$. The acid dissociation constant of $[Co(nta)(H_2O)_2]$, K_{a1} (Scheme 3.3), was determined spectrophotometrically as 6.52(2).

$$[Co(nta)(H_2O)_2] \underset{+\,H^+}{\overset{K_{a_1},\,-\,H^+}{\rightleftharpoons}} [Co(nta)(OH_2)(OH)]^-$$

Scheme 3.3 Acid dissociation reaction of $[Co(nta)(H_2O)_2]$.

3.4.4 ^{1}H NMR spectrum of $[Co(apda)(H_2O)_2]$.

The investigation of $[Co(nta)(gly)]^-$ and $[Co(nta)(l\text{-ala})]^-$ with ^{1}H NMR by Koine *et al.* (1969:1583) provided new possibilities to the identification of Co(III)-nta and related complexes.

The ^{1}H NMR spectra can be used as follows to gain evidence regarding the structures of these complexes: as mentioned in Paragraph 2.2.1, the protons of a specific G ring of nta (H_{G1a} and H_{G1b} in Figure 3.7) are non-equivalent if L = L', while the protons of two different G rings (e.g. H_{G2a} and H_{G1a} in Figure 3.7) are equivalent under the same conditions for L and L'. This results in two doublets with an AB pattern that centres between 3.9 and 4.5 ppm. A singlet in the same region is assigned to the equivalent protons of the remaining acetate ring (R ring), which is co-planar with the bidentate or other ligands. Complexes in which all the ring protons of nta and related ligands like apda are non-equivalent (L ≠ L') will exhibit totally different spectra than the above.

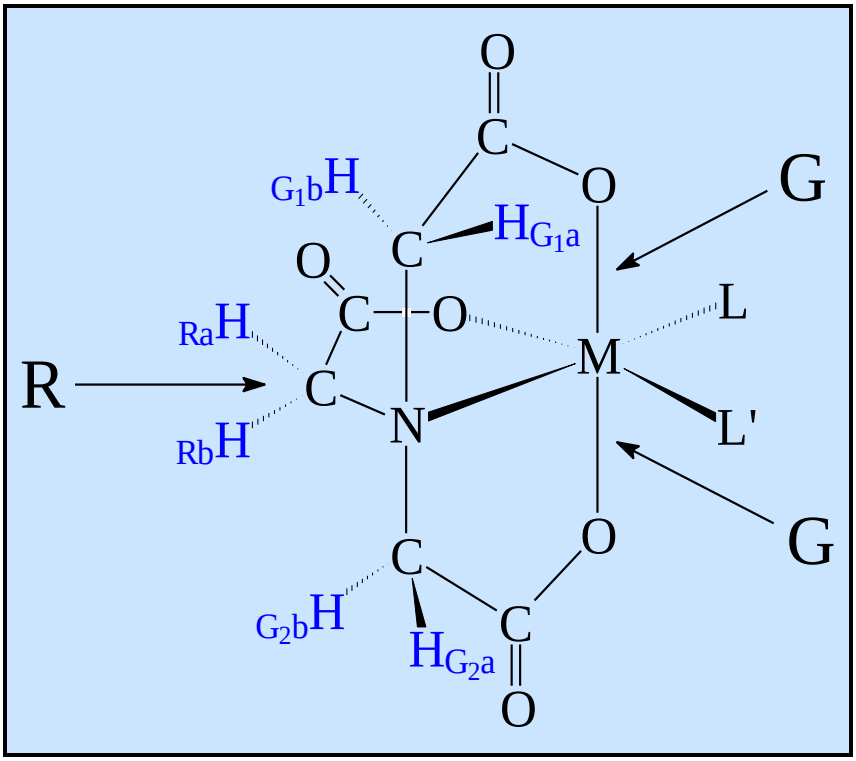

Figure 3.7 Glycinato rings in Co(III)-nta complexes.

As mentioned in Chapter 2, an AB pattern is the phenomenon which is observed when protons are in different chemical environments yielding a doublet that is again split into a doublet by spin-spin interaction, for a total of four peaks of similar intensity.

An example of an AB Pattern occurring in ^{1}H NMR spectra is presented in Figure 3.8.

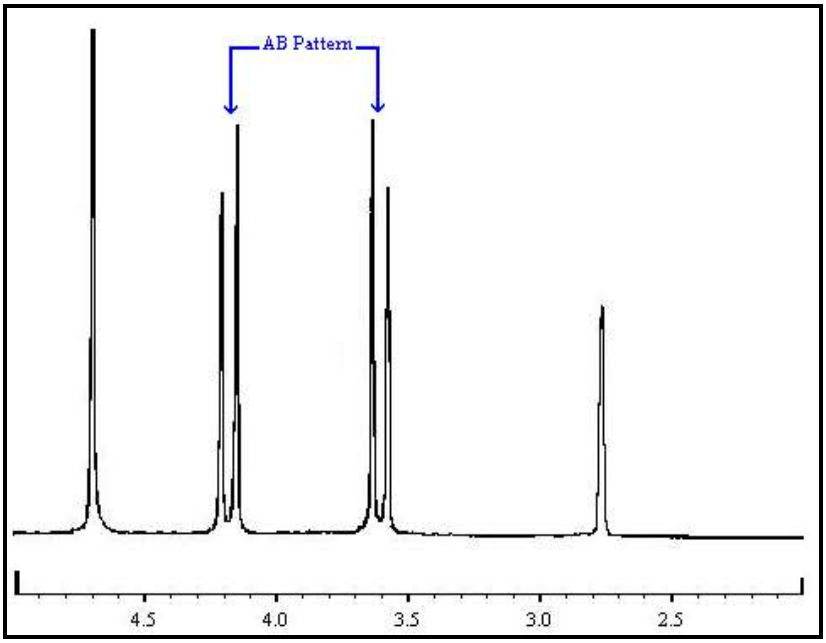

Figure 3.8 An example of an AB Pattern in ^{1}H NMR Spectra.

The same method of identification can be applied to metal complexes with apda where the protons of two glycinato G (equatorial) rings (e.g. H_{G2a} and H_{G1a} in Figure 3.9) are equivalent if L = L' and the longer propionato ring is situated in the R (out-of-plane) position. This would result in two doublets with an AB pattern and two triplets. The two triplets are assigned to the remaining protons on the propionato ring (R ring), which is co-planar with the bidentate or other ligands. Complexes where the propionato chain is in the G position or where L ≠ L' would result in all the ring protons of apda to be non-equivalent. These complexes will exhibit totally different spectra than the above-mentioned pattern.

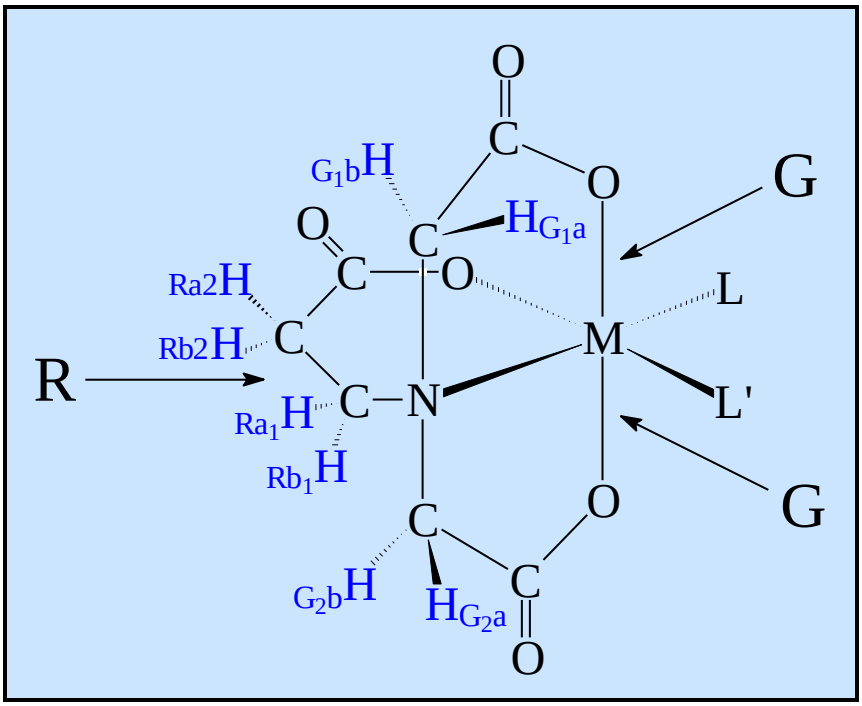

Figure 3.9 Glycinato and propionato rings in Co(III)-apda complexes.

The ^{1}H NMR spectrum (see Figure 3.10) obtained for [Co(apda)(H_2O)$_2$] integrates for eight apda protons but does not exhibit the AB pattern and two triplets one would expect if L = L' = H_2O (Figure 3.9) and with the propionato ring in the R position. All eight the apda protons are non-equivalent, leading to four distinguishable doublets, each integrating for one proton, and two multiplets, each integrating for two protons, occurring in the 2.5 – 4.2 ppm region. These findings indicate that the propionato ring must be situated in a G position since L = L' = H_2O.

These results are corroborated by Gladkikh *et al.* (1997:1346) in their X-ray crystallographic study on [Co(apda)(H_2O)$_2$]. Their results confirmed that the propionato ring occupies the G position in the solid state. The ^{1}H NMR spectrum for [Co(apda)(H_2O)$_2$] is shown in Figure 3.10.

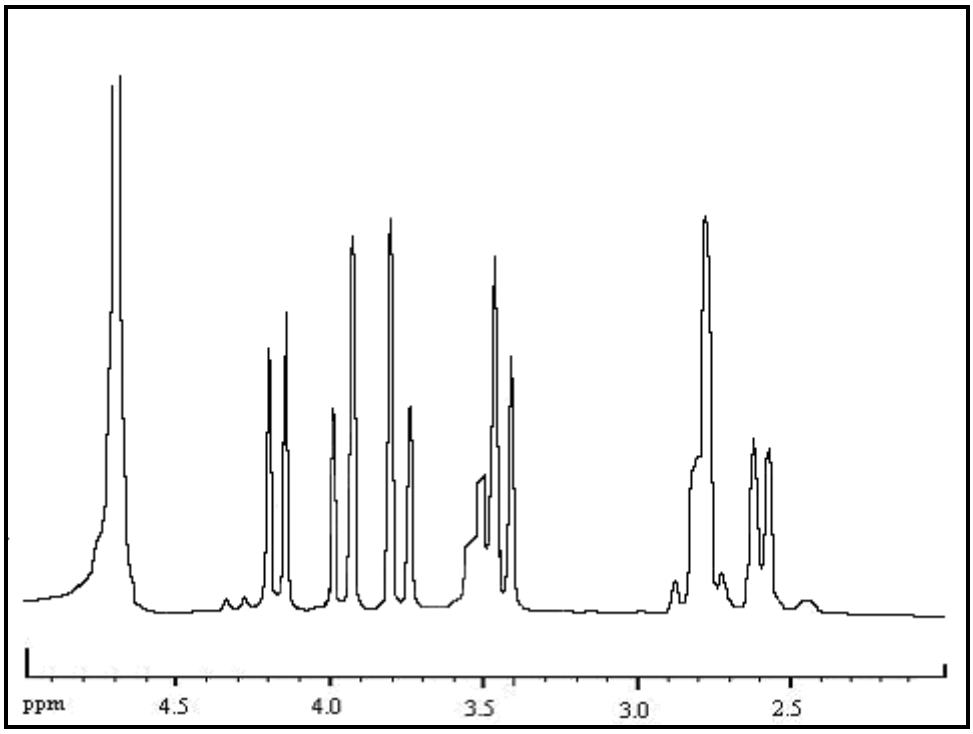

Figure 3.10 ^{1}H NMR spectrum of [Co(apda)(H_2O)$_2$].

The IR results presented in Paragraph 3.4.2 and the ^{1}H NMR results presented in the preceding paragraph confirms the successful synthesis of [Co(apda)(H_2O)$_2$].

3.5 [Co(II)(H_2O)$_6$][Co(III)(Hapda)$_2$]$_2$$H_2O$

3.5.1 Synthesis of [Co(H_2O)$_6$][Co(Hapda)$_2$]$_2$$H_2O$.

$CoCl_2 6H_2O$ (5.7 g, 24.3 mmol) was added to a 25 cm^3 solution containing apda (5.0 g, 24.3 mmol) and $KHCO_3$ (5.0 g, 50 mmol). The mixture was heated on a water bath for about 1 hour. The solution was removed from the water bath and placed on an ice bath. H_2O_2 (1 cm^3, 30 %) was added after which it was stirred for about 20 minutes. The pH of the resultant solution was adjusted to 2 with HCl (conc.) and stirred at room temperature for 24 hours. Ethanol (200 cm^3) was added to the mixture until precipitation occurred. The precipitate was washed with ice water and then re-dissolved in hot water *ca.* 60 ºC after which pink crystals, suitable for X-ray crystallography, separated (10 hours).

It was found however, that a mixture of $[Co(H_2O)_6][Co(Hapda)_2]_2H_2O$ and $[Co(apda)(H_2O)_2]$ precipitates during the synthesis of either of these two complexes if the pH is 2.5.

Due to interference of the $[Co(II)(H_2O)_6]^{2+}$ cation no ^1H NMR data could be recorded.

Yield: 1.67 g (18 %).
IR (υ-$COOH$ (cm^{-1})): 1705(m), 1597(s).

3.5.2 IR spectrum of $[Co(H_2O)_6][Co(Hapda)_2]_2H_2O$.

The spectrum obtained for the $[Co(H_2O)_6][Co(Hapda)_2]_2H_2O$ complex shows stretching frequencies at 1705 and 1597 cm^{-1}. These values indicate both uncoordinated and coordinated COO^- groups, respectively. It was concluded that apda does not act as a tetradentate ligand in $[Co(H_2O)_6][Co(Hapda)_2]_2H_2O$. The stretching frequency for the uncoordinated COO^- group corresponds very well to the stretching frequency of 1706 cm^{-1} which was observed for the free N-(2-carboxyethyl)iminodiacetic acid (apda) (Figure 3.1).

The IR spectrum found for the $[Co(H_2O)_6][Co(Hapda)_2]_2H_2O$ complex is shown in Figure 3.11.

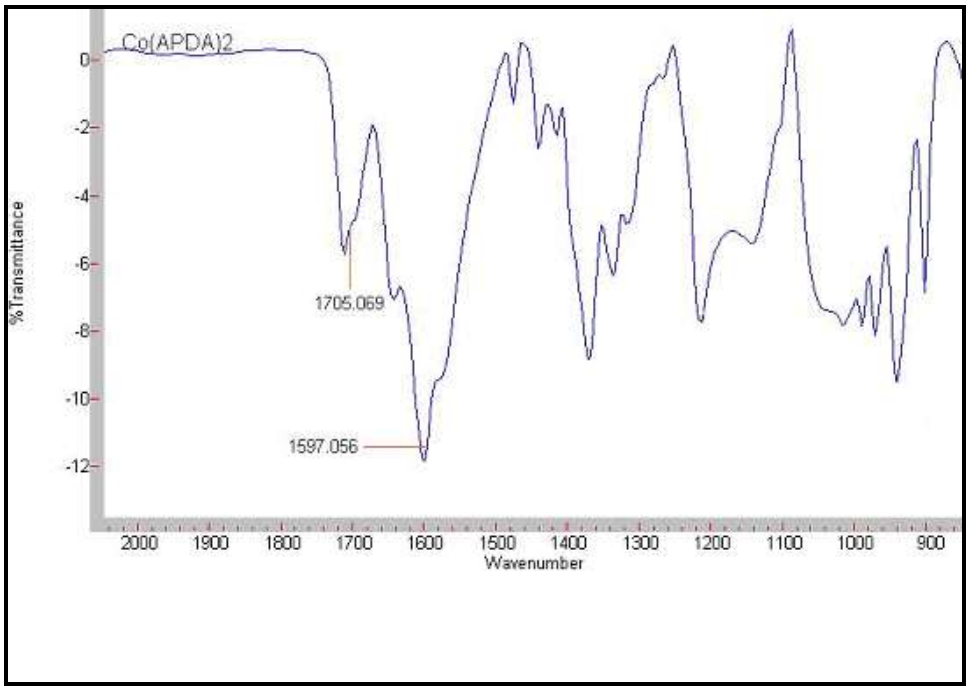

Figure 3.11 IR spectrum of $[Co(H_2O)_6][Co(Hapda)_2]_2H_2O$.

The structure of this complex was confirmed by an X-ray crystallographic study, which is presented in Chapter 4.

3.6 $Na[Co(III)(Hapda)_2]xH_2O$.

3.6.1 Synthesis of $Na[Co(Hapda)_2]xH_2O$.

Anion exchange resin was used in order to separate the $[Co(II)(H_2O)_6]^{2+}$ counter ion from the anionic species (Refer to Chapter 4), $[Co(Hapda)_2]^-$. An ion-exchange column was filled with sufficient strong-base anion-exchange resin to give a 20 cm column. The column was washed with NH_3 (6 M, 50 cm^3) followed by water (100 cm^3) and HCl (2 M, 100 cm^3). The column was washed with a sufficient amount of water until the eluent had a pH of 1.5 – 2.0. $[Co(II)(H_2O)_6][Co(III)(Hapda)_2]_2H_2O$ (3.00 g, 2.7 mmol) was introduced into the column after which it was washed with water (200 cm^3). $Na[Co(Hapda)_2]xH_2O$ was eluted with NaCl (2 M, 150 cm^3). The solution was

evaporated until a pink precipitate formed. The precipitate was filtered and washed with ice cold water (50 cm^3). The precipitate was re-crystallised from hot water (*ca.* 60 ºC).

IR (υ-COOH(cm^{-1})): 1702(s), 1609(m).
^{1}H NMR (D_2O) δ: 2.77 (4 H *t*), 3.59 (4 H *d*), 3.74 (4 H *t*), 4.18 (4 H *d*).
UV/VIS (λ_{max} (nm)(ε, M^{-1} cm^{-1})): 230.0 (1.50 x 10^4), 365.1 (8.4 x 10^1), 515.0 (5.6 x 10^1).

3.6.2 IR spectrum of $Na[Co(Hapda)_2]xH_2O$.

The spectrum obtained for the $Na[Co(Hapda)_2]xH_2O$ complex (Figure 3.12) show stretching frequencies at 1701 and 1608 cm^{-1}. These values are also indicative of uncoordinated and coordinated COO^- groups, respectively. Only minor differences between the COO^- stretching frequencies of $Na[Co(Hapda)_2]xH_2O$ and $[Co(H_2O)_6][Co(Hapda)_2]_2H_2O$ is observed. The stretching frequency for the uncoordinated COO^- group, 1701 cm^{-1} (Figure 3.12), also corresponds very well to the stretching frequency of 1706 cm^{-1} which was observed for the free N-(2-carboxyethyl)iminodiacetic acid (apda) (Figure 3.1).

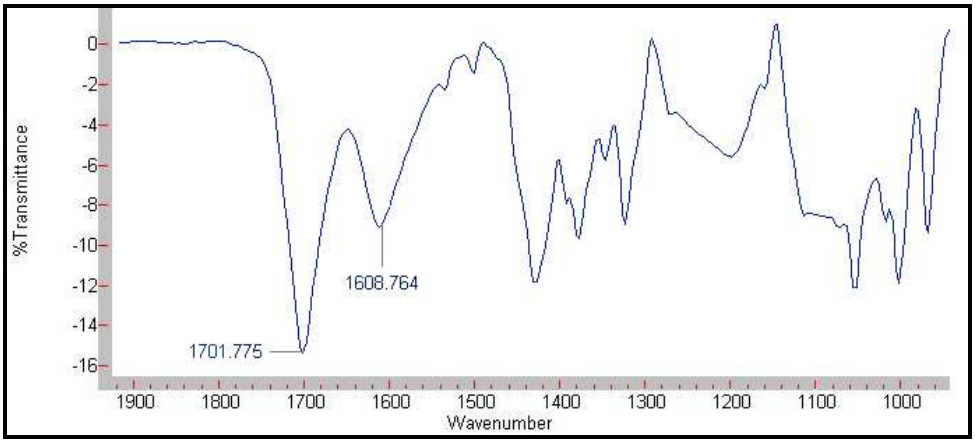

Figure 3.12 IR spectrum of $Na[Co(Hapda)_2]xH_2O$.

3.6.3 UV/VIS spectral studies of $Na[Co(Hapda)_2]xH_2O$.

$Na[Co(Hapda)_2]xH_2O$ crystals were dissolved in water (pH *ca.* 5.5) and the UV/VIS spectrum was recorded which showed peaks at 230.0 and 515.0 nm and a shoulder at 365.1 nm.

In a second experiment, $Na[Co(Hapda)_2]xH_2O$ crystals were dissolved (pH *ca.* 5.5) and the UV/VIS spectrum was recorded (Figure 3.13). The pH was adjusted to 1 (HCl, 1.0 M) and the spectrum was recorded (Figure 3.13). The spectrum shows an immediate decrease in absorption value for both the absorption maximum at 515 nm and the shoulder at 365 nm. The pH was again adjusted to 5.5 (KOH, 1.0 M) and the spectrum was recorded (pH 5.5 (2) in Figure 3.13). This resulted in the immediate increase in absorption for both the absorption maximum at 515 nm and the shoulder at 365 nm, to approximately its original position at pH 5.5. These results indicate a reversible reaction in the pH range investigated.

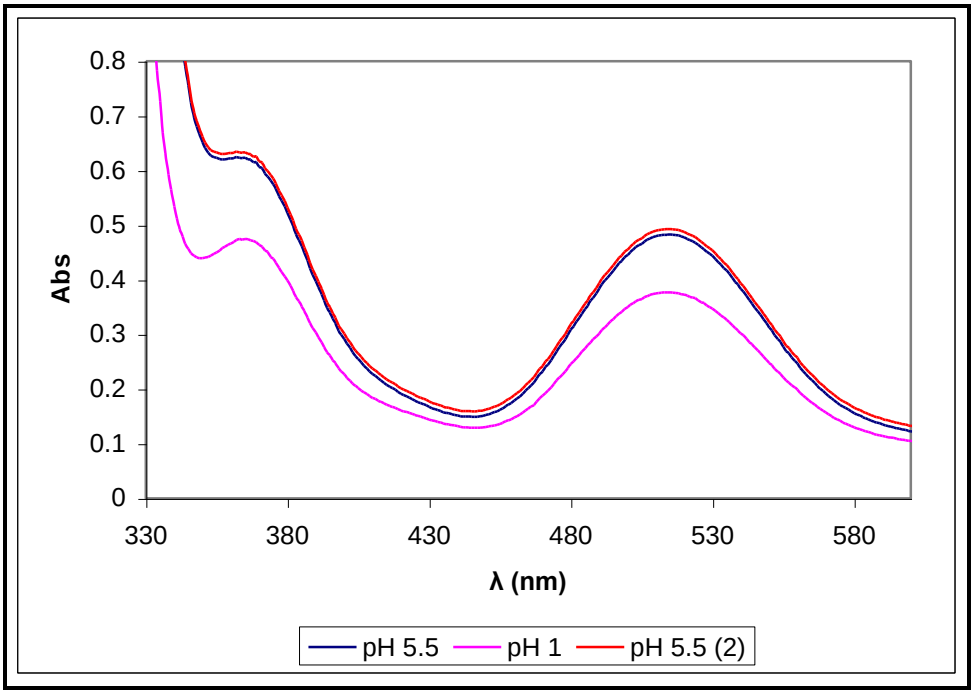

Figure 3.13 UV/VIS spectra of different Co(III)-apda species in solution.

No change in absorption spectrum was observed when the pH was kept at one over time, indicating that the species formed at pH 1 is stable for several hours. The UV/VIS spectrum obtained for the $Na[Co(Hapda)_2]xH_2O$ complex in solution at pH 1 (Figure 3.13) corresponds very well to the UV/VIS spectrum obtained from the reaction solution of $[Co(H_2O)_6][Co(Hapda)_2]_2H_2O$ (Paragraph 3.5.1) and $Na[Co(Hapda)_2]xH_2O$ (Paragraph 3.6.1) at pH 2. These results indicate that $[Co(Hapda)_2]^-$ exist in solution at low pH (*ca.* 1) but that a new species are formed at higher pH (*ca.* 5) (Scheme 3.4).

$$Na[Co(Hapda)_2]\cdot xH_2O \xrightarrow[H_2O]{\text{Dissolved in}} \underset{\text{pH 5.5}}{\text{new species}} \xrightarrow{HCl} \underset{\text{pH 2}}{[Co(Hapda)_2]^-}$$

Scheme 3.4 Co(III)-apda species in solution.

A fresh solution of this complex was again prepared and its spectrum was recorded (Figure 3.14). HCl (1.0 M) was used to adjust the pH to 5 and the spectrum was again recorded. This procedure was repeated 4 times and the spectrum was recorded after each adjustment of pH, until the pH reached a value of 1 (Figure 3.14).

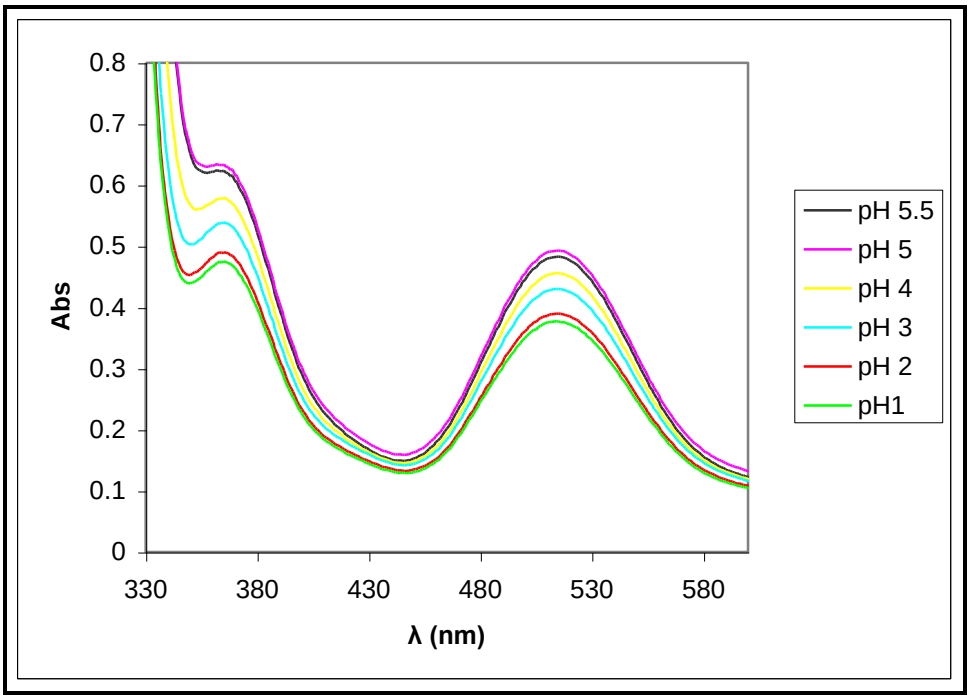

Figure 3.14 UV/VIS spectral change of $Na[Co(Hapda)_2]xH_2O$ on addition of HCl.

The successive scans (Figure 3.14) indicate an increase of the absorption maximum at 265 nm between pH 5 and 1. It will be shown in Chapter 5 that the pH dependence observed in the preceeding paragraph is probably due to the protonation/deprotonation equilibrium of the uncoordinated propionate groups of apda (Scheme 3.5).

$$[Co(Hapda)_2]^- \underset{+ H^+}{\overset{- H^+, K_{a1}'}{\rightleftharpoons}} [Co(apda)(Hapda)]^{2-} \underset{+ H^+}{\overset{- H^+, K_{a2}'}{\rightleftharpoons}} [Co(apda)_2]^{3-}$$

Scheme 3.5 Acid dissociation reaction of $[Co(Hapda)_2]^-$ and $[Co(apda)(Hapda)]^{2-}$.

3.6.4 ^{1}H NMR spectrum of $Na[Co(Hapda)_2]xH_2O$.

The ^{1}H NMR spectrum obtained for $Na[Co(Hapda)_2]xH_2O$ shows two doublets with an AB pattern and two triplets, all integrating for four protons. The two doublets and one of the triplets are in the 3.4 – 4.1 ppm region, while the other triplet occurs at 2.77 ppm. The AB pattern is the result of coupling between the eight protons on the coordinated glycinate rings, as discussed in Paragraph 3.4.4. The possible explanation for the second triplet occurring in a different region than the two doublets is that the longer propionato ring is protonated and no longer bonded to the cobalt centre. This results in the shifting of the H_{Ra2} and H_{Rb2} triplet to a value of 2.77 ppm.

The same pattern of peaks were observed by Obodovskaya *et al.* (1992:295) in their ^{1}H NMR study on $[Co(dien)(Hapda)]ClO_4$ in which apda acts as a tridentate ligand (refer to Figure 2.5). The spectrum obtained for $[Co(dien)(Hapda)]ClO_4$ shows two doublets with an AB pattern and two triplets all integrating for two protons. The two doublets and one of the triplets occur in the 3.5 – 4.2 ppm region while the other triplet occurs at 3.0 ppm. The two doublets were assigned to the protons on the coordinated glycinate rings as discussed in Paragraph 3.4.4. The two triplets were assigned to the four protons on the uncoordinated propionate group. The ^{1}H NMR spectrum obtained for $Na[Co(Hapda)_2]xH_2O$ is shown in Figure 3.15.

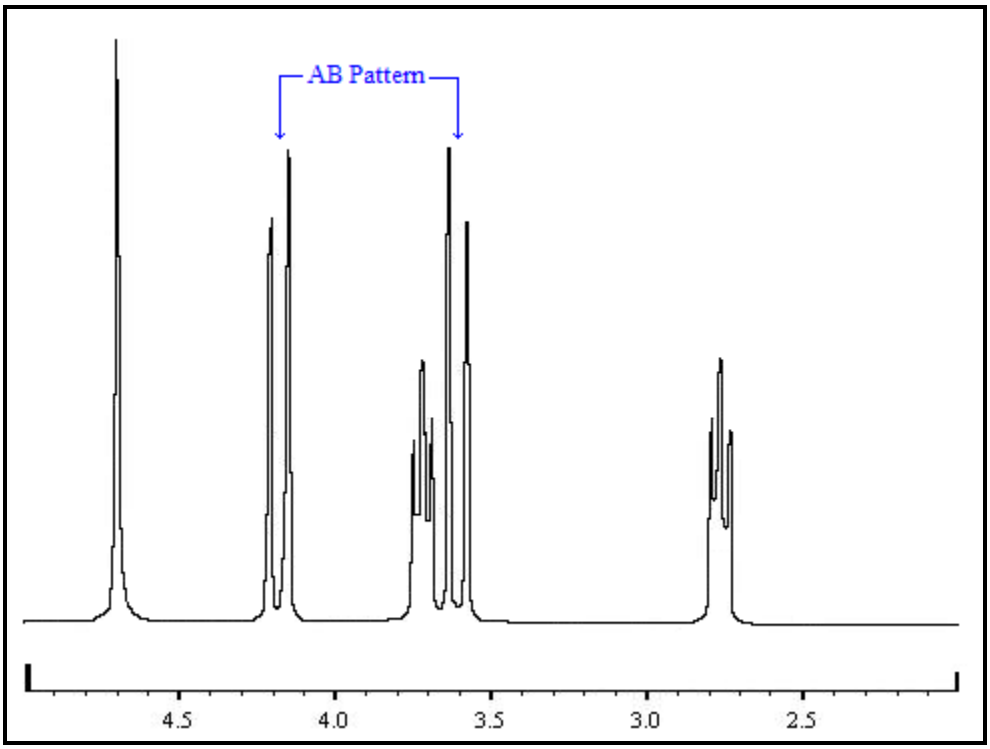

Figure 3.15 ^{1}H NMR spectrum for Na[Co(Hapda)$_2$]xH_2O.

3.7 Conclusion

It can be seen from these discussions that ^{1}H NMR data perhaps provide a better synthetic identification tool for Co(III)-apda complexes than IR data.

As mentioned earlier, [Co(apda)(H_2O)$_2$] is synthesised at a pH between 2.5 and 3.5 while [Co(H_2O)$_6$][Co(Hapda)$_2$]$_2H_2O$ is synthesised at a pH between 1.5 and 2.5. When comparing the UV/VIS spectra of these complexes at pH 1 (Figure 3.4), it can be seen that the spectra are totally different. The same was found true for the UV/VIS spectra at pH 5. These results indicate that [Co(apda)(H_2O)$_2$] does not revert to [Co(H_2O)$_6$][Co(Hapda)$_2$]$_2H_2O$ at pH 1.

It was also shown that [Co(apda)(H_2O)$_2$] can easily be prepared, which will prove very useful in the investigation of the mechanism of substitution reactions of this complex (Thacker & Higginson, 1975:704 and Visser *et al.*, 2002:461).

Synthesis and identification

The Co(III)-apda complexes presented in Scheme 3.1 were successfully characterised by means of ^{1}H NMR, IR and UV/VIS spectra. The findings in this chapter are corroborated by the X-ray crystallographic study of the $[Co(H_2O)_6][Co(Hapda)_2]_2H_2O$ complex in the next chapter, as well as the kinetic study on Co(III)-apda complexes in Chapter 5.

4 X-ray crystallography

In this chapter…

An introduction to the identification of cobalt(III)-apda and related complexes by means of X-ray crystallography is given in Paragraph 4.1, while a detailed discussion on the experimental methods and reagents used is presented in Paragraph 4.2. This chapter focuses on the characterisation of $[Co(H_2O)_6][Co(Hapda)_2]_2H_2O$ *by means of X-ray crystallography. A comparative study with previous Co(III)-apda and related complexes, which were also characterised with X-ray crystallography, is presented at end of this chapter (Paragraph 4.4).*

4.1 Introduction

There are very few examples of crystal structure determinations of Co(III)-apda complexes available in the literature. It was shown in Chapter 2 that the synthesis and identification of cobalt(III)-apda complexes have not yet been conclusively documented. The identification of starting complexes as well as the final products is also vitally important for the kinetic study that was part of this study to help with the determination of the mechanisms of these substitution reactions. The synthesis of different Co(III)-apda complexes as well as the characterisation of these complexes with IR-, UV/VIS-, and ^{1}H NMR spectroscopy were discussed in detail in Chapter 3.

It was shown in previous studies on Co(III)-apda and related complexes (Gladkikh *et al.* 1997:1346, Visser *et al.* 2001:175 and Obodovskaya *et al.* 1992:295) that X-ray crystallography provides very reliable structural information regarding these complexes. X-ray crystallography is an experimental technique that exploits the fact that X-rays are diffracted by crystals. X-rays have the proper wavelength (Å $\approx$ 1 x 10^{-8} cm) to be

scattered by the electron cloud of an atom of comparable size. Based on the diffraction pattern obtained from X-ray scattering off the periodic assembly of molecules or atoms in the crystal, the electron density can be reconstructed. Additional phase information must be extracted either from the diffraction data or from supplementing diffraction experiments to complete the reconstruction of the molecule or crystal composition. A model is then progressively built into the experimental electron density, refined against the data and a very accurate molecular structure is obtained for the compound investigated.

As mentioned earlier, the different bonding modes of apda (Figure 4.1) was illustrated by Uehara *et al.* (1968:2385) in a comprehensive study on Cr(III)–apda complexes. According to their study, apda acts as either a tri- or a tetradentate ligand. This was also observed in Co(III)-apda complexes with apda acting as a tetradentate ligand in $[Co(apda)(H_2O)_2]$ (Gladkikh *et al.* 1997:1346), while acting as a tridentate ligand in $[Co(dien)(Hapda)]ClO_4$ (Obodovskaya *et al.* 1992:295) (refer to Paragraph 2.2.1).

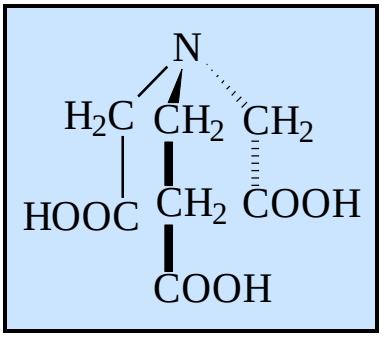

Figure 4.1 N-(2-carboxyethyl)iminodiacetic acid (apda).

This chapter deals mainly with the detailed crystal structure determination of $[Co(H_2O)_6][Co(Hapda)_2]_2H_2O$. The synthesis of $[Co(H_2O)_6][Co(Hapda)_2]_2H_2O$ was presented in Chapter 3. This Co(III)-apda complex was synthesised from equi molar amounts of $CoCl_26H_2O$ and N-(2-carboxyethyl)iminodiacetic acid (apda) (refer to Paragraph 3.5.1).

The IR spectrum obtained for the $[Co(H_2O)_6][Co(Hapda)_2]_2H_2O$ complex (refer to Paragraph 3.5.2) showed stretching frequencies at 1705 and 1597 cm^{-1}. These values indicated both uncoordinated and coordinated COO^- groups, respectively.

The ^1H NMR spectrum obtained for $Na[Co(Hapda)_2]xH_2O$ (refer to Paragraph 3.6.4) shows two doublets with an AB pattern and two triplets. The ^1H NMR spectrum also indicates that apda acts as a tridentate ligand and that the longer propionato ring is protonated and no longer bonded to the cobalt centre. The atoms occupying the other three positions in the Co(III) coordination sphere have up to this point not yet been established.

In the case of $[Co(apda)(H_2O)_2]$, (Scheme 4.1) the spectrum shows stretching frequencies of 1670 and 1580 cm^{-1} (refer to Paragraph 3.4.2). Both these values are indicative of COO^- groups coordinated to a metal centre such as Co(III). These values correlate very well to the values, 1679 and 1584 cm^{-1}, observed by Tsuchiya and co-workers (1969:1886) for their Co(III)-apda complex. The Co(III)-apda complex prepared by Tsuchiya and co-workers was later conclusively characterised by Gladkikh *et al.* (1997:1346) in an X-ray crystallographic study as the *cis* – diaqua, $[Co(apda)(H_2O)_2]$, complex.

The ^1H NMR spectra obtained for $[Co(apda)(H_2O)_2]$ (refer to Paragraph 3.4.4) also indicated that apda acts as a tetradentate ligand and further indicated that the propionato ring is situated in a G position.

The different Co(III)-apda complexes are presented in Scheme 4.1.

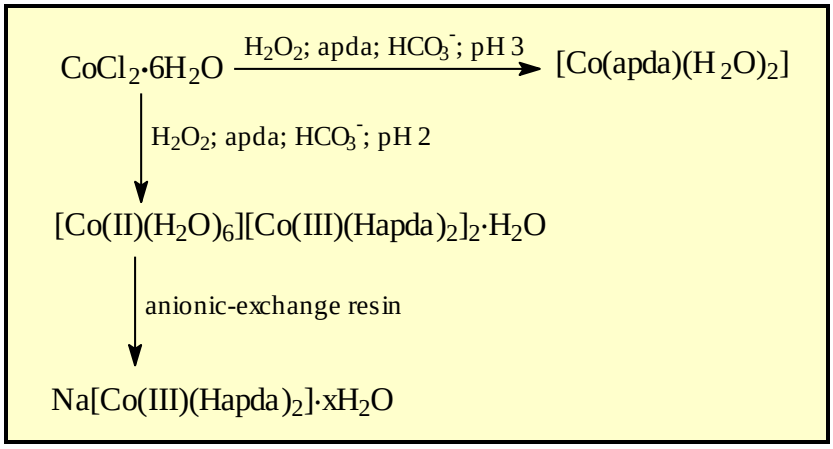

Scheme 4.1 Co(III)-apda complexes prepared (refer to Chapter 3).

4.2 Experimental

The Co(III)-apda complex was synthesised from equi molar amounts of $CoCl_2 6H_2O$ and N-(2-carboxyethyl)iminodiacetic acid (apda) (refer to Paragraph 3.5.1). This complex was isolated as $[Co(H_2O)_6][Co(Hapda)_2]_2 H_2O$ at pH 2.

The density of $[Co(H_2O)_6][Co(Hapda)_2]_2 H_2O$ was determined by flotation in an iodomethane/benzene mixture.

Intensity data were collected by M. Fernandez of Wits University on a Bruker SMART 1K CCD area detector diffractometer with graphite monochromated Mo K_α radiation (50kV, 30mA). The collection method involved ω-scans of width 0.3 °. Data reduction was carried out using the program *SAINT+* (Bruker, 1999) and absorption corrections were made using the program *SADABS* (Sheldrick G.M., 1996).

The crystal structure was solved by the heavy atom method using *SHELXTL* (Bruker, 1999). Non-hydrogen atoms were first refined isotropically followed by anisotropic refinement by full matrix least-squares calculations based on F^2 using *SHELXTL*. With the exception of hydrogen atoms involved in hydrogen bonding, all hydrogen atoms were first located in the difference map, then positioned geometrically and allowed to ride on the adjacent carbon, nitrogen and oxygen atoms (d(C-H) = 0.93 and d(N-H) = 0.86 Å) using an overall isotropic thermal parameter. Hydrogen atoms involved in hydrogen bonding were placed from the difference map, restrained to reasonable O-H distances using DFIX and refined isotropically.

The *SHELXTL* (Bruker, 1999) program was used for all the calculations. Diagrams and publication material were generated using SHELXTL and Diamond (Brandenburg *et al.*, 1998). A final difference Fourier showed no sign of disorder or residual peaks.

4.3 Crystal structures of Co(III)-apda complexes

4.3.1 Crystal structure of $[Co(H_2O)_6][Co(Hapda)_2]_2H_2O$.

A summary of the general crystal data and refinement parameters for $[Co(H_2O)_6][Co(Hapda)_2]_2H_2O$ is presented in Table 4.1.

Table 4.1 Crystal data and structure refinement for $[Co(H_2O)_6][Co(Hapda)_2]_2H_2O$.

Empirical formula	$C_{28}H_{52}Co_3N_4O_{31}$
Formula weight	1133.53
Temperature (K)	293(2)
Wavelength (Å)	0.71073
Crystal system	Triclinic
Space group	P ī (no. 2)
Unit cell dimensions	a = 9.250(1) Å, α= 114.141(3)°
	b = 10.535(2) Å, β= 93.068(3)°
	c = 12.343(2) Å, γ = 104.260(3)°
Volume ($Å^3$)	1047.5(3)
Z	1
Density (calculated) (Mg/m^3)	1.797
Absorption coefficient (mm^{-1})	1.289
F(000)	585
Crystal size (mm^3)	0.36 x 0.14 x 0.10
Theta range for data collection (°)	1.84 to 26.00
Index ranges	$-11 \le h \le 11$, $-12 \le k \le 12$, $-15 \le l \le 12$
Reflections collected	6279
Independent reflections	4079 [R(int) = 0.0228]
Completeness to theta = 26.00°	99.0 %
Absorption correction	Semi-empirical from equivalents
Max. and min. transmission	0.8819 and 0.6540
Refinement method	Full-matrix least-squares on F^2
Data / restraints / parameters	4079 / 10 / 348
Goodness-of-fit on F^2	1.012
Final R indices [I > 2sigma(I)]	$R_1 = 0.0366$, $wR_2 = 0.0754$
R indices (all data)	$R_1 = 0.0555$, $wR_2 = 0.0816$
Largest diff. peak and hole ($e.Å^{-3}$)	0.311 and -0.480

The list of atomic coordinates is presented in Appendix A (Table A.1). The complex crystallises in the space group P ī (no. 2). A perspective drawing of one unit cell (only cobalt atoms) are shown in Figure 4.2.

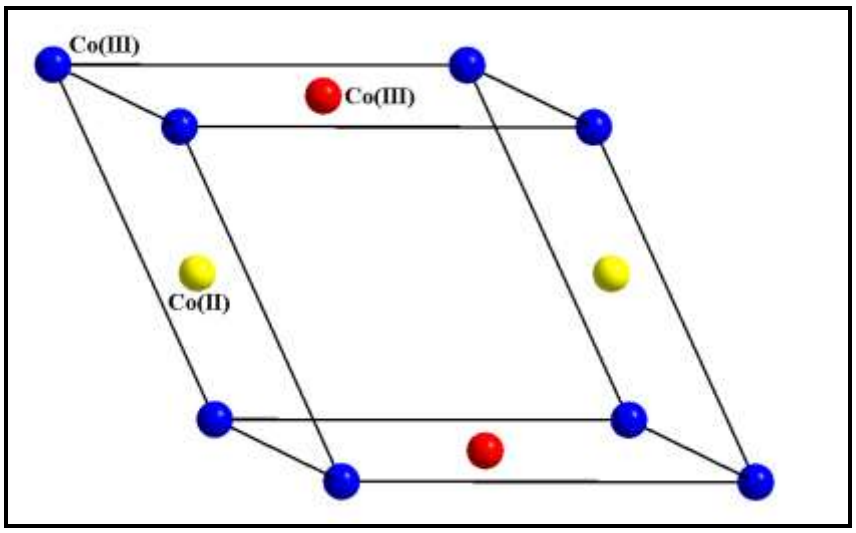

Figure 4.2 Unit cell of $[Co(H_2O)_6][Co(Hapda)_2]_2H_2O$.

The complex was isolated as $[Co(H_2O)_6][Co(Hapda)_2]_2H_2O$ and each unit cell contains two anionic units, $[Co(III)(Hapda)_2]^-$, a cation, $[Co(II)(H_2O)_6]^{2+}$, and one water of crystallisation. The differences between the two anionic units, A and B, in terms of bond lengths, bond angles, strain and octahedral distortion will be discussed later in this chapter.

Perspective drawings that include the numbering scheme of the anionic units, $[Co(Hapda)_2]^-$, A and B as well as the octahedral cation, $[Co(H_2O)_6]^{2+}$, in the $[Co(H_2O)_6][Co(Hapda)_2]_2H_2O$ molecule is shown in Figure 4.3, Figure 4.4 and Figure 4.5, respectively.

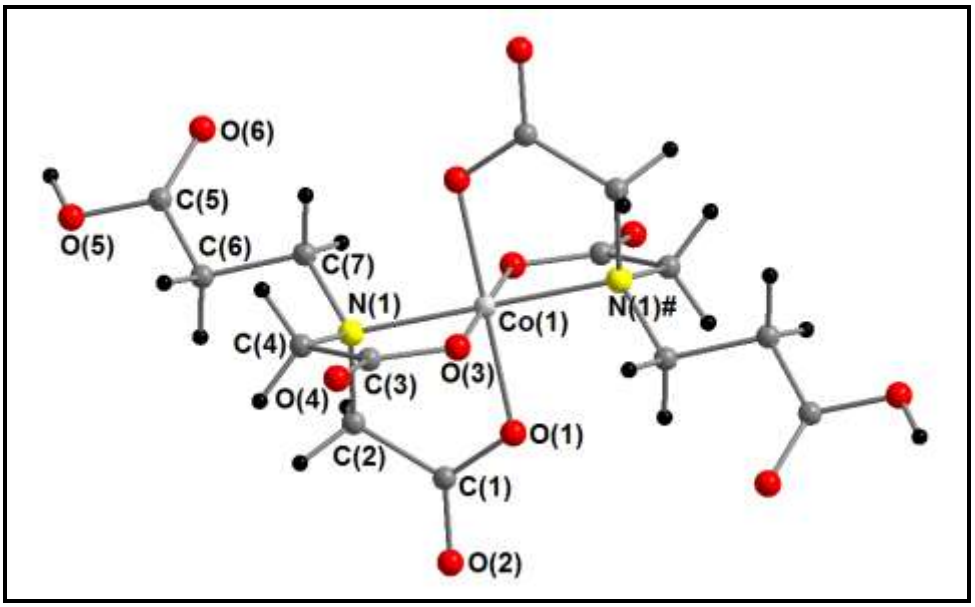

Figure 4.3 Perspective drawing of anionic unit A, $[Co(Hapda)_2]^-$.

The corresponding atoms of the second apda ligand in anionic unit A are referred to with a hash (eg. Nitrogen atom *trans* to N(1) is referred to as N(1)#).

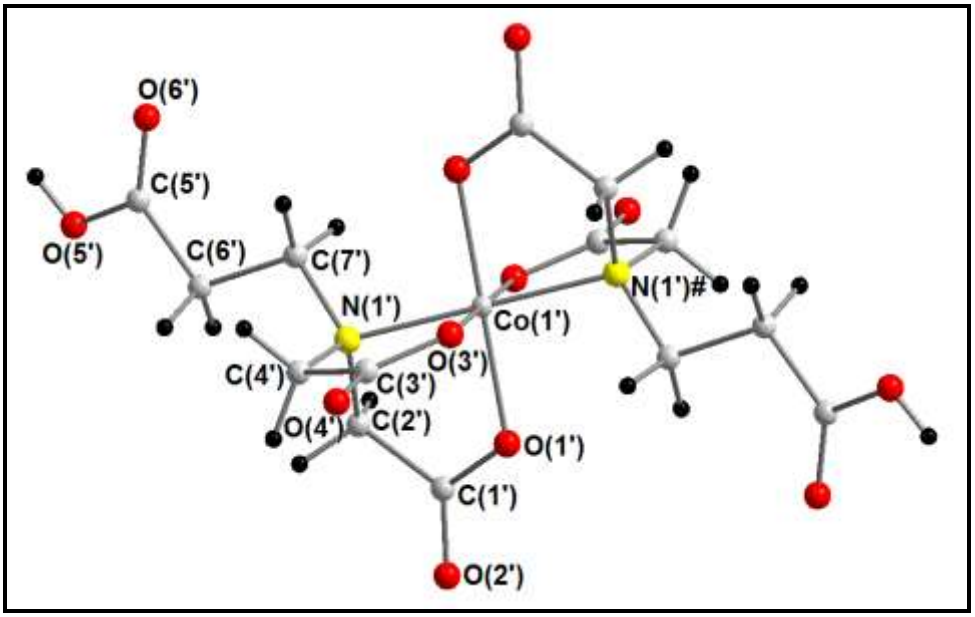

Figure 4.4 Perspective drawing of anionic unit B, $[Co(Hapda)_2]^-$.

The corresponding atoms of the second apda ligand in anionic unit B are referred to with a hash (as illustrated in previous figure).

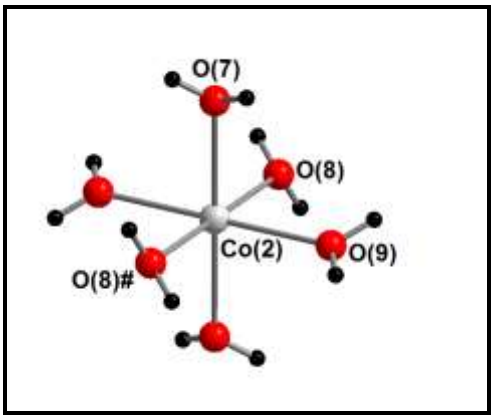

Figure 4.5 Perspective drawing of the octahedral cation $[Co(H_2O)_6]^{2+}$.

The corresponding atoms of the second apda ligand in octahedral cation, $[Co(H_2O)_6]^{2+}$, are referred to with a hash (as illustrated in previous figure).

The most relevant bond distances for the anionic units, $[Co(Hapda)_2]^-$, are presented in Table 4.2.

Table 4.2 Selected bond lengths (Å) for the anionic units, $[Co(Hapda)_2]^-$.

Bond	Length (Å)	Bond	Length (Å)
Co(1)-O(3)	1.880(2)	Co(1')-O(3')	1.879(2)
Co(1)-O(1)	1.880(2)	Co(1')-O(1')	1.900(2)
Co(1)-N(1)	1.976(2)	Co(1')-N(1')	1.973(2)
N(1)-C(4)	1.494(3)	N(1')-C(2')	1.491(4)
N(1)-C(2)	1.495(3)	N(1')-C(7')	1.495(3)
N(1)-C(7)	1.501(3)	N(1')-C(4')	1.501(3)
O(2)-C(1)	1.246(3)	O(2')-C(3')	1.236(3)
O(4)-C(3)	1.235(3)	O(4')-C(1')	1.224(3)
O(6)-C(5)	1.207(3)	O(6')-C(5')	1.209(4)

The most relevant bond angles for the anionic units, $[Co(Hapda)_2]^-$, are presented in Table 4.3.

Table 4.3 Selected bond angles (º) for the anionic units, $[Co(Hapda)_2]^-$.

Bond	Angle (º)	Bond	Angle (º)
O(3)-Co(1)-O(1)	90.54(9)	O(3')-Co(1')-O(1')	89.67(9)
O(3)-Co(1)-N(1)	87.84(9)	O(1')-Co(1')-N(1')	85.07(9)
O(1)-Co(1)-N(1)	87.88(9)	O(3')-Co(1')-N(1')	88.32(9)
C(4)-N(1)-C(2)	112.5(2)	C(4')-N(1')-C(2')	110.6(2)
C(4)-N(1)-C(7)	110.3(2)	C(2')-N(1')-C(7')	110.8(2)
C(2)-N(1)-C(7)	110.1(2)	C(7')-N(1')-C(4')	111.8(2)
C(4)-N(1)-Co(1)	105.4(2)	C(2')-N(1')-Co(1')	103.7(2)
C(2)-N(1)-Co(1)	104.9(2)	C(4')-N(1')-Co(1')	106.4(2)
C(7)-N(1)-Co(1)	113.5(2)	C(7')-N(1')-Co(1')	113.1(2)
C(1)-O(1)-Co(1)	114.9(2)	C(3')-O(3')-Co(1')	115.1(2)
C(3)-O(3)-Co(1)	115.1(2)	C(1')-O(1')-Co(1')	114.5(2)
O(2)-C(1)-O(1)	123.6(3)	O(4')-C(3')-O(3')	123.5(3)
O(2)-C(1)-C(2)	119.7(2)	O(4')-C(3')-C(4')	119.3(3)
O(1)-C(1)-C(2)	116.7(2)	O(3')-C(3')-C(4')	117.1(2)
N(1)-C(2)-C(1)	112.1(2)	N(1')-C(4')-C(3')	112.3(2)
O(4)-C(3)-O(3)	124.4(3)	O(2')-C(1')-O(1')	124.9(3)
O(4)-C(3)-C(4)	119.1(2)	O(2')-C(1')-C(2')	120.0(3)
O(3)-C(3)-C(4)	116.4(2)	O(1')-C(1')-C(2')	115.1(3)
N(1)-C(4)-C(3)	113.0(2)	N(1')-C(2')-C(1')	109.3(2)
O(6)-C(5)-O(5)	122.8(3)	O(6')-C(5')-O(5')	124.0(3)
O(6)-C(5)-C(6)	124.6(3)	O(6')-C(5')-C(6')	124.1(3)
O(5)-C(5)-C(6)	112.6(3)	O(5')-C(5')-C(6')	111.8(3)
C(5)-C(6)-C(7)	111.8(2)	C(5')-C(6')-C(7')	112.8(2)
N(1)-C(7)-C(6)	113.1(2)	N(1')-C(7')-C(6')	112.9(2)

In both the anionic units, $[Co(Hapda)_2]^-$, the Co(III) centre is surrounded by two apda ligands. The structure determination clearly shows that apda acts as a tridentate ligand in both the anionic units with the propionate group remaining uncoordinated in both the anionic units. The same coordination mode of apda was observed in the cobalt(III)-apda complex, $[Co(dien)(Hapda)]ClO_4$ (refer to Figure 2.5), synthesised by Obodovskaya *et al.* (1992:295). It was shown that apda acts as a tridentate ligand and that the propionate group remained uncoordinated. Selected bond distances and angles for the $[Co(dien)(Hapda)]ClO_4$ complex are presented in Table 4.7.

The cobalt(III) centre of both the two anionic units A and B have an octahedral geometry and are surrounded by four oxygen atoms and two nitrogen atoms from two coordinated apda ligands. The Co(III) centre of anionic unit A is surrounded by N(1), N(1)#, O(1), O(1)#, O(3) and O(3)# while the Co(III) centre of anionic unit B is surrounded by N(1'), N(1')#, O(1'), O(1')#, O(3') and O(3')#. The nitrogen atoms in both the anionic units are *trans* with respect to each other and a centre of symmetry is observed around the Co(III) centre. Close inspection on the structural data indicates that the two anionic cobalt(III) units are not similar in terms of bond distances and angles. For anionic A the Co(1)-O(1) and C(1)-O(2) bond distances are 1.880(2) and 1.246(3) Å, respectively, while the distances for the corresponding bonds in anionic unit B are 1.900(2) and 1.224(3) Å, respectively. The Co(1)-N(1)-O(1) and Co(1)-N(1)-O(3) bond angles for anionic A are 87.88(9) and 87.84(9) ^{o}, respectively, while the corresponding bond angles in anionic unit B are 85.07(9) and 88.32(9) ^{o}, respectively. Significant differences in ring strain and octahedral distortion around the metal centre between the two anionic units were also observed.

Unit A has a very slightly distorted octahedron around the cobalt(III) centre with the O-Co-O, O-Co-N and N-Co-N bonding angles ranging between 87.8(1) and 92.1(1) ^{o}, while the *trans*-N-Co-N and O-Co-O angles range between 180.0(1) and 180.0(2) ^{o}. Unit B however, has a slightly more distorted octahedron around the cobalt(III) centre which is clearly illustrated by the larger bond angle deviation from an ideal octahedral configuration with the O-Co-O, O-Co-N and N-Co-N bonding angles ranging between 85.0(1) and 94.9(1) ^{o}, while the *trans*-N-Co-N and O-Co-O angles are all 180.0(1) ^{o}.

The octahedral distortion around the cobalt(III) centres of both anionic units, $[Co(Hapda)_2]^-$, are illustrated in Figure 4.6.

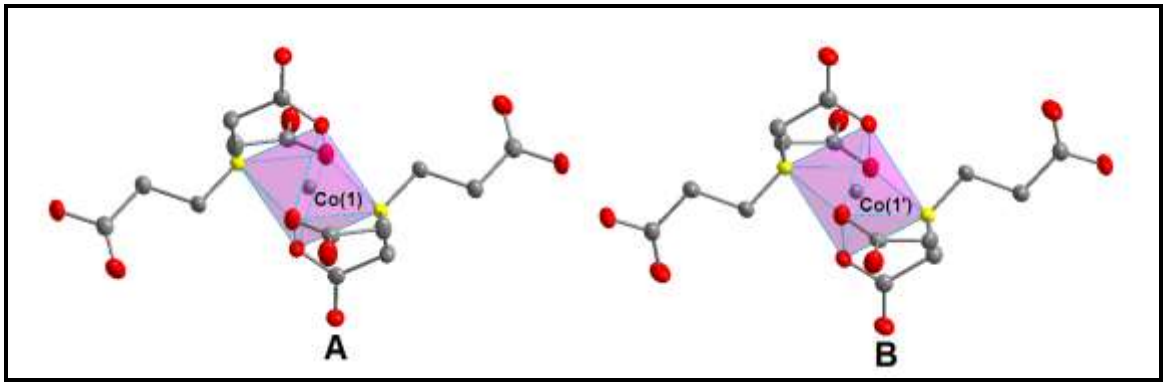

Figure 4.6 Octahedral distortion around cobalt(III) centres of anionic units, $[Co(Hapda)_2]^-$, A and B.

The Co(III)-N_{apda} bonding distances for both anionic units vary between 1.973(2) and 1.976(2) Å. These values are slightly smaller than the Co(III)-N_{apda} bonding distance of 2.019(3) Å observed for the $[Co(dien)(Hapda)]ClO_4$ complex in which apda acts as a tridentate ligand (Obodovskaya *et al.*, 1992:295). These values are also larger than the Co(III)-N_{apda} bonding distance of 1.928(7) Å observed for the $[Co(apda)(H_2O)_2]$ complex in which apda acts as a tetradentate ligand (Gladkikh *et al.*, 1997:1346). The Co(III)-O_{apda} distances vary between 1.879(2) and 1.900(2) Å for both anionic units A and B. These values agree well with those of the $[Co(dien)(Hapda)]ClO_4$ complex with the Co(III)-O_{apda} distances varying between 1.894(3) and 1.901(3) Å (Obodovskaya *et al.*, 1992:295) and are slightly larger than those observed for the $[Co(apda)(H_2O)_2]$ complex with Co(III)-O_{apda} distances varying between 1.873(7) and 1.891(8) Å (Gladkikh *et al.*, 1997:1346). The rest of the N-C, C-C and C-O bond distances of the apda ligand are all considered normal and agree well with those found for $[Co(apda)(H_2O)_2]$ and other similar tripod-type ligands like nta (nta = nitrilotriacetic acid) (Visser *et al.*, 2001:175 and Gladkikh *et al.*, 1997:1346).

The differences between the two anionic units are also illustrated by the sums of the endocyclic angles of the glycinate rings, the torsion angles and distances of Co and N atoms from the CCOO planes. These results are given in Table 4.4.

Table 4.4 Endocyclic angles, distances of N and Co atoms from the CCOO planes and torsion angles for both anionic units, $[Co(Hapda)_2]^-$, A and B.

	Anionic Unit A		**Anionic Unit B**	
	G	**R**	**G**	**R**
Endocyclic angles (º)	536.52	537.77	527.77	539.33
N distance from CCOO* plane (Å)	-0.346(5)	0.155(5)	0.562(5)	0.124(5)
Co distance from CCOO plane (Å)	-0.037(4)	-0.157(4)	-0.059(4)	0.225(4)
Torsion angles (º)				
N-Co-O-C	-7.9(2)	10.5(2)	18.6(2)	6.9(2)
Co-O-C-C	-2.3(3)	-4.0(3)	-1.1(3)	-9.1(3)
N-C-C-O	15.5(4)	-7.7(4)	-24.4(3)	6.6(4)
Co-N-C-C	-19.4(3)	14.3(3)	35.3(3)	-1.0(3)
O-Co-N-C	15.0(2)	-13.3(2)	-29.5(2)	-2.7(2)

The strain in the two anionic units may be expressed by the deviation from planarity of the glycinato rings. Weakliem & Hoard (1959:549) suggested that the sum of the endocyclic bond angles of the rings could be used to determine the ring strain and pointed out that an unstrained glycinato ring should be planar. The ideal value for the sum of the endocyclic bond angles is 538.4 º, which would allow the rings to be nearly planar. The endocyclic angles of the rings in the two cobalt(III) units are 536.52 and 537.77 º for unit A and 527.77 and 539.33 º for unit B. This information is very interesting since it seems that the G ring in anionic unit A is only slightly more strained than the R ring while the G ring in anionic unit B is quite severely strained compared to the R ring in the same unit.

The same was found to be the case in the Co(III)-apda complex in which apda acts as a tridentate ligand (Obodovskaya *et al.*, 1992:295). Both the glycinate rings in $[Co(dien)(Hapda)]ClO_4$ were almost planar but the sums of the endocyclic angles for the G and the R rings were 535.2 and 536.9 º, respectively, indicating that the G ring is slightly more strained than the R ring. The fact that the G ring in anionic unit B is more strained than the R ring agrees very well with previous investigations regarding the ring strain in these types of complexes (Weakliem and Hoard 1959:549, Nagao *et al.*,

1972:1852, Visser *et al.*, 2001:185 and Visser *et al.*, 2001:175). The reason for the more strained G rings in Co(III)-apda complexes is not well understood. It is suggested that the extra electron density donated to the Co(III) centre by the electron rich apda ligand gives it more of a d^7 than d^8 character. This implies stabilisation of the metal dx^2-y^2 orbitals and destabilisation of the dz^2 orbitals, which in turn means better overlap in the equatorial (R ring) position. It is obvious that more evidence is needed to explain with total conviction why the R rings in these complexes are less strained than the G rings.

As mentioned earlier, Weakliem and Hoard (1959:549) attributed the strain in the R rings primarily to angular strain about the coordinated nitrogen atoms. They argued that each ring attempts to impose its own stereochemical requirements on the nitrogen atom, while the nitrogen is also constrained to approximately tetrahedral geometry. These results not only manifest itself to angle and bond abnormalities in the G rings, but also to significant distortions of the nitrogen tetrahedron.

The nitrogen tetrahedra of both the anionic units are slightly distorted from the ideal tetrahedral geometry. The C-N-C angles for anionic unit A vary between 110.1(2) and 112.5(2) ^{o}, compared to between 110.6(2) and 111.8(2) ^{o} for anionic unit B. These results indicate that the strain about the nitrogen tetrahedron is more severe in anionic unit A, compared to anionic unit B. In the study of the [Co(dien)(Hapda)]ClO_4 complex (Obodovskaya *et al.* 1992:295) the apda nitrogen was significantly distorted from the tetrahedral geometry with values for C-N-C angles varying between 108.6(7) and 111.5(7) ^{o}. These values correlate well with those found for other metal complexes with similar tripod-type ligands like nta (nta = nitrilotriacetic acid) with C-N-C angles varying between 112.0(3) and 114.3(2) ^{o} for Cs_2[Co(nta)(CO_3)]H_2O and 110.5(2) ^{o} for [Co(nta)(*N*,*N*-Et_2en)] (Visser *et al.*, 2001:185 and Visser *et al.*, 2001:175).

The angular strain around the nitrogen atom of apda can also be demonstrated by the non-planarity of the G rings, see Table 4.4. Deviations of the N atom from the CCOO planes vary between 0.155(5) and 0.346(5) Å for anionic unit A and 0.124(5) and 0.562(5) Å for anionic unit B. Similarly the out-of-plane distances for cobalt were calculated to be between 0.037(4) and 0.157(4) Å for anionic unit A and between 0.059(4) and 0.225(4) Å for anionic unit B. The deviation of N from the planes decrease in the order G > R for both anionic units, while the deviation of Co from the planes increase in the order G > R for both anionic units. The main reason for this is possibly that the nitrogen atom is more displaced from the CCOO plane (0.346(5) and 0.562(5) Å) in the G rings of anionic unit A and B, respectively, which forces the Co atom into the G plane and out of the R plane (Co distance from R plane in anionic unit A and B is surprisingly long, 0.157(4) and 0.225(4) Å, respectively).

The nitrogen tetrahedra of anionic unit A, $[Co(Hapda)_2]^-$, is shown in Figure 4.7.

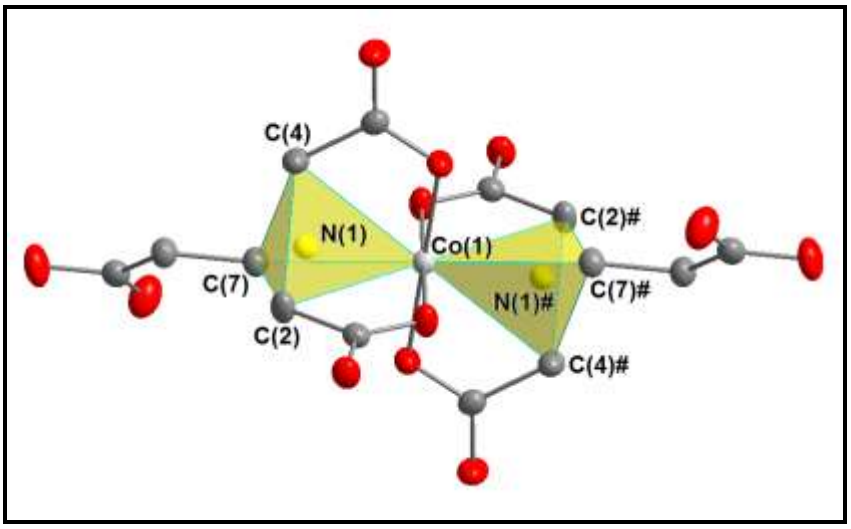

Figure 4.7 Nitrogen tetrahedra of anionic unit A, $[Co(Hapda)_2]^-$.

A projection of $[Co(H_2O)_6][Co(Hapda)_2]_2H_2O$ along the a axis is shown in Figure 4.8.

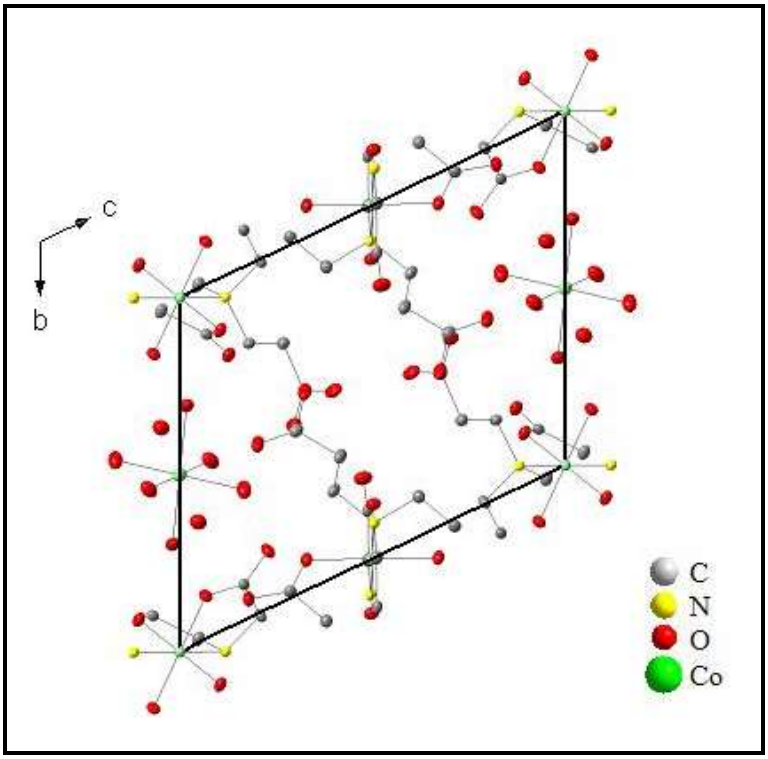

Figure 4.8 Projection of $[Co(H_2O)_6][Co(Hapda)_2]_2H_2O$ along the a axis.

A projection of $[Co(H_2O)_6][Co(Hapda)_2]_2H_2O$ along the a axis reveals that the complex molecules are packed in layers that stretch vertically along the bc plane with the octahedral cation in the centre of the cell edges in the b direction. Quite strong hydrogen bonding was observed between the G ring oxygen, O(2), of anionic unit A and a hydroxy group, O(5')-H(5'), of another anionic unit B (O – O contact distance is 2.621(3) Å) and between the G ring oxygen, O(2'), of anionic unit B and a hydroxy group, O(5)-H(5), of another anionic unit A (O – O contact distance is 2.752(3) Å). The different types and lengths of hydrogen interactions experienced by the G and R rings of anionic units A and B are presented in Table 4.5.

Table 4.5 Types and lengths of hydrogen interactions experienced by the G and R rings of anionic units A and B.

Bond	Anionic Unit A		Anionic Unit B	
O-H…O	**G (O…O)**	**R (O…O)**	**G (O…O)**	**R (O…O)**
O(5')-H(5')….O(2)#	2.621(3) Å			
O(5')-H(5')….O(1)#	3.211(3) Å			
O(7)-H(7F)….O(2)#	2.844(3) Å			
O(9)-H(9B)….O(4)#		2.789(3) Å		
O(7)-H(7E)….O(2')#			2.693(3) Å	
O(5)-H(5)….O(4')#				2.752(3) Å

Close inspection of these results indicates that the R ring in anionic unit A experiences one hydrogen interaction while the G ring in anionic unit A experiences three hydrogen interactions. The G and R rings of anionic unit B experience one hydrogen interaction each. The R ring in anionic unit B experiences only one hydrogen interaction (O(7)-H(7E)….O(2')#) compared to the three hydrogen interactions experienced by the R ring in anionic unit A. These hydrogen interactions may be responsible for the fact that the strain about the nitrogen tetrahedron is more severe in anionic unit A than in anionic unit B, although more evidence is needed to explain the strain about the nitrogen tetrahedra with more confidence.

This information is of course insufficient to make any definite deductions, except that it seems that the reason for the difference in strain in G and R rings of tripod-type ligands like nta and apda can also be attributed to packing effects, especially since the G ring in anionic unit B are quite severely strained and both the glycinato rings in [Co(dien)(Hapda)]ClO_4 experienced almost no strain (Obodovskaya *et al.,* 1992:594).

The most relevant bond distances and angles for the octahedral cation, $[Co(H_2O)_6]^{2+}$, are presented in Table 4.6.

Table 4.6 Selected bond lengths (Å) and angles (º) for octahedral cation, $[Co(H_2O)_6]^{2+}$.

Bond	Length (Å)	Bond	Angle (º)
Co(2)-O(7)	2.091(2)	O(8)-Co(2)-O(7)	89.4(1)
Co(2)-O(8)	2.051(2)	O(8)-Co(2)-O(9)	93.0(1)
Co(2)-O(9)	2.115(2)	O(7)-Co(2)-O(9)	90.8(1)

The octahedral cation $[Co(H_2O)_6]^{2+}$ is slightly distorted (Figure 4.9) but centrosymmetric, with the atom Co(2) at the inversion centre. The Co-O distances vary between 2.051(2) and 2.115(2) Å and the O-Co-O right angles between 86.9(1) and 93.0(1) º. This compares very well with several different crystal structures where $[Co(H_2O)_6]^{2+}$ had been used as the counter ion eg., $[Co(H_2O)_6][CoCl_4]C_{12}H_{24}O_6C_3H_6O$ with Co-O bond lengths varying between 2.042(3) and 2.118(3) Å and Co-O bond angles varying between 86.2(2) and 93.1(2) º (Vance *et al.*, 1980:150).

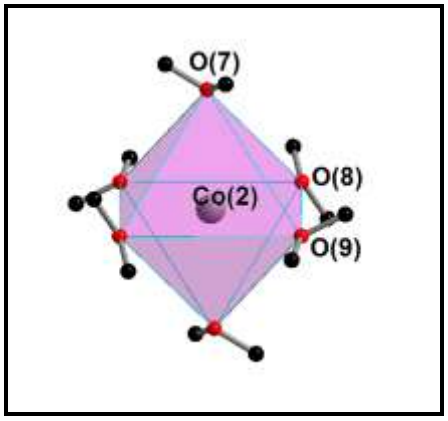

Figure 4.9 Perspective drawing of the slightly distorted octahedral cation $[Co(H_2O)_6]^{2+}$.

4.4 Conclusion

Since the isolation of $[Co(dien)(Hapda)]ClO_4$ by Obodovskaya *et al.*, (1992:295) and $\{[Co(dien)(apda)]_2Cu(H_2O)\}_2(ClO_4)_4 8H_2O$ by Polyakova *et al.* (1997:1509) no other Co(III)-apda complexes in which apda acts as a tridentate ligand have been isolated and characterised by means of X-ray crystallographic studies. The title Co(III)-apda

complex, $[Co(H_2O)_6][Co(Hapda)_2]_2H_2O$, has been isolated and characterised with X-ray crystallography for the first time.

From the discussion above it is obvious that anionic units A and B differ in terms of bond lengths and angles as well as strain experienced by the glycinato rings of the apda ligand. The only reasonable explanation for the difference in strain could be that these rings experience different external pushing/pulling effects due to intermolecular hydrogen bonding and other Van der Waals interactions.

It is obvious from the above discussion that more evidence is required to explain with total conviction why the G ring in the anionic unit B of $[Co(H_2O)_6][Co(Hapda)_2]_2H_2O$ is quite severely strained while the R ring of anionic unit B and both the G and R rings in anionic unit A experience almost no strain.

A comparison of selected features of known structures of Co(III)-apda and -nta complexes is shown in Table 4.7. The following observations can be made.

(1) The Co-N_{ligand} bond distances vary slightly, especially when moving from $[Co(apda)(H_2O)_2]$ to $[Co(dien)(Hapda)]^-$ where a difference of 0.091 Å is observed. An increase is observed in the Co-N_{ligand} bond distances when apda acts as a tridentate ligand.

(2) The average strain in the G rings (G_{end}) in the complexes with a tetradentate ligand is equal.

(3) The strain in the G rings (G_{end}) in the complexes with a tridentate ligand differ significantly with endocyclic bond angles varying between 527.8 and 536.5 º.

(4) The R rings are almost perfectly planar in all the structures.

(5) The R ring bite angles are closer to 90 º than the average G ring bite angles.

(6) The angular strain experienced by the nitrogen of the tetradentate ligand is most pronounced in the C_G-N-C_G angles, which are almost similar for all the complexes studied except the $[Co(apda)(H_2O)_2]$ complex. This is expected since the longer propionato ring of apda experiences more strain than the glycinato rings of nta (refer to Paragraph 2.2.1).

(7) All the other bonding features of the different Co(III)-nta and -apda complexes are the same within experimental error, even though there are substantial differences in charge and therefore packing features as well as bidentate ligand ring sizes.

Table 4.7 Selected features of different Co(III)-apda and -nta complexes.

Complex	**[a]Co-N_{lig} (Å)**	**[b]G_{end} (º)**	**[c]G_{bite} (º)**	**[d]R_{bite} (º)**	**[e]O_G-Co-O_G (º)**	**[f]C_G-N-C_G (º)**	**Reference**
$[Co(apda)(H_2O)_2]$	1.928(7)	-	84.1	88.0(3)	176.1(4)	110.6(6)	Gladkikh *et al.*, (1997:1346)
$[Co(dien)(Hapda)]^-$	2.019(3)	535.2	85.4	87.2(1)	-	-	Obodovskaya *et al.*, (1992:594)
A: $[Co(Hapda)_2]^-$	1.976(2)	536.5	87.9	87.8(1)	-	-	This study
B: $[Co(Hapda)_2]^-$	1.973(2)	527.8	85.1	85.1(1)	-	-	This study
$[Co(nta)(\mu\text{-}OH)]_2^{2-}$	1.992(6)	529.0	86.1	88.1(2)	172.0(2)	115.7(6)	Visser *et al.*, (1997:2851)
$[Co(nta)(CO_3)]^{2-}$	1.920(2)	529.0	87.3	88.52(9)	173.62(9)	114.3(2)	Visser *et al.*, (2001:185)
[Co(nta)(en)]	1.946(3)	529.8	86.5	87.6(1)	172.6(1)	116.3(3)	Gladkikh *et al.*, (1992:1231)
$[Co(nta)(gly)]^-$	1.928(8)	531.3	86.4	89.3(3)	172.5(3)	115.6(7)	Gladkikh *et al.*, (1992:908)
[Co(nta)(viol)]	1.942(7)	529.9	86.5	89.4(3)	172.8(3)	115.3(7)	Almazan *et al.*, (1990:2565)
[Co(nta)(N,N-Et_2en)]	1.950(4)	530.3	85.5	87.9(2)	170.6(2)	116.8(4)	Visser *et al.*, (2001:175)
[Co(nta)(propen)]	1.962(2)	529.5	85.3	86.8(1)	170.5(1)	115.5(4)	Swaminathan *et al.*, (1989:566)

[a] Bonding distance from Co to nitrogen of ligand

[b] Average of the sums of the endocyclic angles of G rings

[c] Average of N-O bite angles of G rings

[d] R ring bite angles

[e] Bonding angle of Co to G ring oxygen atoms

[f] Bonding angle of N of the ligand to C atoms of G rings

5 Kinetic study of the reactions of Co(III)-apda complexes

In this chapter…

The first part of the chapter focuses on the pH dependence of $Na[Co(Hapda)_2]xH_2O$ and $[Co(apda)(H_2O)_2]$, while the latter part of this chapter focuses on the substitution reactions of $[Co(apda)(H_2O)_2]/[Co(apda)(H_2O)(OH)]^-$ with NCS^- ions.

5.1 Introduction

It was mentioned in Chapter 2 that there are only a few kinetic studies of metal-apda complexes available in the literature.

This chapter deals with the influence of H^+ ions on the behaviour of the Co(III)-apda system in aqueous medium (Scheme 5.1) and with the substitution reactions of $[Co(apda)(H_2O)_2]/[Co(apda)(H_2O)(OH)]^-$ with NCS^- ions. The first pH study involves the protonation/deprotonation properties of the $Na[Co(Hapda)_2]xH_2O$ complex, while the second part of the chapter deals with the protonation/deprotonation properties of $[Co(apda)(H_2O)_2]$. The last part of this chapter deals with the substitution reactions between $[Co(apda)(H_2O)_2]/[Co(apda)(H_2O)(OH)]^-$ and NCS^- ions.

The influence of H^+ ions on the behaviour of the almost similar Co(III)-nta system in aqueous medium as well as the substitution reactions of $[Co(nta)(H_2O)_2]/[Co(apda)(H_2O)(OH)]^-$ with NCS^- ions have been investigated by other groups (Thacker & Higginson, 1975:704 and Visser *et al.*, 2002:461) and have been discussed in detail in Chapter 2.

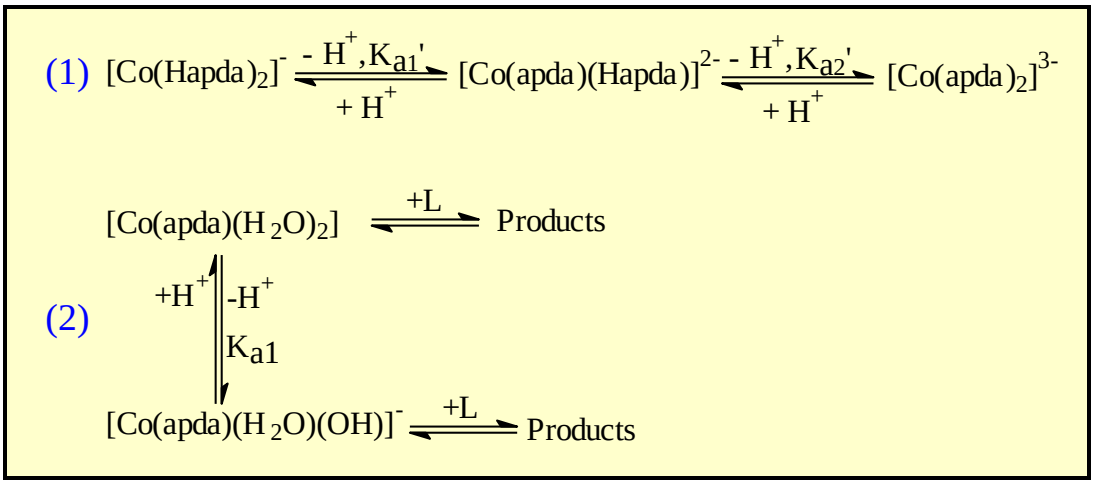

Scheme 5.1 pH dependence of Co(III)-apda complexes studied.

5.2 Experimental procedures

All reagents and chemicals were of analytical grade and double distilled water was used in all experiments. All pH measurements were performed on a pH 211 microprocessor pH meter, calibrated with pH 7.01 (HI7007) and pH 4.01 (HI7004) buffer solutions, all obtained form Hanna instruments. Kinetic measurements were performed on a Cary 50 (Conc.) spectrophotometer equipped with constant temperature cell holders (accuracy within 0.1ºC). Scientist (Micromath, 1990) was used to fit the data. All the kinetic runs were performed under pseudo first-order conditions with the ligand in excess in each case. The ionic strength of all the reaction solutions was kept constant by addition of $NaClO_4$. Linear plots of $\log(A - A_t)$ *vs.* time were obtained for at least two half-lives under all conditions. The solid lines and the figures represent computer least squares fits of data, while the experimentally determined values are represented by dots. Detailed tables of the experimental values are given in Appendix A (Section II).

5.3 Results and discussion

5.3.1 Influence of H^+ ions on the Co(III)-apda system

5.3.1.1 pH dependence of $Na[Co(Hapda)_2]xH_2O$

The UV/VIS results reported earlier (Paragraph 3.6.3) indicated that crystals of $Na[Co(Hapda)_2]xH_2O$ give a stable Co(III)-apda species in solution (pH 5.5), which when acidified to pH 1 yields $[Co(Hapda)_2]^-$ that is stable at pH 1 (Scheme 3.4).

During a potentiometric titration study, $HClO_4$ (1.0 M) (20 x 0.05 cm^3) was added to a 50 cm^3 of a solution that was obtained by dissolving $Na[Co(Hapda)_2]xH_2O$ in water (pH 5.5). The pH of the solution was measured after each addition of 0.05 cm^3 $HClO_4$ (1.0 M). The data obtained (Appendix A, Table A.8) indicated that two moles of acid react with one mole of the starting complex. However, the values of K_{a1}' and K_{a2}' could not be determined from this data, probably because their values were too close to separate. The proposed acid dissociation reactions of $[Co(Hapda)_2]^-$ and $[Co(Hapda)(apda)]^{2-}$ are shown in Scheme 5.2.

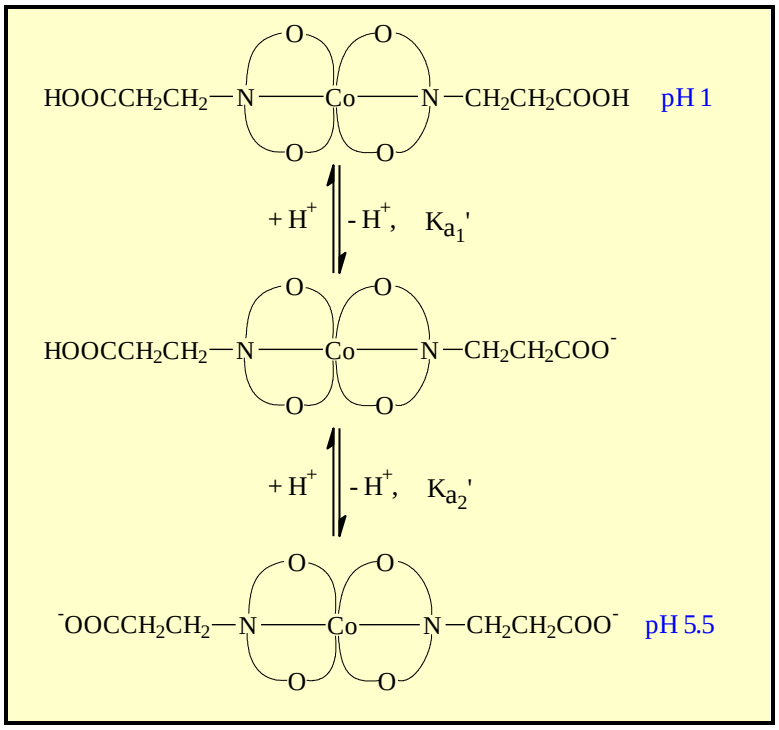

Scheme 5.2 Proposed acid dissociation reaction of $[Co(Hapda)_2]^-$ and $[Co(Hapda)(apda)]^{2-}$.

The pH dependence of $Na[Co(Hapda)_2]xH_2O$ was studied at room temperature between pH 1 and 5.5. In general, for protonation of a diprotic species as defined by Equations 5.1 and 5.2, UV/VIS studies of the acid base behaviour of diprotic complexes such as H_2A is given by Equation 5.3 (Appendix A, Section III).

$$\mathbf{H_2A \overset{K_{a_1}'}{\rightleftharpoons} HA^- + H^+} \qquad \textbf{(5.1)}$$

$$\mathbf{HA^- \overset{K_{a_2}'}{\rightleftharpoons} A^{2-} + H^+} \qquad \textbf{(5.2)}$$

$$\mathbf{A_{tot} = \frac{A_{H_2A} + A_{HA^-}(K_{a1}'/[H^+]) + A_{A^{2-}}(K_{a1}'K_{a2}'/[H^+]^2)}{1 + (K_{a1}'/[H^+] + K_{a1}'K_{a2}'/[H^+]^2)}} \qquad \textbf{(5.3)}$$

In Equation 5.3, A_{tot} = absorbance at a specific $[H^+]$, A_{H_2A} = absorbance of the H_2A species, A_{HA^-} = absorbance of the HA^- species, $A_{A^{2-}}$ = absorbance of the A^{2-} species and K_{a1}' and K_{a2}' are the acid dissociation constants.

The acid dissociation constants of $[Co(Hapda)_2]^-$ and $[Co(Hapda)(apda)]^{2-}$, K_{a1}' and K_{a2}' (Scheme 5.2), were spectrophotometrically determined at λ = 348 nm at 25 ºC by adjusting the pH of a $[Co(apda)_2]^{3-}$ solution from pH 5.28 to 0.98 (4.5×10^{-3} M) with HCl (1 M) and immediately measuring the absorbance (Figure 5.1). The spectrophotometric data (Appendix A, Table A.7) were fitted to Equation 5.5 (solid line in Figure 5.1) and the values for pK_{a1}' and pK_{a2}' were determined as 2.6(1) and 2.8(1), respectively

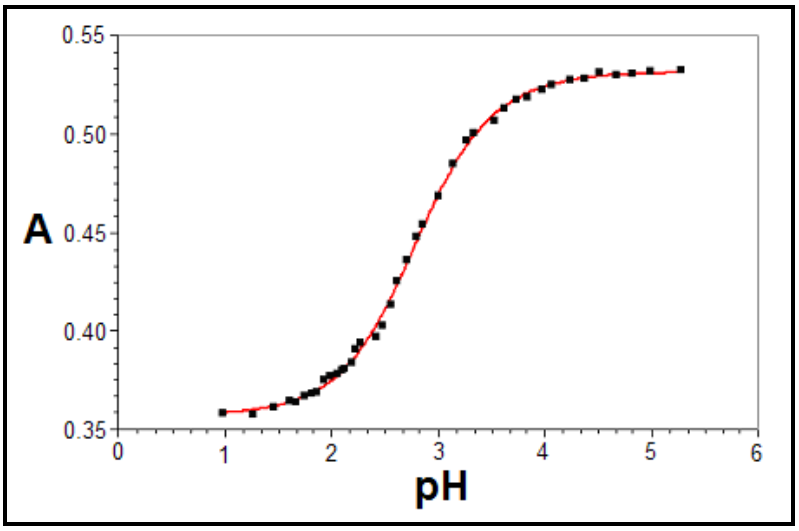

Figure 5.1 Plot of Abs (λ = 348 nm) *vs.* pH for $Na[Co(Hapda)_2]xH_2O$ (4.5×10^{-3} M), 25 ºC, μ = 1.0 M ($NaClO_4$).

The values obtained for pK_{a1}' and pK_{a2}' are very close. This is expected since the chemical environments for the dissociation of the first hydrogen and the second hydrogen from the $[Co(Hapda)_2]^-$ and $[Co(Hapda)(apda)]^{2-}$ complexes are almost similar.

In the pH range studied (pH 1 – 5), no ligand substitution reactions for the $Na[Co(Hapda)_2]xH_2O$ complex were observed.

5.3.1.2 pH dependence of $[Co(apda)(H_2O)_2]$

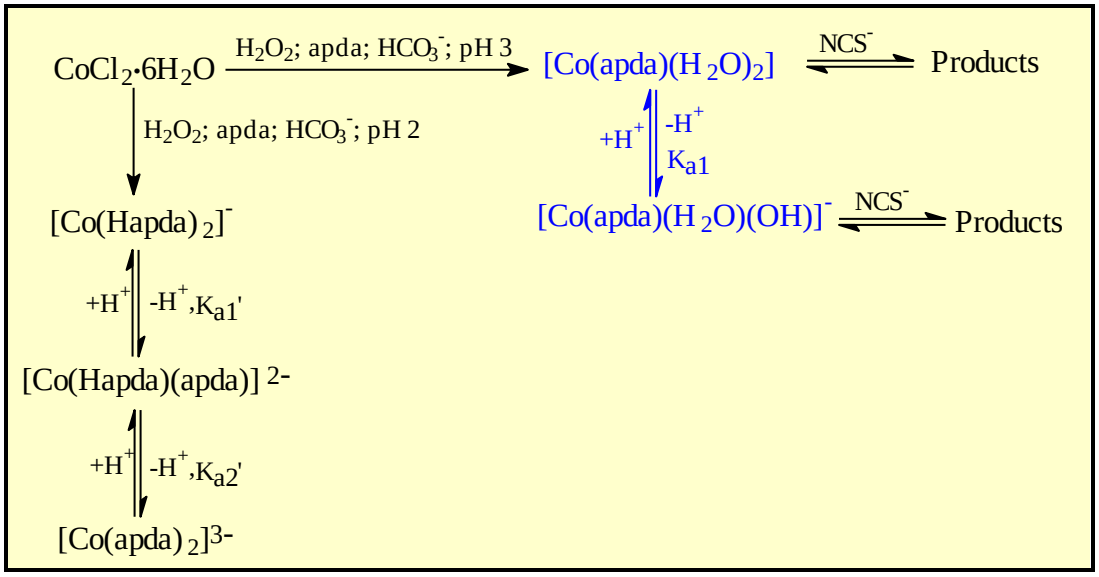

Scheme 5.3 pH dependence of $[Co(apda)(H_2O)_2]$ (Blue print).

It was shown earlier (Paragraph 3.4.3) that $[Co(apda)(H_2O)_2]$ is stable in acidic solution (pH *ca.* 2). Initial potentiometric titration values indicated that one mole H^+ reacts with one mole $[Co(apda)(H_2O)_2]$ between pH 4.30 and 7.80. A protonation/deprotonation equilibrium, accounting for one mole H^+ per one mole $[Co(apda)(H_2O)_2]$, was proposed between pH 2 – 7 (refer to Scheme 3.2).

In order to avoid complication by competitive reactions observed at pH values > 7 (refer to Paragraph 3.4.3), it was decided to keep the reaction conditions between pH 2 – 7.

UV/VIS studies of the protonation behaviour of monoprotic complexes such as HB (as defined by Equation 5.4) are given by Equation 5.5 (Appendix A, Section III).

$$\mathbf{HB \overset{K_{a_1}}{\rightleftharpoons} B^- + H^+} \qquad \textbf{(5.4)}$$

$$\mathbf{A_{tot} = \frac{A_{HB} + A_{B^-}(K_{a1}/[H^+])}{1 + (K_{a1}/[H^+])}} \qquad \textbf{(5.5)}$$

In Equation 5.5, A_{tot} = absorbance at a specific $[H^+]$, A_{HB} = absorbance of the HB species, A_{B^-} = absorbance of the B^- species and K_{a1} is the acid dissociation constant.

The acid dissociation constant, K_{a1}, of $[Co(apda)(H_2O)_2]$ (Scheme 5.4) was determined spectrophotometrically at λ = 559 nm at 25 ºC by adjusting the pH of a $[Co(apda)(H_2O)_2]$ solution (8 x 10^{-3} M) with KOH (1 M) and immediately measuring the absorbance. The data were fitted to Equation 5.5 and the results are illustrated in Figure 5.2.

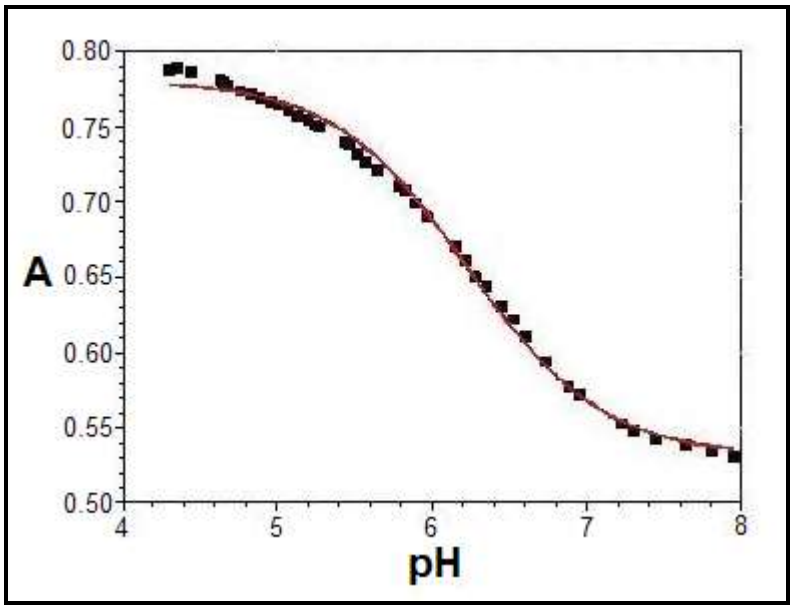

Figure 5.2 Plot of Abs (λ = 559 nm) *vs.* pH for $[Co(apda)(H_2O)_2]$ (8 x 10^{-3} M), 25 ºC, μ = 1.0 M ($NaClO_4$).

The proposed acid dissociation reaction of $[Co(apda)(H_2O)_2]$ is shown in Scheme 5.4.

$$[Co(apda)(H_2O)_2] \underset{+\ H^+}{\overset{K_{a_1},\ -\ H^+}{\rightleftharpoons}} [Co(apda)(H_2O)(OH)]^-$$

Scheme 5.4 Acid dissociation reaction of $[Co(apda)(H_2O)_2]$.

The value for pK_{a1} was determined as 6.23(2). This compares very well with the value of 6.52(2) determined by Visser and co-workers (2002:461) for $[Co(nta)(H_2O)_2]$. The pK_{a1} value is also higher than the value of 5.43 found for the similar acid dissociation equilibrium involving $[Cr(nta)(H_2O)_2]$ (Hualin & Xu, 1990:137).

5.3.2 Substitution reactions of Co(III)-apda complexes with NCS^- ions

5.3.2.1 Substitution reactions of $[Co(apda)(H_2O)_2]$/$[Co(apda)(H_2O)(OH)]^-$ with NCS^- ions.

As in the case of $[Co(nta)(H_2O)_2]$ (Visser *et al.,* 2002:461), the UV/VIS studies of the $[Co(apda)(H_2O)_2]$ complex (refer to Paragraph 3.4.3) indicated competitive reactions at pH values > 7, possibly due to dimer formation. In order to avoid complications by these reactions, the substitution reactions of $[Co(apda)(H_2O)_2]$/$[Co(apda)(H_2O)(OH)]^-$ with NCS^- ions were studied in the pH range between 2 and 7. The ligand substitution of $[Co(apda)(H_2O)_2]$/$[Co(apda)(H_2O)(OH)]^-$ with various ligands (NCS^-, N_3^- etc.) were studied. In the pH 2 - 7 range, only ligand substitution of $[Co(apda)(H_2O)_2]$/ $[Co(apda)(H_2O)(OH)]^-$ with NCS^- ions provided satisfactory results.

Thacker and Higginson (1975:704) also investigated the substitution reactions between $[Co(nta)(H_2O)_2]$ and different incoming ligands (NCS^-, HCN, N_3^-/thiourea). Unfortunately, none of these ligands provided satisfactory results. HCN did not react with $[Co(nta)(H_2O)_2]$ in the pH range 2 - 7, while the reactions between $[Co(nta)(H_2O)_2]$ and N_3^-/thiourea were complicated by the reduction of the metal centre in each case. They concluded that only NCS^- ions did not reduce the metal centre in the pH range studied.

The initial UV/VIS spectra revealed two distinguishable reactions with rate constants which differ considerably (*ca.* 100 times) upon adding an excess of NCS^- to solutions of $[Co(apda)(H_2O)_2]$/$[Co(apda)(H_2O)(OH)]^-$. The UV/VIS spectrum obtained for the first substitution reaction of $[Co(apda)(H_2O)_2]$ with NCS^- is shown in Figure 5.3. The

decrease in absorption at 556 nm is representative of a typical reaction under pseudo first-order reaction conditions. The isosbestic point at 478 nm disappears with time as the second reaction takes place.

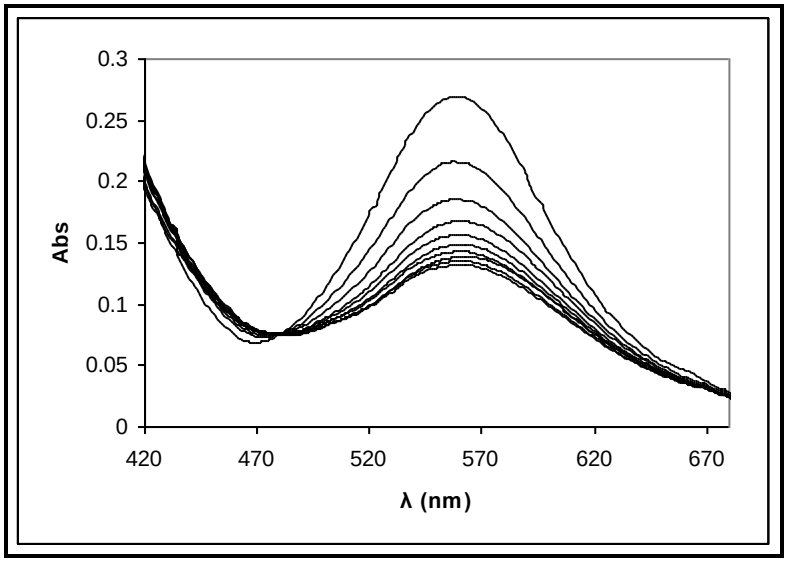

Figure 5.3 UV/VIS spectral change for the first reaction between $[Co(apda)(H_2O)_2]$ and NCS^- ions.

At these pH values, where both the Co(III)-apda species can react with NCS^-, the following reaction scheme is proposed:

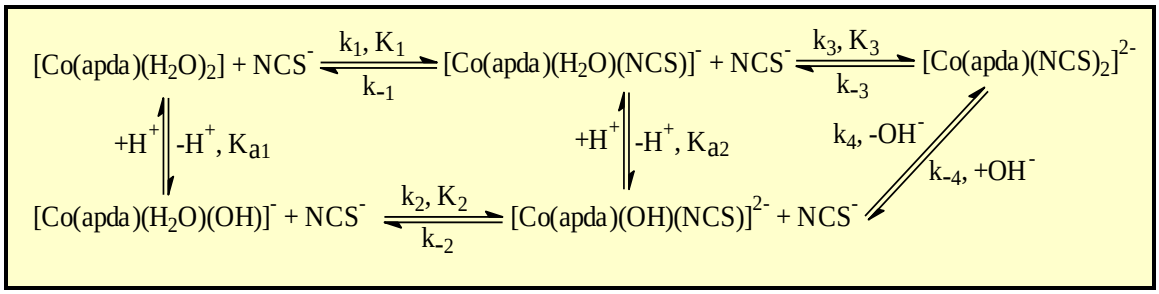

Scheme 5.5 Reactions of $[Co(apda)(H_2O)_2]/[Co(apda)(H_2O)(OH)]^-$ with NCS^- ions.

The total rate law, according to Scheme 5.5, is given by Equation 5.6.

$$\mathbf{R = k_1[Co(apda)(H_2O)_2][NCS^-] + k_2[Co(apda)(H_2O)(OH)^-][NCS^-] + k_3[Co(apda)(H_2O)(NCS)^-][NCS^-] + k_4[Co(apda)(NCS)(OH)^{2-}][NCS^-] - k_{-1}[Co(apda)(H_2O)(NCS)^-] - k_{-2}[Co(apda)(NCS)(OH)^{2-}] - k_{-3}[Co(apda)(NCS)_2^{2-}] - k_{-4}[Co(apda)(NCS)_2^{2-}]} \quad \mathbf{(5.6)}$$

The total Co(III) concentration, $[Co]_{tot}$, is indicated by Equation 5.7.

$$\mathbf{[Co]_{tot} = [Co(apda)(H_2O)_2] + [Co(apda)(H_2O)(OH)]^-} \quad \textbf{(5.7)}$$

The total concentration of the Co(III)-monothiocyanide complex, $[Co\text{-}NCS_{tot}]$, is illustrated by Equation 5.8.

$$\mathbf{[Co\text{-}NCS_{tot}] = [Co(apda)(H_2O)(NCS)^-] + [Co(apda)(NCS)(OH)^{2-}]} \quad \textbf{(5.8)}$$

The acid dissociation constants, K_{a1} and K_{a2}, are given in Equations 5.9 and 5.10 respectively.

$$\mathbf{K_{a_1} = \frac{[Co(apda)(H_2O)(OH)^-][H^+]}{[Co(apda)(H_2O)_2]}} \quad \textbf{(5.9)}$$

$$\mathbf{K_{a_2} = \frac{[Co(apda)(OH)(NCS)^{2-}][H^+]}{[Co(apda)(H_2O)(NCS)^-]}} \quad \textbf{(5.10)}$$

Under pseudo first-order conditions with $[Co]_{tot} << [NCS^-]$ and $[Co\text{-}NCS_{tot}] << [NCS^-]$, the observed rate, k_{obs}, can be derived from Equations 5.6 – 5.10 (Appendix A, Section III).

$$\mathbf{k_{obs} = \frac{k_1[H^+] + k_2K_{a_1}}{(K_{a_1} + [H^+])}[NCS^-] + \frac{k_3[H^+] + k_4K_{a_2}}{(K_{a_2} + [H^+])}[NCS^-] + \frac{k_{-1}[H^+] + k_{-2}K_{a_2}}{(K_{a_2} + [H^+])} + k_{-3} + k_{-4}[OH^-]} \quad \textbf{(5.11)}$$

In the pH range studied (2 – 7.5) the $[OH^-]$ is very small, with the result that the contribution of the $k_{-4}[OH^-]$ term in Equation 5.11 becomes negligibly small. A provisional fit of the experimental data to Equation 5.11 (excluding the $k_{-4}[OH^-]$ factor) also gave a value for k_4 approaching zero.

In order to verify the latter assumption, the first reaction between $[Co(apda)(H_2O)_2]$ and NCS^- ions were allowed to go to completion at low pH after which the pH of the reaction solution was increased to ~ 6.5. The spectroscopic results did not indicate that hydroxide ions are substituted (k_4 pathway). In general the replacement of an OH^- ligand by any other ligand is not observed in complexes related to $[Co(apda)(H_2O)_2]$ (Leipoldt *et al.*, 1993:241). Taking the above into consideration Equation 5.11 can be simplified to Equation 5.12.

$$\mathbf{k_{obs} = \frac{k_1[H^+] + k_2K_{a_1}}{(K_{a_1} + [H^+])}[NCS^-] + \frac{k_3[H^+]}{(K_{a_2} + [H^+])}[NCS^-] + \frac{k_{-1}[H^+] + k_{-2}K_{a_2}}{(K_{a_2} + [H^+])} + k_{-3}} \quad \textbf{(5.12)}$$

Initial calculations showed that $K_{a2} \approx 6.6$. At pH 2.00 the contributions for K_{a1} (6.23(2) from Figure 5.2) and K_{a2} become negligible so that Equation 5.12 can be simplified to Equation 5.13.

$$\mathbf{k_{obs} = k_1[NCS^-] + k_{-1} + k_3[NCS^-] + k_{-3}} \quad \textbf{(5.13)}$$

The substitution of the second aqua ligand from the coordination sphere (k_3 in Scheme 5.5) is almost a 100 times slower than the first aqua substitution step (k_1 step) so that the rate equation for the formation of $[Co(apda)(H_2O)(NCS)]^-$ and $[Co(apda)(NCS)]^{2-}$ in consecutive substitution steps, but different time scales, can be described by Equations 5.14 and 5.15 respectively.

$$\mathbf{k_{obs} = k_1[NCS^-] + k_{-1}} \quad \textbf{(5.14)}$$

$$\mathbf{k_{obs} = k_3[NCS^-] + k_{-3}} \quad \textbf{(5.15)}$$

Plots of k_{obs} *vs.* $[NCS^-]$ for the first reaction at pH 2.00 and at 15.1, 25.0 and 35.1 ºC are shown in Figure 5.4. Due to the fact that the second reaction is very slow at 15.0 ºC,

plots of k_{obs} *vs.* [NCS^-] for the second substitution reaction at pH 2.00 at 25.0, 35.1 and 45.2 ºC are shown in Figure 5.5. The plots for the first and second reactions were linear (refer to Figures 5.4 and 5.5) and the k_1, k_{-1}, k_3 and k_{-3} values were calculated, see Table 5.1.

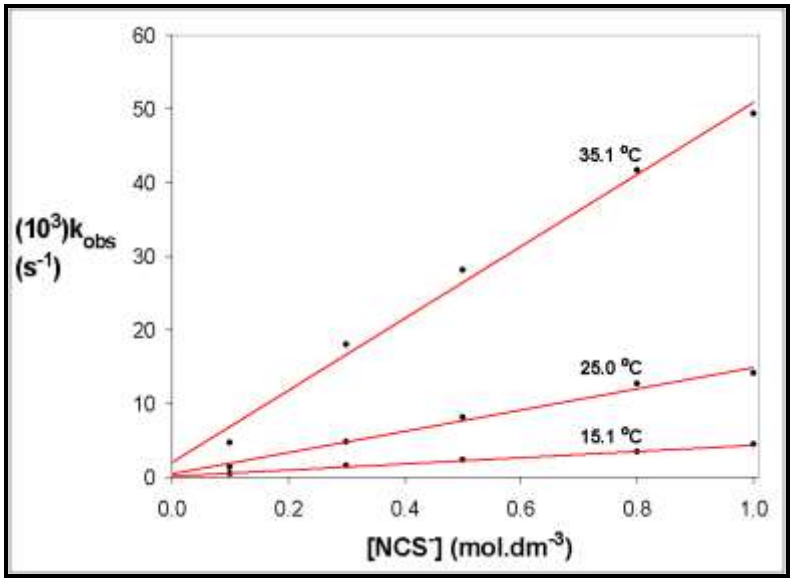

Figure 5.4 Plot of k_{obs} *vs.* [NCS^-] for first reaction (k_1 step, Scheme 5.5) at different temperatures, μ = 1.0 M ($NaClO_4$), λ = 556 nm, [$Co(apda)(H_2O)_2$] = 2.5 x 10^{-3} M.

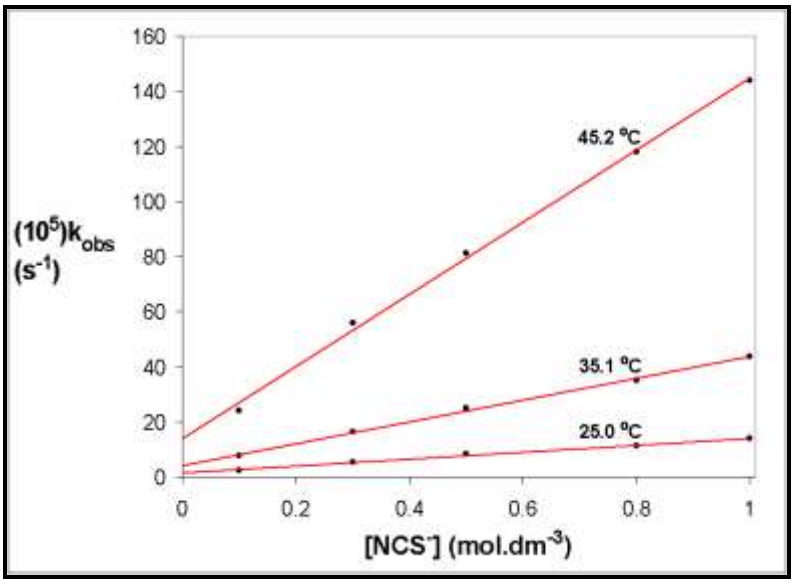

Figure 5.5 Plot of k_{obs} *vs.* [NCS^-] for second reaction (k_3 step, Scheme 5.5) at different temperatures, μ = 1.0 M ($NaClO_4$), λ = 556 nm, [$Co(apda)(H_2O)_2$] = 2.5 x 10^{-3} M.

According to Scheme 5.5 the concentration of $[Co(apda)(H_2O)(OH)]^-$ will increase with an increase in pH. The results in Figure 5.6 clearly indicate an increase in substitution rate with an increase in pH. As mentioned earlier, the UV/VIS spectrum of $[Co(apda)(H_2O)(OH)]^-$ at pH > 7 indicated competing reactions, possibly due to dimer formation. In order to prevent further complication of the reaction scheme it was decided to investigate the reaction between Co(III)-apda and NCS^- ions between pH 2 – 7. This meant that the values of k_2, k_{-2} and pK_{a2} could only be determined from Equation 5.12 and that the influence of the k_1 and k_3 pathways as well as the dissociation constants K_{a1} and K_{a2} could not be ignored under these conditions.

The values of k_2, k_{-2} and pK_{a2} were calculated by fitting the data of a plot of k_{obs} *vs.* $[NCS^-]$ at pH 7.0 (Figure 5.7) simultaneously with the data in Figure 5.6 into Equation 5.12. This was achieved by keeping the values of k_1, k_{-1}, k_3, k_{-3} and pK_{a1}, that was already determined in the previous paragraphs, constant. These results are also reported in Table 5.1.

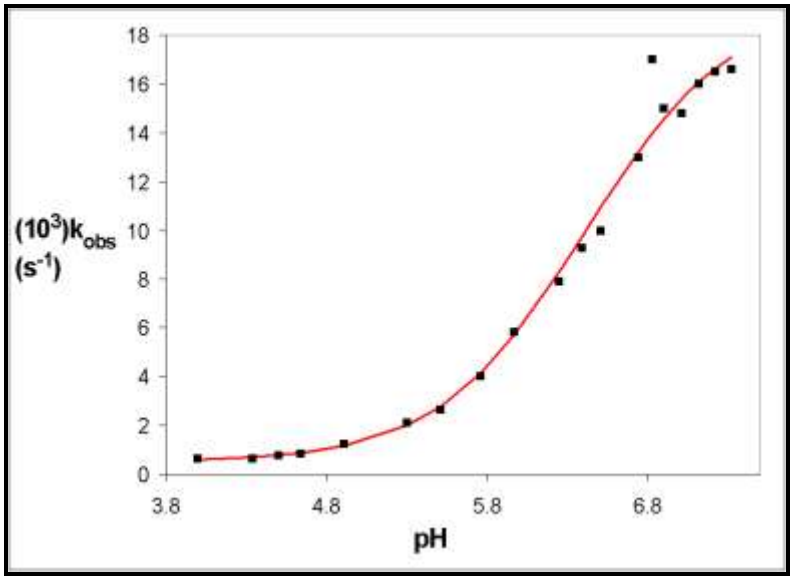

Figure 5.6 Plot of k_{obs} *vs.* pH at 25 ºC $[NCS^-]$ for first reaction between $[Co(apda)(H_2O)_2]$ and NCS^- ions. μ = 1.0 M ($NaClO_4$), λ = 556 nm, $[NCS^-] = 1.0 \times 10^2$ M, $[Co(apda)(H_2O)_2] = 5.0 \times 10^{-4}$ M.

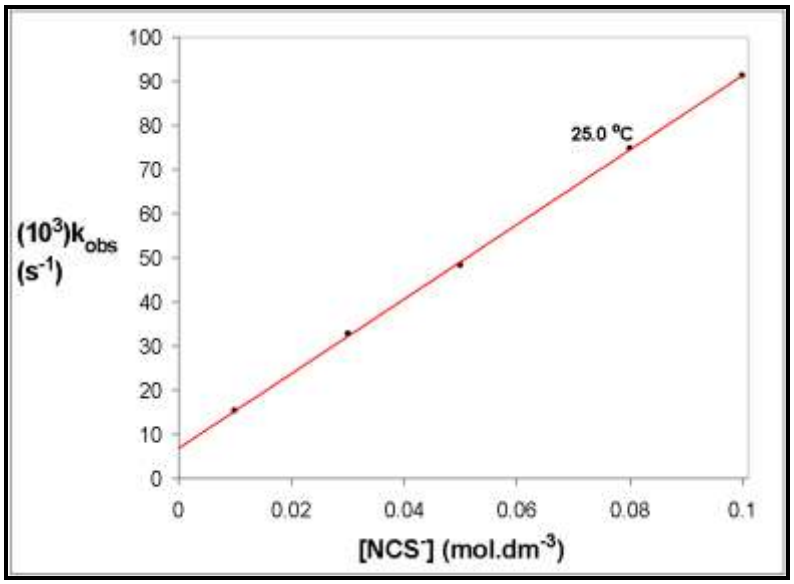

Figure 5.7 Plot of k_{obs} *vs.* $[NCS^-]$ for first reaction at pH = 7.00, 25 ºC, μ = 1.0 M ($NaClO_4$), λ = 556 nm, $[Co(apda)(H_2O)_2] = 5.0 \times 10^{-4}$ M.

The calculation of activation parameters from kinetic data supplies information regarding the reaction mechanism. The Eyring Equation that is used to calculate the activation parameters, $\Delta H^{\#}$ and $\Delta S^{\#}$, is shown in Equation 5.16.

$$\ln\left(\frac{k}{T}\right) = \ln\left(\frac{k_b}{h}\right) + \frac{\triangle S^{\#}}{R} - \frac{\triangle H^{\#}}{RT} \qquad \textbf{(5.16)}$$

In Equation 5.16, T = Temperature in Kelvin, k_b = Boltzman's constant, h = Planck's constant and R = universal gas constant. The activation parameters $\Delta H^{\#}$ and $\Delta S^{\#}$ can be obtained experimentally from a plot of **ln(k/T)** vs. **(1/T)**. The activation enthalpy, $\Delta H^{\#}$, is calculated from the slope **{-$\Delta H^{\#}$/R}** of the graph while the activation entropy, $\Delta S^{\#}$, is calculated from the section **{ln(k_b/h) + ($\Delta S^{\#}$/R)}** of the graph.

Table 5.1 Summary of the rate constants and activation parameters for the reaction between $[Co(apda)(H_2O)_2]$/$[Co(apda)(H_2O)(OH)]^-$ and NCS^- ions.

Temperature (°C)	**15.1**	**25.0**	**35.1**	**45.2**
$(10^3)k_1$ (M^{-1} s^{-1})	4.2(2)	14(1)	48(3)	
$(10^4)k_{-1}$ (s^{-1})	1.2(1)	3.8(6)	19(2)	
K_1 (M^{-1})[a]	35(3)	37(5)	25(4)	
$(10^4)k_3$ (M^{-1} s^{-1})		1.2(6)	3.9(1)	13(4)
$(10^5)k_{-3}$ (s^{-1})		1.6(4)	4.3(6)	14(2)
K_3 (M^{-1})[a]		7.5(6)	9.1(4)	9.3(6)
pK_{a1} (Spectrophotometrically determined)		6.23(2)		
k_2 (M^{-1} s^{-1})		0.986(8)		
$(10^3)k_{-2}$ (s^{-1})		9.5(8)		
K_2 (M^{-1})[a]		103(6)		
pK_{a2} (kinetically determined)		6.6(1)		
$\Delta H^{\#}$ (k_1) (kJ mol^{-1})		80(2)		
$\Delta S^{\#}$ (k_1) (J mol^{-1} K^{-1})		-4.0(2)		

[a] determined as k_n/k_{-n}

From Table 5.1 and the preceeding figures it is clear that the experimental data fits well with the rate law (Equation 5.6) and we conclude that Scheme 5.5 is a fair representation of the mechanism of the substitution reactions between $[Co(apda)(H_2O)_2]$ and NCS^- ions.

The stability constant, K_1, of $[Co(apda)(H_2O)(OH)]^-$ at 25.0 °C was calculated as 37(5) M^{-1}. This value correlates very well with the value of 40(7) obtained by Visser *et al.* (2002:461) for $[Co(nta)(H_2O)(OH)]^-$ at 24.7 °C. The value obtained is almost 70 times smaller than the similar value obtained for $[Co(TPPS)(H_2O)(NCS^-)]^{4-}$ and 160 times smaller than the value obtained for the formation of $[Co(TMpyP)(H_2O)(NCS^-)]^{4+}$ (2.6(4) x 10^3 M^{-1} and 6.4(2) x 10^3 M^{-1}, respectively, Ashley & Leipoldt, 1981:2326) (TPPS and TMpyP are both N donor ligands). The increase in stability for the porphyrine complexes is probably due to the fact that the formal charge on these complexes is spread over a very large planar surface area, which does not exist for the apda or nta complexes. The mode of bonding of the thiocyanide ion is unknown, but one would anticipate that the ligand is nitrogen bonded because of the apparent hard acid character of cobalt(III) (Huheey *et al.*, 2'nd Edition, p278).

The values obtained for K_1 are 2 – 3 times higher than that obtained for K_3 and 2 times lower than the value obtained for K_2. The reason for the higher K_2 value could be expected as the hydroxo ligand will be able to donate more electron density to the metal centre at higher pH, thereby slightly increasing the stability of the complexes at high pH.

The $[Co(apda)(H_2O)(OH)]^-$ complex reacts about 70 times faster at 25.0 °C with NCS^- than the $[Co(apda)(H_2O)_2]$ complex with NCS^- (k_2 = 0.986(8) M^{-1} s^{-1} *vs.* 14(1) x 10^{-3} M^{-1} s^{-1} for k_1 at 25.0 °C). A corresponding increase was observed in the similar reaction of $[Co(nta)(H_2O)(OH)]^-$/$[Co(nta)(H_2O)_2]$ with NCS^- ions (Visser *et al.*, 2002:461). This clearly indicates that the hydroxo ligand labilises the *cis*-aqua bond so than an increase in rate is observed. This *cis*-labilising effect of the hydroxo ligand was also observed in the reaction of $[Cr(nta)(H_2O)(OH)]^-$/$[Cr(nta)(H_2O)_2]$ with NCS^- ions where an increase of 8 times was observed (Visser *et al.* 1994:1051). The same increase was also observed in the formation of $[Co(TPPS)(H_2O)(NCS^-)]^{4-}$ and $[Co(TMpyP)(H_2O)(NCS^-)]^{4+}$ (Ashley & Leipoldt 1981:2326).

The rate of substitution of the first aqua ligand of $[Co(apda)(H_2O)_2]$ (k_1 = 14(1) x 10^{-3} M^{-1} s^{-1} at 25.0 °C) at low pH is about 125 times faster than the rate of substitution of the second aqua ligand (k_3 = 1.2(6) x 10^{-4} M^{-1} s^{-1} at 25.0 °C). The same was observed by Visser *et al.* (2002:461) for the reaction of $[Co(nta)(H_2O)_2]$ with NCS^- ions. They observed that the rate of substitution of the first aqua ligand at low pH was about 120 times faster than the rate of substitution of the second aqua ligand. The reason for this is not well understood, but one would not expect the NCS^- ligand to have a high *cis*-labilising effect on the remaining aqua ligand. It is possible that additional d $\rightarrow$ π^* backbonding for strengthening the Co-NCS bond will enhance the σ–donation of H_2O to Co and thus strengthen this Co-H_2O bond in the ground state. More information, e.g. crystallographic data, is required in order to explain this decrease in rate successfully.

The value of k_1 at 25.0 °C is in the same order of magnitude as the value calculated for the reaction of $[Co(nta)(H_2O)_2]$ with NCS^- ions (k_1 = 2.4(1) x 10^{-2} M^{-1} s^{-1} at 24.7 °C, Visser *et al.* 2002:461) as well as the value calculated for the reaction of

$[Co(TPPS)(H_2O)_2]^{3-}$ with NCS^- ions (k_1 = 3.24(2) x 10^{-2} M^{-1} s^{-1}, Ashley & Leipoldt, 1981:2326) and about 105 times faster than the reaction of $[Co(NH_3)_5(H_2O)]^{3+}$ with NCS^- ions (Van Eldik *et al.*, 1979:1520). This indicates that ligands such as apda and nta exert a very high labilising effect on cobalt(III) complexes. This labilisation can be contributed to the fact that apda donates electron density to the central metal ion which in turn weakens the metal-aqua bond. This also indicates that the electron donating ability of the apda ligand is in the same order of magnitude as that of the porphine ligand. This trend was also observed for the similar Cr(III)-nta complexes (Visser *et al.*, 1994:1051).

In the study by Visser *et al.*, (2002:461) the k_1 value of the substitution of the first aqua ligand in the reaction of $[Co(nta)(H_2O)_2]$ with NCS^- ions was 4 times faster than the k_1 value obtained for the reaction of $[Cr(nta)(H_2O)_2]$ with NCS^- ions (k_1 was determined as 5.8 x 10^{-3} M^{-1} s^{-1} for the chromium complex, Visser *et al.* 1994:1051). The value of k_2 at 24.7 °C (1.68(5) M^{-1} s^{-1}) was approximately 70 times faster than the value obtained for the similar reaction of $[Cr(nta)(H_2O)(OH)]^-$/$[Cr(nta)(H_2O)_2]$ with NCS- ions at 35.0 °C. This indicated that Co(III) complexes are more labile than Cr(III) complexes. This was also observed for several M(III)-porphyrin (M = Co/Cr) complexes (Ashley *et al.*, 1980:1608).

In contrast to the activation enthalpy ($\Delta H^{\#}$), the activation entropy ($\Delta S^{\#}$) supplies more information regarding the reaction mechanism. Positive $\Delta S^{\#}$ values are indicative of a dissociative mechanism while negative $\Delta S^{\#}$ values are indicative of an associative mechanism in most cases. The values for $\Delta H^{\#}$ and $\Delta S^{\#}$ for the substitution of the first aqua ligand (k_1) in the reaction of $[Co(apda)(H_2O)_2]$ with NCS^- ions is 80(2) kJ mol^{-1} and -4.0(2) J mol^{-1} K^{-1}, respectively. The low negative value for $\Delta S^{\#}$ suggests an I_d mechanism. The activation parameters for the substitution of the first aqua ligand (k_1) in the reaction of $[Co(nta)(H_2O)_2]$ with NCS^- ions as well as the reactions of Co(III)-porphyrin complexes suggested an I_d mechanism (Visser *et al.*, 2002:461 and Ashley & Leipoldt, 1981:2326). However, additional information such as high pressure kinetic studies are necessary in order to establish the intimate mechanism of substitution for Co(III)-apda complexes with certainty.

6 Critical evaluation

In this chapter…

The successes of this study and the future research possibilities are discussed in this chapter.

All the initial aims of this study have to a large extent successfully been met. The synthesis and characterisation of $[Co(apda)(H_2O)_2]$ by way of ^1H NMR and IR together with the X-ray crystallographic study by Gladkikh *et al.* (1997:1346) have removed a lot of doubt regarding the Co(III)-apda complex first prepared by Tsuchiya and co-workers (1969:1886). The various Co(III)-apda complexes that were isolated and characterised (Chapters 3 and 4) can successfully be used as biological model complexes in future studies. These complexes could for example be used to simulate the bonding of metal ions to functional groups of wool fibre or might have uses as models in pharmacology.

The new ^1H NMR and IR data of Co(III)-apda complexes should be of assistance in future studies.

The synthesis of $[Co(H_2O)_6][Co(Hapda)_2]\cdot 2H_2O$ at low pH (*ca.* 2) was the first Co(III)-apda complex with two tridentate apda ligands bonded to the same cobalt centre. This complex was also synthesised in the absence of competing ligands. Other Co(III)-apda complexes with apda acting as a tridentate ligand were all prepared in the presence of a competing ligand like diethylenetriamine (Obodovskaya *et al.*, 1992:295).

The strain experienced by the glycinato rings of tridentate bonded apda has been investigated in detail. Comparisons with other studies have been attempted for the first time.

Critical evaluation

Due to the uncoordinated COO^- groups in the $[Co(apda)_2]^{3-}$ complex, the ability of this complex to act as a ligand in other complexes will also be investigated in future studies.

The study of the pH dependence of $[Co(apda)(H_2O)_2]$ and pH dependence of $[Co(apda)_2]^{3-}$ was successful and acid dissociation reaction constants of both these complexes were determined.

The study of the substitution reactions of $[Co(apda)(H_2O)_2]$ with thiocyanide at different pH values in order to determine the mechanism was successful and the value for pK_{a2} (Scheme 5.5) was determined successfully. High pressure kinetic studies will provide more information on the intimate mechanism of these substitution reactions in the future.

Appendix A: Supplementary data

Section I Crystal data

Crystal data for $[Co(H_2O)_6][Co(Hapda)_2]_2H_2O$ (I)

Table A.1 Atomic coordinates ($x10^4$) and equivalent isotropic displacement parameters ($Å^2 \times 10^3$) for (I). U(eq) is defined as one third of the trace of the orthogonalised Uij tensor.

Atom	x	y	z	U(eq)
Co(1)	0	0	0	17(1)
N(1)	1848(2)	615(2)	1188(2)	18(1)
O(1)	739(2)	-1473(2)	-1056(2)	25(1)
O(2)	2754(2)	-2286(2)	-1276(2)	26(1)
O(3)	-934(2)	-1229(2)	678(2)	25(1)
O(4)	-671(2)	-1649(2)	2294(2)	34(1)
O(5)	6028(2)	4726(2)	3989(2)	36(1)
O(6)	4306(3)	5141(2)	2960(2)	39(1)
C(1)	2088(3)	-1396(3)	-697(3)	21(1)
C(2)	2907(3)	-120(3)	482(3)	25(1)
C(3)	-189(3)	-1031(3)	1668(2)	22(1)
C(4)	1357(3)	72(3)	2093(3)	27(1)
C(5)	4771(3)	4306(3)	3215(3)	25(1)
C(6)	4025(3)	2696(3)	2685(3)	24(1)
C(7)	2569(3)	2234(3)	1799(3)	22(1)
Co(1')	5000	10000	5000	19(1)
N(1')	2911(3)	9011(2)	5046(2)	19(1)
O(3')	4309(2)	11526(2)	4978(2)	26(1)
O(4')	2347(2)	12401(2)	5240(2)	33(1)
O(1')	5243(2)	10869(2)	6710(2)	26(1)
O(2')	4232(2)	10558(2)	8210(2)	31(1)
O(5')	-973(3)	4369(3)	3247(2)	43(1)
O(6')	175(3)	5197(2)	2027(2)	46(1)
C(3')	2939(3)	11432(3)	5123(2)	22(1)
C(4')	1991(3)	10020(3)	5100(3)	23(1)
C(1')	4248(3)	10205(3)	7137(3)	23(1)
C(2')	3054(3)	8876(3)	6200(3)	25(1)
C(5')	-20(3)	5343(3)	3027(3)	27(1)
C(6')	795(3)	6665(3)	4166(3)	29(1)
C(7')	2263(3)	7548(3)	4002(3)	25(1)
Co(2)	5000	5000	10000	26(1)
O(7)	5118(3)	3137(2)	10180(2)	30(1)
O(8)	6889(3)	4988(3)	9203(2)	38(1)
O(9)	3506(3)	3706(3)	8333(2)	43(1)
O(10)	1280(3)	6585(3)	483(3)	40(1)

Table A.2 Bond angles (º) for (I).

Bond	Angle (º)	Bond	Angle (º)
O(3)-Co(1)-O(3)#1	180.0(2)	O(3')-Co(1')-N(1')	88.32(9)
O(3)-Co(1)-O(1)	90.54(9)	O(1')-Co(1')-N(1')	85.07(9)
O(3)#1-Co(1)-O(1)	89.46(9)	O(1')#2-Co(1')-N(1')	94.93(9)
O(3)-Co(1)-O(1)#1	89.46(9)	O(3')#2-Co(1')-N(1')#2	88.32(9)
O(3)#1-Co(1)-O(1)#1	90.54(9)	O(1')-Co(1')-N(1')#2	91.68(9)
O(1)-Co(1)-O(1)#1	180.0(2)	O(1')-Co(1')-N(1')#2	94.93(9)
O(3)-Co(1)-N(1)	87.84(9)	O(1')#2-Co(1')-N(1')#2	85.07(9)
O(3)#1-Co(1)-N(1)	92.16(9)	N(1')-Co(1')-N(1')#2	180.00(7)
O(1)-Co(1)-N(1)	87.88(9)	C(2')-N(1')-C(7')	110.8(2)
O(1)#1-Co(1)-N(1)	92.12(9)	C(2')-N(1')-C(4')	110.6(2)
O(3)-Co(1)-N(1)#1	92.16(9)	C(7')-N(1')-C(4')	111.8(2)
O(3)#1-Co(1)-N(1)#1	87.84(9)	C(2')-N(1')-Co(1')	103.7(2)
O(1)-Co(1)-N(1)#1	92.12(9)	C(2')-N(1')-Co(1')	113.2(2)
O(1)#1-Co(1)-N(1)#1	87.88(9)	C(4')-N(1')-Co(1')	106.5(2)
N(1)-Co(1)-N(1)#1	87.88(9)	C(3')-O(3')-Co(1')	115.1(2)
C(4)-N(1)-C(2)	112.5(2)	C(1')-O(1')-Co(1')	114.6(2)
C(4)-N(1)-C(7)	110.3(2)	O(4')-C(3')-C(4')	119.3(3)
C(2)-N(1)-C(7)	110.1(2)	O(3')-C(3')-C(4')	117.1(2)
C(4)-N(1)-Co(1)	105.4(2)	N(1')-C(4')-C(3')	112.3(2)
C(2)-N(1)-Co(1)	104.9(2)	O(2')-C(1')-O(1')	124.9(3)
C(7)-N(1)-Co(1)	113.5(2)	O(2')-C(1')-C(2')	120.0(3)
C(1)-O(1)-Co(1)	114.9(2)	O(1')-C(1')-C(2')	115.1(3)
C(3)-O(3)-Co(1)	115.1(2)	N(1')-C(2')-C(1')	109.3(2)
O(2)-C(1)-O(1)	123.6(3)	O(6')-C(5')-O(5')	108.3(2)
O(2)-C(1)-C(2)	119.7(2)	O(6')-C(5')-C(6')	124.1(3)
O(1)-C(1)-C(2)	116.7(2)	O(5')-C(5')-C(6')	111.8(3)
N(1)-C(2)-C(1)	112.1(2)	C(5')-C(6')-C(7')	112.8(2)
O(4)-C(3)-O(3)	124.4(3)	N(1')-C(7')-C(6')	112.9(2)
O(4)-C(3)-C(4)	119.1(2)	O(8)#3-Co(2)-O(8)	180.000(1)
O(3)-C(3)-C(4)	116.4(2)	O(8)#3-Co(2)-O(7)	90.5(1)
N(1)-C(4)-C(3)	113.0(2)	O(8)-Co(2)-O(7)	89.5(1)
O(6)-C(5)-O(5)	122.8(3)	O(8)#3-Co(2)-O(7)#3	89.5(1)
O(6)-C(5)-C(6)	124.6(3)	O(8)-Co(2)-O(7)#3	90.5(1)
O(5)-C(5)-C(6)	112.6(3)	O(7)-Co(2)-O(7)#3	180.000(1)
C(5)-C(6)-C(7)	111.8(2)	O(8)#3-Co(2)-O(9)	87.0(1)
N(1)-C(7)-C(6)	113.1(2)	O(8)-Co(2)-O(9)	93.0(1)
O(3')#2-Co(1')-O(3')	180.000(1)	O(7)-Co(2)-O(9)	90.8(1)
O(3')#2-Co(1')-O(1')	90.33(9)	O(7)#3-Co(2)-O(9)	89.2(1)
O(3')-Co(1')-O(1')	89.67(9)	O(8)#3-Co(2)-O(9)#3	93.0(1)
O(3')#2-Co(1')-O(1')#2	89.67(9)	O(8)-Co(2)-O(9)#3	86.8(1)
O(3')-Co(1')-O(1')#2	90.33(9)	O(7)-Co(2)-O(9)#3	89.2(1)
O(1')-Co(1')-O(1')#2	180.000(1)	O(7)#3-Co(2)-O(9)#3	90.8(1)
O(3')#2-Co(1')-N(1')	91.68(9)	O(9)-Co(2)-O(9)#3	180.000(1)

Symmetry transformations used to generate equivalent atoms:

$1^{\#}$ -x,-y,-z

$2^{\#}$ -x+1,-y+2,-z+1

$3^{\#}$ -x+1,-y+1,-z+2

Table A.3 Bond lengths (Å) for (I).

Bond	Length (Å)	Bond	Length (Å)
Co(1)-O(3)	1.881(2)	Co(1')-O(1')#2	1.901(2)
Co(1)-O(3)#1	1.881(2)	Co(1')-N(1')	1.973(2)
Co(1)-O(1)	1.881(2)	Co(1')-N(1')#2	1.973(2)
Co(1)-O(1)#1	1.881(2)	N(1')-C(2')	1.491(4)
Co(1)-N(1)	1.976(2)	N(1')-C(7')	1.495(3)
Co(1)-N(1)#1	1.976(2)	N(1')-C(4')	1.501(3)
N(1)-C(4)	1.494(3)	O(3')-C(3')	1.275(3)
N(1)-C(2)	1.495(3)	O(4')-C(3')	1.236(3)
N(1)-C(7)	1.501(3)	O(1')-C(1')	1.283(3)
O(1)-C(1)	1.274(3)	O(5')-C(5')	1.308(4)
O(2)-C(1)	1.246(3)	O(6')-C(5')	1.209(4)
O(3)-C(3)	1.281(3)	C(3')-C(4')	1.517(4)
O(4)-C(3)	1.235(3)	C(1')-C(2')	1.515(4)
O(5)-C(5)	1.320(4)	C(5')-C(6')	1.501(4)
O(6)-C(5)	1.207(3)	C(6')-C(7')	1.520(4)
C(1)-C(2)	1.509(4)	Co(2)-O(8)	2.051(2)
C(3)-C(4)	1.508(4)	Co(2)-O(8)#3	2.051(2)
C(6)-C(7)	1.526(4)	Co(2)-O(7)	2.091(2)
Co(1')-O(3')#2	1.879(2)	Co(2)-O(7)#3	2.091(2)
Co(1')-O(3')	1.879(2)	Co(2)-O(9)	2.115(2)
Co(1')-O(1')	1.901(2)	Co(2)-O(9)#3	2.115(2)

Table A.4 Anisotropic displacement parameters ($Å^2 \times 10^3$) for (I).

Atom	U_{11}	U_{22}	U_{33}	U_{23}	U_{13}	U_{12}
Co(1)	16(1)	18(1)	17(1)	8(1)	2(1)	4(1)
N(1)	19(1)	17(1)	18(1)	7(1)	3(1)	4(1)
O(1)	20(1)	24(1)	23(1)	3(1)	0(1)	8(1)
O(2)	24(1)	25(1)	26(1)	6(1)	5(1)	10(1)
O(3)	22(1)	28(1)	26(1)	16(1)	1(1)	-1(1)
O(4)	33(1)	38(1)	30(1)	23(1)	2(1)	-3(1)
O(5)	25(1)	25(1)	43(1)	8(1)	-8(1)	-2(1)
O(6)	49(2)	24(1)	36(1)	11(1)	-8(1)	7(1)
C(1)	21(1)	21(1)	23(2)	12(1)	5(1)	5(1)
C(2)	19(2)	26(2)	24(2)	5(1)	1(1)	8(1)
C(3)	25(2)	21(2)	19(2)	9(1)	5(1)	7(1)
C(4)	26(2)	30(2)	23(2)	16(1)	1(1)	-1(1)
C(5)	23(2)	26(2)	22(2)	9(1)	5(1)	5(1)
C(6)	24(2)	22(2)	24(2)	9(1)	0(1)	3(1)
C(7)	22(2)	18(1)	24(2)	9(1)	1(1)	3(1)
Co(1')	14(1)	19(1)	19(1)	6(1)	2(1)	4(1)
N(1')	18(1)	19(1)	19(1)	6(1)	4(1)	5(1)
O(3')	20(1)	23(1)	35(1)	11(1)	5(1)	7(1)
O(4')	26(1)	28(1)	48(2)	16(1)	9(1)	13(1)
O(1')	22(1)	27(1)	20(1)	6(1)	0(1)	-1(1)
O(2')	37(1)	31(1)	20(1)	9(1)	2(1)	4(1)

Table A.4 continued

O(5')	43(2)	34(1)	27(1)	6(1)	5(1)	-15(1)
O(6')	58(2)	37(1)	23(1)	8(1)	5(1)	-10(1)
C(3')	23(2)	23(2)	16(2)	5(1)	1(1)	6(1)
C(4')	17(1)	27(2)	26(2)	10(1)	5(1)	9(1)
C(1')	22(2)	22(2)	25(2)	11(1)	3(1)	9(1)
C(2')	22(2)	27(2)	24(2)	11(1)	2(1)	4(1)
C(5')	22(2)	24(2)	29(2)	8(1)	4(1)	3(1)
C(6')	27(2)	27(2)	24(2)	5(1)	6(1)	1(1)
C(7')	21(2)	21(2)	24(2)	3(1)	4(1)	3(1)
Co(2)	25(1)	25(1)	29(1)	11(1)	5(1)	7(1)
O(7)	34(1)	25(1)	30(1)	11(1)	3(1)	10(1)
O(8)	37(1)	51(2)	42(2)	29(1)	17(1)	22(1)
O(9)	35(2)	46(2)	31(1)	14(1)	2(1)	-8(1)
O(10)	42(2)	40(1)	41(2)	21(1)	9(1)	11(1)

Table A.5 Hydrogen coordinates ($\times 10^4$) and isotropic displacement parameters ($Å^2 \times 10^3$) for (I).

Atom	x	y	z	U(eq)
H(5)	$6.47(4) \times 10^3$	$5.62(3) \times 10^3$	$4.23(3) \times 10^3$	$6(1) \times 10^1$
H(2A)	3441	-457	958	30
H(2B)	3653	577	320	30
H(4A)	1344	891	2834	32
H(4B)	2090	-365	2272	32
H(6A)	3793	2418	3329	29
H(6B)	4721	2189	2271	29
H(7A)	1853	2695	2228	27
H(7B)	2794	2577	1190	27
H(5')	$-1.50(4) \times 10^3$	$3.72(4) \times 10^3$	$2.58(3) \times 10^3$	$6(1) \times 10^1$
H(2C)	1529	10238	5816	28
H(2D)	1184	9537	4404	28
H(4C)	3339	8006	6075	30
H(4D)	2090	8795	6479	30
H(6C)	1018	6364	4785	35
H(6D)	136	7278	4441	35
H(7C)	2999	7010	3893	30
H(7D)	2076	7673	3276	30
H(7E)	$4.87(5) \times 10^3$	$2.41(3) \times 10^3$	$9.53(2) \times 10^3$	$7(2) \times 10^1$
H(7F)	$5.89(3) \times 10^3$	$3.11(4) \times 10^3$	$10.50(3) \times 10^3$	$5(1) \times 10^1$
H(8A)	$6.81(5) \times 10^3$	$4.95(5) \times 10^3$	$8.52(2) \times 10^3$	$7(2) \times 10^1$
H(8B)	$7.40(4) \times 10^3$	$4.48(4) \times 10^3$	$9.26(4) \times 10^3$	$8(2) \times 10^1$
H(9A)	$3.79(5) \times 10^3$	$3.56(5) \times 10^3$	$7.69(2) \times 10^3$	$9(2) \times 10^1$
H(9B)	$2.69(2) \times 10^3$	$3.10(3) \times 10^3$	$8.20(4) \times 10^3$	$6(1) \times 10^1$
H(10A)	$0.78(5) \times 10^3$	$6.13(4) \times 10^3$	$-0.19(2) \times 10^3$	$8(2) \times 10^1$
H(10B)	$0.67(4) \times 10^3$	$6.46(5) \times 10^3$	$0.92(4) \times 10^3$	$9(2) \times 10^1$

Table A.6 Hydrogen bonds for (I) (Å and °).

D-H…A	d(D-H) (Å)	d(H...A) (Å)	d(D...A) (Å)	<(DHA) (°)
O(5)-H(5)...O(4')#2	0.84(3)	1.91(3)	2.752(3)	175(4)
O(5')-H(5')...O(2)#1	0.85(3)	1.78(3)	2.621(3)	173(4)
O(5')-H(5')...O(1)#1	0.85(3)	2.64(4)	3.211(3)	126(3)
O(7)-H(7E)...O(2')#4	0.82(1)	1.88(3)	2.693(3)	169(4)
O(7)-H(7F)...O(2)#5	0.81(3)	2.08(4)	2.844(3)	157(4)
O(8)-H(8A)...O(6)#6	0.82(3)	2.01(2)	2.771(3)	155(4)
O(8)-H(8B)...O(10)#6	0.82(4)	1.94(4)	2.757(4)	175(5)
O(9)-H(9A)...O(6)#6	0.82(3)	2.34(3)	2.973(4)	135(4)
O(9)-H(9B)...O(4)#7	0.82(3)	1.98(3)	2.789(3)	173(4)
O(10)-H(10A)...O(6')#8	0.82(3)	2.11(3)	2.914(4)	169(5)
O(10)-H(10B)...O(6')	0.83(4)	2.26(3)	2.928(4)	138(4)

Symmetry transformations used to generate equivalent atoms:

$1^{\#}$ -x,-y,-z

$2^{\#}$ -x+1,-y+2,-z+1

$3^{\#}$ -x+1,-y+1,-z+2

$4^{\#}$ x,y-1,z

$5^{\#}$ -x+1,-y,-z+1

$6^{\#}$ -x+1,-y+1,-z+1

$7^{\#}$ -x,-y,-z+1

$8^{\#}$ -x,-y+1,-z

Section II Kinetic data

The tables in this section give the observed first-order rate constant for the reactions described in Chapter 5. Where applicable, the figure number representing a specific data set is included in brackets after the Table number.

Table A.7 (Figure 5.1) Plot of Abs (λ = 348 nm) *vs.* pH for $Na[Co(Hapda)_2]xH_2O$ (4.5×10^{-3} M), 25 ºC, μ = 1.0 M ($NaClO_4$).

pH	A	pH	A
5.28	0.5322	2.62	0.4250
4.99	0.5318	2.56	0.4133
4.82	0.5306	2.48	0.4026
4.67	0.5301	2.42	0.3973
4.51	0.5311	2.28	0.3938
4.38	0.5281	2.23	0.3908
4.24	0.5273	2.19	0.3841
4.07	0.5248	2.13	0.3810
3.98	0.5226	2.10	0.3801
3.84	0.5184	2.06	0.3783
3.74	0.5174	1.99	0.3767
3.62	0.5128	1.93	0.3751
3.53	0.5066	1.86	0.3687
3.34	0.5004	1.82	0.3680
3.27	0.4965	1.75	0.3672
3.14	0.4847	1.67	0.3638
3.01	0.4683	1.61	0.3642
2.86	0.4538	1.46	0.3613
2.80	0.4479	1.27	0.3578
2.71	0.4361	0.98	0.3581

Table A.8 Potentiometric titration data, $Na[Co(Hapda)_2]xH_2O$ = 1×10^{-2} M, (5×10^{-4} mol).

$HClO_4$ (1.0 M) (cm^{-3})	$HClO_4$ (10^4 mol)	pH	$HClO_4$ (1.0 M) (cm^{-3})	$HClO_4$ (10^4 mol)	pH
0.000	0.0	4.44	0.550	5.5	2.55
0.050	0.5	4.28	0.600	6.0	2.43
0.100	1.0	4.11	0.650	6.5	2.33
0.150	1.5	3.95	0.700	7.0	2.24
0.200	2.0	3.87	0.750	7.5	2.18
0.250	2.5	3.72	0.800	8.0	2.11
0.300	3.0	3.53	0.850	8.5	2.06
0.350	3.5	3.36	0.900	9.0	2.02
0.400	4.0	3.19	0.950	9.5	1.97
0.450	4.5	2.91	1.000	10.0	1.93
0.500	5.0	2.72			

Table A.9 (Figure 5.2) Plot of Abs (λ = 559 nm) *vs.* pH for $[Co(apda)(H_2O)_2]$ (8 x 10^{-3} M), 25 ºC, μ = 1.0 M ($NaClO_4$).

pH	A	pH	A
4.30	0.7896	5.78	0.7093
4.36	0.7878	5.83	0.7066
4.44	0.7850	5.89	0.6984
4.63	0.7803	5.97	0.6894
4.65	0.7784	6.15	0.6701
4.68	0.7761	6.21	0.6605
4.76	0.7729	6.28	0.6503
4.83	0.7711	6.35	0.6433
4.89	0.7684	6.45	0.6300
4.96	0.7656	6.52	0.6213
5.01	0.7631	6.60	0.6102
5.07	0.7603	6.73	0.5933
5.13	0.7565	6.88	0.5770
5.20	0.7534	6.95	0.5709
5.25	0.7503	7.22	0.5520
5.27	0.7491	7.30	0.5478
5.44	0.7394	7.44	0.5414
5.47	0.7376	7.64	0.5380
5.52	0.7311	7.80	0.5342
5.57	0.7262	7.95	0.5301
5.64	0.7202		

Table A.10 (Figure 5.4) Plot of k_{obs} *vs.* $[NCS^-]$ for first reaction (k_1 step, Scheme 5.5) at different temperatures, μ = 1.0 M ($NaClO_4$), λ = 556 nm, $[Co(apda)(H_2O)_2]$ = 2.5 x 10^{-3} M.

$[NCS^-]$ ($mol.dm^{-3}$)	**(10^3) k_{obs} (s^{-1})**		
	15.1	**25.0**	**35.1**
0.1	0.44(1)	1.35(6)	4.7(1)
0.3	1.52(4)	4.8(3)	18.0(1)
0.5	2.3(1)	8.1(1)	28.1(3)
0.8	3.4(1)	12.6(2)	41.7(8)
1.0	4.4(2)	14.1(1)	49.3(4)

Table A.11 (Figure 5.5) Plot of k_{obs} *vs.* [NCS^-] for second reaction (k_3 step, Scheme 5.5) at different temperatures, μ = 1.0 M ($NaClO_4$), λ = 556 nm, [$Co(apda)(H_2O)_2$] = 2.5 x 10^{-3} M.

[NCS^-] ($mol.dm^{-3}$)	**(10^5) k_{obs} (s^{-1})**		
	25.0	**35.1**	**45.2**
0.1	2.5(1)	7.8(1)	24.2(5)
0.3	5.3(2)	16.3(1)	56.0(3)
0.5	8.4(4)	24.8(2)	81(2)
0.8	11.3(3)	35.2(3)	118(2)
1.0	13.8(4)	43.8(4)	143(3)

Table A.12 (Figure 5.6) Plot of k_{obs} *vs.* pH at 25 ºC [NCS^-] for first reaction between [$Co(apda)(H_2O)_2$] and NCS^- ions. μ = 1.0 M ($NaClO_4$), λ = 556 nm, [NCS^-] = 1.0 x 10^2 M, [$Co(apda)(H_2O)_2$] = 5.0 x 10^{-4} M.

PH	**(10^3) k_{obs} (s^{-1})**	**pH**	**(10^3) k_{obs} (s^{-1})**
4.00	0.62(2)	6.39	9.3(5)
4.34	0.64(5)	6.51	10(2)
4.50	0.775(6)	6.74	13(1)
4.64	0.84(1)	6.83	17(3)
4.91	1.23(4)	6.90	15(4)
5.30	2.1(2)	7.01	14.8(8)
5.51	2.64(6)	7.12	16(3)
5.76	4.0(4)	7.22	16.5(7)
5.97	5.8(1)	7.32	16.6(8)
6.25	7.9(4)		

Table A.13 (Figure 5.7) Plot of k_{obs} *vs.* [NCS^-] for first reaction at pH = 7.00, 25 ºC, μ = 1.0 M ($NaClO_4$), λ = 556 nm, [$Co(apda)(H_2O)_2$] = 5.0 x 10^{-4} M.

[NCS^-] ($mol.dm^{-3}$)	**(10^3) k_{obs} (s^{-1})**
0.01	1.50(4)
0.03	3.2(2)
0.05	4.9(1)
0.08	7.5(3)
0.10	9.2(4)

Section III Theoretical aspects of kinetics

Spectrophotometric determination of ionisation constants:

For diprotic species:

$$H_2A \underset{}{\overset{K_{a1}'}{\rightleftharpoons}} HA^- + H^+ \overset{K_{a2}'}{\rightleftharpoons} A^{2-} + H^+ \qquad \textbf{(A.1)}$$

The observed absorption coefficient, ε at the analytical wavelength for a given pH value, when all three species are present, is

$$\varepsilon = \varepsilon_{A^{2-}} \cdot F_{A^{2-}} + \varepsilon_{HA^-} \cdot F_{HA^-} + \varepsilon_{H_2A} F_{H_2A} \qquad \textbf{(A.2)}$$

where $\varepsilon_{A^{2-}}$, ε_{HA^-} and ε_{H_2A} are the molar absorption coefficients for the *di*protonated, *mono*protonated and *non*protonated species, respectively. The fractions of these species present are given by

$$F_{H_2A} = [H^+]^2/G \qquad \textbf{(A.3)}$$

$$F_{HA^-} = K_{a1}'[H^+]/G \qquad \textbf{(A.4)}$$

$$F_{A^{2-}} = K_{a1}'K_{a2}'/G \qquad \textbf{(A.5)}$$

Where G, the denominator, is $[H^+]^2 + K_{a1}'[H^+] + K_{a1}'K_{a2}'$. Substituting these relevant factors into the total molar absorption coefficient equation, multiplying with the denominator and rearranging, yields

$$[H^+]^2(\varepsilon - \varepsilon_{H_2A}) + K_{a1}'[H^+](\varepsilon - \varepsilon_{HA^-}) + K_{a1}'K_{a2}'(\varepsilon - \varepsilon_{A^{2-}}) = 0 \qquad \textbf{(A.6)}$$

Provided that the same total concentration is used for all measurements, the expression may be written with the appropriate absorbance (A) replacing the molar absorption (ε).

The equation can then be arranged to:

$$[H^+]^2(A_{tot} - A_{H_2A}) + K_{a1}'[H^+](A_{tot} - A_{HA^-}) + K_{a1}'K_{a2}'(A_{tot} - A_{A^{2-}}) = 0 \quad \textbf{(A.7)}$$

Rearrangement of this expression after dividing this equation by $[H^+]^2$ throughout gives:

$$A_{tot} = \frac{A_{H_2A} + A_{HA^-}(K_{a1}'/[H^+]) + A_{A^{2-}}(K_{a1}'K_{a2}'/[H^+]^2)}{1 + K_{a1}'/[H^+] + K_{a1}'K_{a2}'/[H^+]^2} \quad \textbf{(A.8)}$$

For monoprotic species:

$$HB \overset{K_{a1}}{\rightleftharpoons} B^- + H^+ \quad \textbf{(A.9)}$$

The total absorbance A_{tot} is the sum of the ionised species, A_{B^-}, and the molecular species, A_{HB}.

$$A_{tot} = A_{HB} + A_{B^-} \quad \textbf{(A.10)}$$

The absorbance of either component is related to its molar concentration (c) by a general expression ($A = \varepsilon lc$), where ε is the molar absorption coefficient of the particular species and l is the optical length of the cell. The concentration of the ionised species in the mixture is $F_{B^-}c$, where F_{B^-} is the fraction ionised. Equation A.11 gives the fraction ionised for acids.

$$F_{B^-} = [B^-]/([B^-] + [HB]) \quad \textbf{(A.11)}$$

Hence the contribution of F_{B^-} to the observed absorbance of the mixture is $\varepsilon_B F_B lc$. Similarly the contribution of the molecular species to the observed absorbance of the mixture is $\varepsilon_{HB}F_{HB}lc$, where F_{HB} is the fraction present in the molecular form. The terms

ε_{HB} and ε_{B^-} are the molar absorption coefficients of the molecular and ionised species, respectively, which are related directly to absorbance. The ionisation constant is defined by the expression:

$$K_{a1} = \frac{[H^+][B^-]}{[HB]} \qquad \textbf{(A.12)}$$

The fractions of ionised and molecular species are then given by expressions obtained by replacing [HB] with $[H^+][B^-]/K_{a1}$:

$$F_{B^-} = K_{a1}/([H^+] + K_{a1}) \qquad \textbf{(A.13)}$$

$$F_{HB} = [H^+]/([H^+] + K_{a1}) \qquad \textbf{(A.14)}$$

If the same cell optical length is used throughout then

$$A = (\varepsilon_{B^-} \cdot F_{B^-} + \varepsilon_{HB} \cdot F_{HB}) \qquad \textbf{(A.15)}$$

and therefore, because $\varepsilon = A/c$, and F_{B^-} and F_{HB} are defined above,

$$\varepsilon = ((\varepsilon_{B^-} \cdot K_{a1})/([H^+] + K_{a1})) + ((\varepsilon_{HB} \cdot [H^+])/([H^+] + K_{a1})) \qquad \textbf{(A.16)}$$

Provided that the same total concentration is used for all measurements, the expression may be written with the appropriate absorbance (A) replacing the molar absorption (ε). The equation can then be arranged to:

$$A_{tot} = \frac{A_{HB} + A_{B^-}(K_{a1}/[H^+])}{1 + (K_{a1}/[H^+])} \qquad \textbf{(A.17)}$$

Pseudo-first-order reactions (mono-variation)

The rate of a reaction is defined by the change in concentration of any of the reacting species per time unit. For the reaction

$$A + B \xrightarrow{k} C \qquad \textbf{(A.18)}$$

the rate can be expressed in terms of the disappearance of A or B or in terms of the formation of C, as shown in Equation A.19.

$$\text{Rate} = \frac{-d[A]}{dt} = \frac{-d[B]}{dt} = \frac{d[C]}{dt} \qquad \textbf{(A.19)}$$

Equation A.20 is representative of a typical rate law for Reaction A.18, if the rate of the reaction is only dependent on the concentrations of A and B.

$$\text{Rate} = k[A]^a[B]^b \qquad \textbf{(A.20)}$$

In Equation A.20, k represents the rate constant whilst a and b represents the order of the reaction with respect to the concentrations of A and B. The total order of the reaction is given by the sum of a and b. If a reaction proceeds by more than one step, the order of the reaction is determined by the reactions that precede the rate-determining step.

It is often impossible to determine the order of the reaction with respect to the different reactants in one kinetic experiment. The problem can be solved to a large extent by the method of mono-variation (isolation). This type of experiment is conducted where [A] << [B], which causes [B] to be constant during the whole reaction. The rate of this reaction is presented in Equation A.21.

$$\text{Rate} = k_{obs}[A]^a \qquad \textbf{(A.21)}$$

In Equation A.21, k_{obs} is the observed rate constant with

$$k_{obs} = k[B]^b \quad \textbf{(A.22)}$$

It often happens that a = 1, which means that the kinetics of Reaction A.18 simplifies to that of a first order reaction where k_{obs} is the pseudo-first-order rate constant.

In practice k_{obs} is determined at different concentrations of [B]. If the reaction were first-order with respect to [B], a plot of k_{obs} versus [B] would, according to Equation A.22, produce a straight line though the origin. The slope of the graph then gives the second-order rate constant.

If the straight line does not pass through the origin of the graph it indicates that there is a second reaction independent of [B]. The rate of the reaction is then given by Equation A.23.

$$\text{Rate} = k_1[A][B] + k_2[A] \quad \textbf{(A.23)}$$

From Equation A.23 and the above discussion, the pseudo-first-order reaction constant is given by Equation A.24.

$$k_{obs} = k_1[B] + k_2 \quad \textbf{(A.24)}$$

A plot of k_{obs} vs. [B] would produce a straight line with slope k_1 and a section of k_2.

Appendix B: Hazardous Chemicals

β-Alanine 

Physical state; Appearance:

White crystalline powder.

Physical dangers:

May act as an irritant.

Ammonium Hydroxide   

Physical state; Appearance:

Very volatile, colourless solution of ammonia in water, with pungent odour.

Chemical dangers:

Reacts with many heavy metals and their salts forming explosive compounds. Attacks many metals forming flammable/explosive gas. The solution in water is a strong base, it reacts violently with acids.

Routes of exposure:

The substance can be absorbed into the body by inhalation of its vapour or aerosol and by ingestion.

Inhalation risk:

A harmful contamination of the air can be reached very quickly on evaporation of this substance at 20 °C.

Effects of short-term exposure:

The substance is corrosive to the eyes, the skin and the respiratory tract. Corrosive on ingestion as well. Inhalation of high concentrations of vapour may cause laryngeal oedema, inflammation of the respiratory tract, and pneumonia. The effects may be delayed.

Effects of long-term exposure:

Lungs may be affected by repeated or prolonged exposure to the vapour or aerosol.

Chloroacetic Acid

Physical state; Appearance:

Colourless, hygroscopic crystals, with pungent odour.

Chemical dangers:

The substance decomposes on burning producing toxic fumes including hydrogen chloride, phosgene. The solution in water is a medium strong acid. Attacks metal.

Routes of exposure:

The substance can be absorbed into the body by inhalation and through the skin and by ingestion.

Inhalation risk:

No indication can be given about the rate in which a harmful concentration in the air is reached on evaporation of this substance at 20 °C.

Effects of short-term exposure:

The substance is corrosive to the eyes, the skin and the respiratory tract. Inhalation of aerosol may cause lung oedema. The substance may cause effects on the cardiovascular system and central nervous system, resulting in cardiac disorders, convulsions and kidney

impairment. Exposure at high levels may result in death. The effects may be delayed. Medical observation is indicated.

Cobalt(II)-chloride

Physical state; appearance:

Purple, hygroscopic crystals.

Chemical dangers:

Reacts violently with alkali metals such as potassium and sodium causing a fire and explosion hazard.

Routes of exposure:

The substance can be absorbed into the body by inhalation of its aerosol and by ingestion.

Inhalation risk:

Evaporation at 20 °C is negligible; a harmful concentration of airborne particles can, however, be reached quickly when dispersed.

Effects of short-term exposure:

The substance irritates the eyes, the skin and the respiratory tract. Inhalation of aerosol may cause asthmatic reactions.

Effects of long-term exposure:

Repeated or prolonged contact may cause skin sensitisation. Repeated or prolonged inhalation exposure may cause asthma. The substance may have effects on the heart, resulting in cardiomyopathy. This substance is possibly carcinogenic to humans.

Ethanol

Physical state; Appearance:

Colourless liquid, with characteristic odour.

Physical dangers:

The vapour mixes well with air and explosive mixtures are easily formed.

Chemical dangers:

Reacts slowly with calcium hypochlorite, silver oxide and ammonia, causing fire and explosion hazard. Reacts violently with strong oxidants such as nitric acid, silver nitrate, mercuric nitrate or magnesium perchlorate, causing fire and explosion hazard.

Routes of exposure:

The substance can be absorbed into the body by inhalation of its vapour and by ingestion. Inhalation risk. A harmful contamination of the air will be reached rather slowly on evaporation of this substance at 20 °C.

Effects of short-term exposure:

The substance irritates the eyes. Inhalation of high concentration of vapour may cause irritation of the eyes and respiratory tract. The substance may cause effects on the central nervous system.

Effects of long-term or repeated exposure:

The liquid defats the skin. The substance may have effects on the upper respiratory tract and central nervous system, resulting in irritation, headache, fatigue and lack of concentration.

Hydrochloric Acid

Physical state; Appearance:

Colourless liquid, with pungent odour.

Physical dangers:

Corrosive acid.

Chemical dangers:

The solution in water is a strong acid, it reacts violently with bases and is corrosive. Reacts violently with oxidants forming toxic gas. Attacks many metals in the presence of water, forming combustible gas.

Routes of exposure:

The substance can be absorbed into the body by inhalation.

Inhalation risk:

A harmful concentration of this gas in the air will be reached very quickly on loss of containment.

Effects of short-term exposure:

Rapid evaporation of the liquid may cause frostbite. The substance is corrosive to the eyes, the skin and the respiratory tract. Inhalation of high concentrations of the gas may cause pneumonitis and lung oedema, resulting in reactive airways dysfunction syndrome (RADS). The effects may be delayed. Medical observation is indicated.

Effects of long-term or repeated exposure:

The substance may have effects on the lungs, resulting in chronic bronchitis. The substance may have effects on the teeth, resulting in erosion.

Hydrogen Peroxide



Physical state; Appearance:

Colourless liquid.

Chemical dangers:

The substance decomposes on warming or under influence of light producing oxygen, which increases fire hazard. The substance is a strong oxidant and reacts violently with combustible and reducing materials causing fire and explosion hazard particularly in the presence of metals. Attacks many organic substances, e.g., textile and paper.

Routes of exposure:

The substance can be absorbed into the body by inhalation of its vapour and by ingestion.

Inhalation risk:

A harmful contamination of the air can be reached rather quickly on evaporation of this substance at 20 °C.

Effects of short-term exposure:

The substance is corrosive to the eyes and the skin. The vapour irritates the respiratory tract. Ingestion of this substance may produce oxygen bubbles (embolism) in the blood, resulting in shock.

Effects of long-term or repeated exposure:

Lungs may be affected by inhalation of high concentrations. The substance may have effects on the hair, resulting in bleaching.

Nitrogen

Physical state; Appearance:

Odourless, colourless compressed gas.

Physical dangers:

Gas mixes readily with air.

Routes of exposure:

The substance can be absorbed into the body by inhalation.

Inhalation risk:

On loss of containment this gas can cause suffocation by lowering the oxygen content of the air in confined areas.

Perchloric acid

Physical state; Appearance:

Colourless liquid, with pungent odour.

Chemical dangers:

May explode on heating. The substance decomposes on heating producing toxic and corrosive fumes. The substance is a strong oxidant and reacts violently with combustible and reducing materials, organic materials and strong bases, causing fire and explosion hazard. Attacks many metals forming flammable/explosive gas. The acid is unstable if the concentration is over 72 %; may explode by shock or concussion when dry or drying. Mixtures with combustible material (such as paper) may ignite spontaneously at room temperature.

Routes of exposure:

The substance can be absorbed into the body by inhalation and by ingestion.

Inhalation risk:

No indication can be given about the rate in which a harmful concentration in the air is reached on evaporation of this substance at 20 °C.

Effects of short-term exposure:

Corrosive. The vapour is very corrosive to the eyes, the skin and the respiratory tract. Inhalation of vapour or mist may cause lung oedema. The effects may be delayed. Medical observation is indicated.

Potassium Bicarbonate

Physical state; Appearance:

White powder or granules.

Routes of exposure:

The substance can be absorbed into the body by inhalation of its aerosol and by ingestion.

Inhalation risk:

May cause respiratory tract irritation.

Effects of short-term exposure:

Irritation.

Potassium and Sodium Hydroxide


Physical state; Appearance:

White, deliquescent solid, with no odour.

Chemical dangers:

The substance is a strong base, it reacts violently with acid and is corrosive in moist air to metals such as zinc, aluminium, tin and lead forming a combustible/explosive gas. Reacts with ammonium salts to produce ammonia and causing fire hazard. Attacks some forms of plastics, rubber or coatings. Rapidly absorbs carbon dioxide and water from air. Contact with moisture or water will generate heat.

Routes of exposure:

The substance can be absorbed into the body by inhalation of its aerosol and by ingestion.

Inhalation risk:

Evaporation at 20 °C is negligible; a harmful concentration of airborne particles can, however, be reached quickly.

Effects of short-term exposure:

Corrosive. The substance is very corrosive to the eyes, the skin and the respiratory tract. Corrosive on ingestion. Inhalation of an aerosol of this substance may cause lung oedema.

Effects of long-term or repeated exposure:

Repeated or prolonged contact with skin may cause dermatitis.

Bibliography

ALMAZAN, F., GARCIA-ESPANA, E., MOLLAR, M., LLORET, F., JULVE, M., FAUS, J., SOLANS, X. and ALINS, N., 1990. *J. Chem. Soc. Dalton Trans.,* p. 2565.

ASHLEY, K.R., LEIPLODT, J.G. and JOSHI, V.K., 1980. *Inorg. Chem.,* 19:1608.

ASHLEY, K.R. & LEIPLODT, J.G., 1981. *Inorg. Chem.,* 20:2326.

BATTAGLIA, L.P., CORRADI, A.B. and TANI, M.E.V., 1975. *Acta Cryst.,* B31:1160.

BESWICK, C.L., SHALDERS, R.D. and SWADDLE, T.W., 1996. *Inorg. Chem.,* 35:1991.

BHATTACHARYYA, S.K. & BANJEREE, R., 1997. *Polyhedron,* 16:849.

BHATTACHARYYA, S.K. & BANJEREE, R., 1997. *Polyhedron,* 16:4217.

BOCARSLEY, J.R. & BARTON, J.K., 1992. *Inorg. Chem.,* 31:2827.

BOCARSLY, J.R., CHIANG, M.Y., BRYANT, L. and BARTON, J.K., 1990. *Inorg. Chem.,* 29:4898.

BRANDENBURG, K., & BERNDT, M., 1998. Visual Crystal Structure Information System, Version 2.1, Germany.

BRUKER (1999), *SAINT+*. Version 6.02 (includes XPREP and SADABS). Bruker AXS INC., Madison, Wisconsin, USA.

BRUKER (1999), *SHELXTL*. Version 5.1 (includes XS, XL, XP, XSHELL). Bruker AXS INC., Madison, Wisconsin, USA.

COOPER, J.A., BLACKWELL, L.F. and BUCKLEY, P.D., 1984. *Inorg. Chim. Acta,* 92:23.

CREMER, D. & POPLE, J.A., 1975. *J. Am. Chem. Soc.,* 97:1354.

DASGUPTA, T.P. & HARRIS, G.M., 1974. *Inorg. Chem.,* 13:1275.

DEMAINE, M.M. & HUNT, J.B., 1971. *Inorg. Chem.,* 10:2106.

DUNG, N.H., VIOSSAT, B. and BUSNOT, A., 1987. *Inorg. Chem.,* 26:2365.

EL-AWADAY, A.A. & HUGUS, Z.Z., 1971. *Inorg. Chem.,* 10:1415.

ELLIS, D., SCOTT, K.L. and WHARTON, R.K., 1972. *Inorg. Chem.,* 11:2565.

FALLAB, S., 1967. *Angew. Chem. (Int. Ed.),* 6:496.

GARNETT, P.J. & WATTS, D.W., 1947. *Inorg. Chim. Acta,* 8:307.

GLADKIKH, O.P., POLYNOVA, T.N., PORAI-KOSHITS, M.A. and POZNYAK, A.L., 1991. *Koord. Khim.,* 17:945.

GLADKIKH, O.P., POLYNOVA, T.N., PORAI-KOSHITS, M.A. and POZNYAK, A.L., 1992. *Koord. Khim.,* 18:908.

GLADKIKH, O.P., POLYNOVA, T.N., PORAI-KOSHITS, M.A. and POZNYAK, A.L., 1992. *Koord. Khim.,* 18:1231.

GLADKIKH, O.P., POLYNOVA, T.N., PORAI-KOSHITS, M.A. and POZNYAK, A.L., 1992. *Koord. Khim.,* 18:1125.

GLADKIKH, O.P., POLYNOVA, T.N., PORAI-KOSHITS, M.A. and POZNYAK, A.L., 1992. *Koord. Khim.,* 18:1131.

GLADKIKH, O.P., POLYNOVA, T.N., PORAI-KOSHITS, M.A. and POZNYAK, A.L., 1992. *Koord. Khim.,* 18:1156.

GLADKIKH, O.P., POZNYAK, A.L., POLYNOVA, T.N. and PORAI-KOSHITS, M.A., 1997. *Russian J. Inorg. Chem.,* 42:1346.

GONZALES-PEREZ, J.M. and NICLOS-GUTIEREZ, J., 1981. *J. Ars Pharm.,* 22:429.

GONZALES-PEREZ, J.M., NICLOS-GUTIEREZ, J. and DUNGN, H., 1991. *Inorg. Chim. Acta,* 184:243.

GORDON, P.F. & GREGORY, P., 1983. *Organic Chemistry in colour.* Berlin: Springer-Verlag.

GRANT, D.M. & HAMM, R.E., 1958. *J. Am. Chem. Soc.,* 80:4166.

HALLORAN, L.J., CAPUTO, R.E., WILLET, R.D. and LEGG, J.I., 1975. *Inorg. Chem.,* 14:1762.

HAY, R.W., 1984. *Coord. Chem. Rev.,* 57:1.

HAULIN, Z. & XU, Z., 1990. *Polyhedron,* 9:137.

HAYLOCK, S.J., BUCKLEY, P.D. & BLACKWELL, L.F., 1983. *J. Inorg. Biochem.,* 19:105.

HELIS, H.M., DE MEESTER, P. and HODGSON, D.J., 1977. *J. Am. Chem. Soc.,* 99:3309.

HOFFMAN, A.B. & TAUBE, H., 1968. *Inorg. Chem.,* 7:903.

HUHEEY, J.E., KEITER, E.A., KEITER, R.L., *Inorganic Chemistry: Principles, Structure and Reactivity,* Second Edition, p278.

ILYUKHIN, A.B., SHKOL'NIKOVA, L.M. and POZNYAK, A.L., 1990. *Koord. Khim.,* 16:1597.

JAHN & TELLER, 1937. *Proc. Roy. Soc.,* A161:220.

JITSUKAWA ,K., MORIOKA, T., MASUDA, H., OGOSHI, H. and EINAGA, H., 1994. *Inorg. Chim. Acta,* 216:249.

KANAMORI, K., KUMANDA, J., YAMAMOTO, M., OKAYASU, T. and OKAMOTO, K., 1995. *Bull. Chem. Soc. Jpn.,* 68:3445.

KOINE, N., BIANCHINI, J. and LEGG, I., 1983. *Inorg. Chem.,* 25:2835.

KOINE, N., SAKOTA, N., HIDAKA, J. and SHIMURA, Y., 1969. *Bull. Chem. Soc. Jpn.,* 42:1583.

KUSHI, Y., IDENDO, T., YASUI, T. and YONEDA, H., 1983. *Bull. Chem. Soc. Jpn.,* 56:2845.

LEE HIN-FAT & HIGGINSON, W.C.E., 1971. *J. Chem. Soc.,* A:2589.

LEIPOLDT, J.G. & MEYER, H., 1987. *Polyhedron,* 6:1631.

LINHARDT, V.M. & SIEBERT, H., 1969. *Z. Anorg. Allg. Chem.,* 364:24.

MELOON, D.R. & HARRIS, G.M., 1977. *Inorg. Chem.,* 16:434.

MERTZ, W. 1975. *Nutr. Revs.,* 33:129.

MOORE, P., 1984. (In Twigg, M.V., ed. Mechanisms of Inorganic and Organometallic Reactions, Volume 2. New York: Plenum Press).

MIZUTA, T., YOSHIDA, T. and MIYOSHI, K., 1989. *Inorg. Chim. Acta,* 165:65.

MORI, M., SHIBATA, M., KYUNO, E. and OKUBO, Y., 1958. *Studies on the Synthesis of Metal Complexes,* 31:940.

NAGAO, R., FUMIYUKI, M. and SAITO, Y., 1972. *Acta Cryst.,* B28:1852.

NAKAMOTO, K., 1963. Infrared Spectra of Inorganic and Coordination Compounds. New York: John Wiley & Sons.

OBODOVSKAYA, A.E., SCKOL'NIKOVA, L.M. and POZNYAK, A.L., 1992.

Russian J. Inorg. Chem., 37:295.

OGINO, H., WATANBE, T. and TANAKA, N., 1975. *Inorg. Chem.,* 14:2093.

OKAMOTO, K., HIDAKA, J., FUKAGAWA, M. and KANAMORI, K., 1992. *Acta Cryst.,* C48:1025.

PLANISEK, F & NEWKIRK, J.B., 1979. Cobalt and cobalt alloys. (In GRAYSON, M., ed. Kirk-Othmer Encyclopedia of Chemical Technology. New York: John Wiley & Sons. P. 481 - 494).

POLYKOVA, I.N., SERGIENKO, V.S., POZNYAK, A.L. and ELLERT, O.G., 1997. *Russian J. Inorg. Chem.,* 42:1509.

PORAI-KOSHITS, M.A. & POLYNOVA, T.N., 1984. *Koord. Khim.,* 10:725.

PURCELL, F.P. & KOTZ, J.C., 1985. *Inorganic Chemistry,* Japan: W.B. Saunders Company. p. 710.

SADLER, G.G. & DASGUPTA, T.P., 1987. *Inorg. Chim. Acta,* 130:185.

SADLER, G.G. & DASGUPTA, T.P., 1987. *Inorg. Chem.,* 26:3254.

SANTOS, T.M., DE JESUS, J.P. and O'BRIEN, P., 1992. *Polyhedron,* 11:1687.

SCIENTIST FOR WINDOWS, 1990. Least Square Parameter Estimation, Version 4.00, Micromath.

SHELDRICK, G.M., (1996), SADABS. Version 2.03. University of Gottingen, Germany.

SKRZYPCZAK-JANKUN, E., and SMITH, D.A., 1994. *Acta Cryst.,* Section C:1097.

SMITH, B.B. & SAWYER, T., 1968. *Inorg. Chem.,* 7:923.

SMITH, G.S. & HOARD, J.L., 1959. *J. Am. Chem. Soc.,* 81:556.

SUDMEIER, J.L. & OCCUPATI, 1968. *Inorg. Chem.,* 7:2524.

SULFAB, Y., TAYLOR, R.S. and SYKES, A.G., 1976. *Inorg. Chem.,* 15:2388.

SWAMINATHAN, K., SINHA, U.C., CHATTERJEE, C., PHULAMBRIKAR, A., PADMANABHAN, V.M. and BOHRA, R., 1989. *Acta Cryst.,* 45:566.

SYKES, A.G. & WEIL, J.A., 1970. (In. Edwards, J.O. ed. Inorganic Reaction Mechanisms, Volume 13. New York: John Wiley and Sons).

TERRIL, J.B. & REILLY, C.N., 1966. *Inorg. Chem.,* 5:1988.

THACKER, M.A. & HIGGINSON, W.C.E., 1975. *J. Chem. Soc. Dalton Trans.,* p. 704.

TOEPFER, E.W., MERTZ, W., POLANSKY, M.M., ROGINSKY, E.E., and WOLF, W.R., 1977. *J. Agric. Food Chem.,* 25:162.

TOFTLUND, H. & SPRINGBORG, J., 1976. *J. Chem. Soc. Chem. Comm.,* p. 1017.

TSUCHIYA, R., UEHARA, A. and KYUNO, E., 1969. *Bull. Chem. Soc. Jpn.,* 42:1886.

UEHARA, A., KYUNO, E. and TSUCHIYA, R., 1968. *Bull. Chem. Soc. Jpn.,* 41:2385.

VANCE, T.B., HOLT, E.M., PIERPONT, C.G. and HOLT, S.L., 1980. *Acta Cryst.,* B36:150.

VAN ELDIK, R., PALMER, D.A. and KELM, H., 1979. *Inorg. Chem.,* 18:1520.

VISSER, H.G., LEIPLODT, J.G., PURCELL, W. and MOSTERT, D., 1994. *Polyhedron,* 13:1051.

VISSER, H.G., PURCELL, W., BASSON, S.S. and CLAASEN, Q., 1997. *Polyhedron,* 16:2851.

VISSER, H.G., PURCELL, W. and BASSON, S.S., 2001. *Trans. Metal Chem.,* 26:175.

VISSER, H.G., PURCELL, W. and BASSON, S.S., 2001. *Polyhedron,* 20:185.

VISSER, H.G., PURCELL, W. and BASSON, S.S., 2002. *Trans. Metal Chem.,* 27:461.

VISSER, H.G., PURCELL, W. and BASSON, S.S., 2003. *Trans. Metal Chem.,* 28:235.

VOGEL, A.I., 1989. Vogel's Textbook of Quantitative Chemical Analysis, Fifth Edition. Essex: Longman. P.317.

WEAKLIEM, H.A. & HOARD, J.L., 1959. *J. Am. Chem. Soc.,* 81:549.

WEYH, J.A., MAYNARD, R.B. and BAKER, T.J., 1976. *Inorg. Chem.,* 15:2298.

WEYH, J.A., NEWLUN, A.K., BAKER, T.J. and SHIOYAMA, T.K., 1973. *Inorg. Chem.,* 12:2374.

WITHLOW, S.H., 1972. *Acta Cryst.,* B28:1914.

WOLCOTT, D. & HUNT, J.B., 1968. *Inorg. Chem.,* 7:755.

Abstract

The synthesis and reactions of Co(III) complexes with tripod-type ligands such as N-(2-carboxyethyl)iminodiacetic acid (apda) have a widespread interest, mainly because of the fact that these complexes can be used as biological model complexes and because apda labilises usually inert metal centres. The first Co(III)-apda complex was prepared by Tsuchiya and co-workers (1969:1886), this complex was later conclusively characterised by Gladkikh and co-workers (1997:1346) as $[Co(apda)(H_2O)_2]$ by means of X-ray crystallography. Since then very few metal complexes containing apda as ligand are cited and little or no kinetic studies have been published on these types of complexes.

The question regarding the identity of the different Co(III)-apda species in solution at different pH levels has been accounted for in this study (refer to Scheme 1).

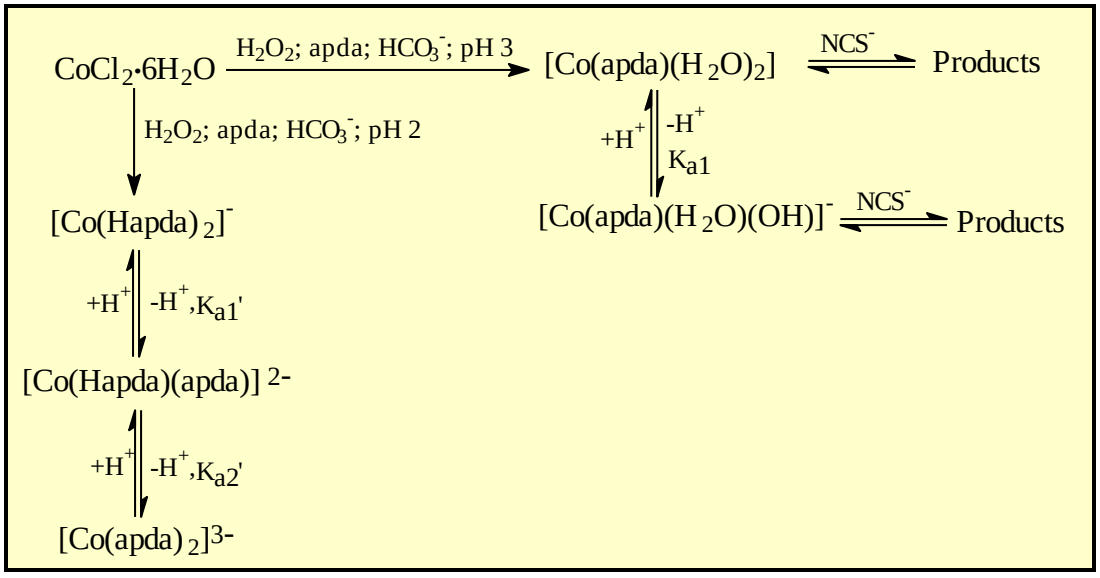

Scheme 1 Complexes and reactions of cobalt(III)-apda.

N-(2-carboxyethyl)iminodiacetic acid (apda) was synthesised according to a method obtained from Niclós Gutiérrez (University of Granada). The synthesis of apda was confirmed by means of IR and ^1H NMR spectrometry.

Abstract

$[Co(apda)(H_2O)_2]$ was prepared similar to the method described by Tsuchiya and co-workers (1969:1886). The synthesis of $[Co(apda)(H_2O)_2]$ was confirmed by means of IR, UV/VIS and ^1H NMR spectrometry. The IR stretching frequencies obtained for $[Co(apda)(H_2O)_2]$ are indicative of COO^- groups coordinated to a metal centre such as Co(III). The ^1H NMR spectrum also indicated that apda acts as a tetradentate ligand with the longer propionato ring in the G (out-of-plane) position.

An acid base equilibrium is observed when the pH of a $[Co(apda)(H_2O)_2]$ solution is increased. It was concluded that the newly formed species is $[Co(apda)(H_2O)(OH)]^-$ which is unstable at pH > 7, possibly due to dimer formation. The pK_a was spectrophotometrically determined as 6.23(2).

The substitution reactions between $[Co(apda)(H_2O)_2]$/$[Co(apda)(H_2O)(OH)]^-$ and NCS^- ions have been investigated. At pH = 2.00 NCS^- ions substitute the aqua ligands in a stepwise fashion. The substitution of the first aqua ligand of $[Co(apda)(H_2O)_2]$ (k_1 = 14(1) x 10^{-3} M^{-1} s^{-1} at 25.0 °C) at low pH is about 125 times faster than the rate of substitution of the second aqua ligand (k_3 = 1.2(6) x 10^{-4} M^{-1} s^{-1} at 25.0 °C). The $[Co(apda)(H_2O)(OH)]^-$ complex reacts about 70 times faster at 25.0 °C with NCS^- than the $[Co(apda)(H_2O)_2]$ complex with NCS^- (k_2 = 0.986(8) M^{-1} s^{-1} *vs.* 14(1) x 10^{-3} M^{-1} s^{-1} for k_1 at 25.0 °C). This clearly indicates that the hydroxo ligand labilises the *cis*-aqua bond so that an increase in rate is observed. Hydroxide is not substituted by NCS^- ions at higher pH so that only one reaction is observed spectrophotometrically.

The synthesis and characterisation of a Co(III)-apda complex with apda acting as a tridentate ligand were also undertaken. This complex was characterised by means of IR spectroscopy and X-ray crystallography as $[Co(H_2O)_6][Co(Hapda)_2]_2H_2O$. This complex crystallises in the triclinic space group P $\bar{1}$ (R = 0.0228). The two anionic units, $[Co(III)(Hapda)_2]^-$, differ in terms of bond lengths and angles as well as strain experienced by the glycinato rings of the apda ligand. This is the first Co(III)-apda complex with two tridentate apda ligands bonded to the same cobalt centre. This complex was also synthesised in the absence of competing ligands.

Abstract

The strain experienced by the glycinato rings of the coordinated apda decreases in the order G > R for all the complexes studied. The R rings in all the complexes are almost perfectly planar in all cases, whilst the G rings are non-planar.

The synthesis and characterisation of $Na[Co(Hapda)_2]xH_2O$ were also undertaken. This complex was characterised by means of IR, UV/VIS and ^1H NMR spectrometry.

Two acid base equilibria are observed when the pH of a $Na[Co(Hapda)_2]xH_2O$ solution is decreased. It was concluded that the species present at pH 5.5 is $[Co(apda)_2]^{3-}$ and that the $[Co(Hapda)(apda)]^{2-}$ and $[Co(Hapda)_2]^-$ complexes form upon the addition of H^+ to this solution. The two acid dissociation constants, pK_{a1}' and pK_{a2}', were spectrophotometrically determined as 2.6(1) and 2.8(1), respectively.

The various Co(III)-apda complexes that were isolated and characterised can successfully be used as biological model complexes in future studies. These complexes could for example be used to simulate the bonding of metal ion to functional groups of wool fibre or might have uses as models in pharmacology.

Keywords: cobalt(III), N-(2-carboxyethyl)iminodiacetic acid, ionisation constants, substitution reactions, X-ray crystallography.

Opsomming

Die sintese en reaksies van Co(III) komplekse met driepoot-tipe ligande soos N-(2-karboksieetiel)iminodiasynsuur (apda) lok wye belangstelling omdat hierdie komplekse as biologiese modelkomplekse gebruik kan word en omdat die apda ligand metaalsentra wat gewoonlik inert is, labiliseer. Die eerste Co(III)-apda kompleks is berei deur Tsuchiya en medewerkers (1969:1886), hierdie kompleks is later gekarakteriseer deur Gladkikh en medewerkers (1997:1346) as $[Co(apda)(H_2O)_2]$ deur middel van X-straal kristalstruktuurbepaling. Sedertdien is weinig ander komplekse met apda as ligand gekarakteriseer en is byna geen kinetiese studies in verband met hierdie tipe komplekse gepubliseer nie.

Die vraag rondom die indentiteit van die verskillende Co(III)-apda spesies in oplossing (sien Skema 1) by verskillende pH's is grootliks in hierdie studie beantwoord.

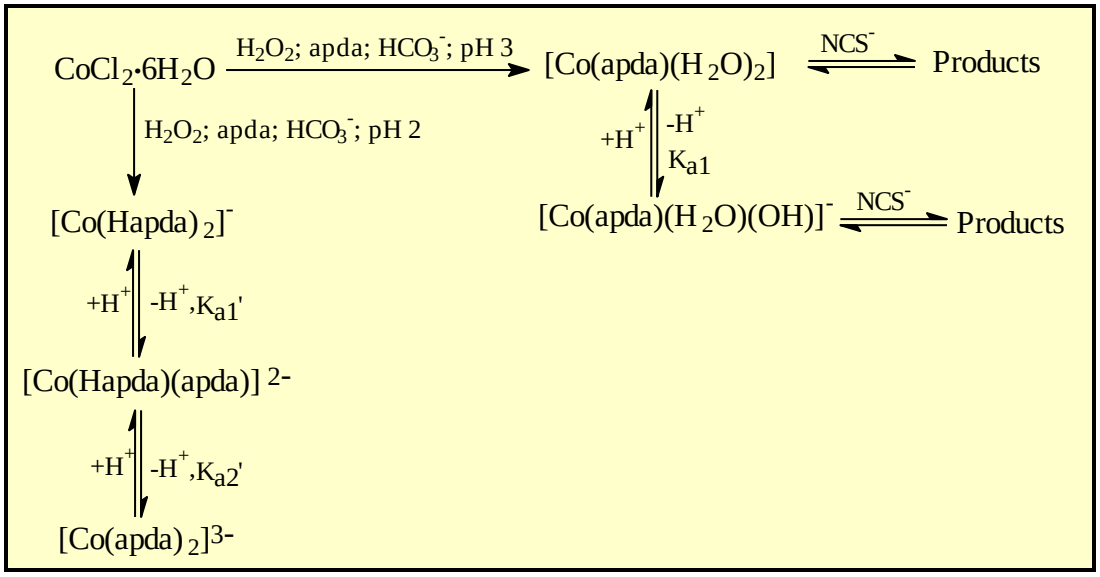

Skema 1 Komplekse en reaksies van cobalt(III)-apda.

N-(2-karboksieetiel)iminodiasynsuur (apda) is gesintetiseer volgens 'n metode wat van Niclós Gutiérrez (Universiteit van Granada) verkry is. Die sintese van apda is bevestig met behulp van IR en ^{1}H KMR spektrometrie.

Opsomming

$[Co(apda)(H_2O)_2]$ is gesintetiseer volgens die metode wat beskryf is deur Tsuchiya en medewerkers (1969:1886). Die sintese van $[Co(apda)(H_2O)_2]$ is bevestig met behulp van IR, UV/VIS en ^1H KMR spektrometrie. Die IR strekkingsfrekwensies van die $[Co(apda)(H_2O)_2]$ kompleks dui op COO^- groepe wat gekoördineerd is aan metale soos Co(III). Die ^1H KMR spektrum dui ook aan dat apda as ‘n tetradentate ligand in hierdie kompleks optree met die langer proprionato ring wat die G (uit-die-vlak) posisie beklee.

‘n Suur-basis ewewig is waargeneem toe die pH van ‘n $[Co(apda)(H_2O)_2]$ oplossing verhoog is. Daar is tot die gevolgtrekking gekom dat die nuwe spesie wat vorm die $[Co(apda)(H_2O)(OH)]^-$ spesie is wat onstabiel is by pH > 7, moontlik as gevolg van dimeer vorming. Die pK_a is spektrofotometries as 6.23(2) bepaal.

Die substitusiereaksies tussen $[Co(apda)(H_2O)_2]$/$[Co(apda)(H_2O)(OH)]^-$ en NCS^- ione is ook ondersoek. NCS^- substitueer die akwaligande stapsgewys by pH = 2.00. Die substitusie van die eerste akwa ligand van $[Co(apda)(H_2O)_2]$ (k_1 = 14(1) x 10^{-3} M^{-1} s^{-1} by 25.0 °C) by lae pH is ongeveer 125 keer vinniger as die tempo van die tweede akwa-substitusie (k_3 = 1.2(6) x 10^{-4} M^{-1} s^{-1} by 25.0 °C). Die $[Co(apda)(H_2O)(OH)]^-$ kompleks reageer ongeveer 70 keer vinniger by 25.0 °C met NCS^- as die $[Co(apda)(H_2O)_2]$ kompleks met NCS^- (k_2 = 0.986(8) M^{-1} s^{-1} *vs.* 14(1) x 10^{-3} M^{-1} s^{-1} vir k_1 by 25.0 °C). Hierdie resultate toon duidelik dat die hidroksoligand die *cis*-akwa binding sodanig labiliseer dat ‘n toename in tempo waargeneem word. Verder toon dit aan dat die hidroksie ligande nie deur NCS^- ione by hoër pH gesubstitueer word nie aangesien slegs een reaksie by hierdie pH waargeneem word.

Die sintese en karakterisering van ‘n Co(III)-apda kompleks, waar apda as tridentate ligand optree, is ook onderneem. Hierdie kompleks is gekarakteriseer met behulp van IR spektroskopie en X-straal kristalstruktuurbepaling as $[Co(H_2O)_6][Co(Hapda)_2]_2H_2O$. Hierdie kompleks kristalliseer in die trikliniese ruimtegroep P ī (R = 0.0228). Die twee anioniese eenhede, $[Co(III)(Hapda)_2]^-$, verskil in terme van bindingsafstande en hoeke sowel as die verwringing wat deur die glisinato ringe van die apda ligand ondervind word. Hierdie is die eerste Co(III)-apda kompleks met twee tridentaat-gekoördineerde

adpa ligande wat aan dieselfde metal sentra bind. Hierdie kompleks is ook in die afwesigheid van kompeterende ligande gesintetiseer.

Die verwringing van die glisinato ringe van gekoordineerde apda neem af in die volgorde G > R vir al die komplekse wat ondersoek is. Die R ringe is amper ten volle planêr vir al die gevalle, terwyl die G ringe almal nie-planêr is.

Die sintese en karakterisering van $Na[Co(Hapda)_2]xH_2O$ is ook onderneem. Hierdie kompleks is gekarakteriseer met behulp van IR, UV/VIS en ^1H NMR spektrometrie.

Twee suur-basis ewewigte is waargeneem tydens die verlaging van die pH van ‘n $Na[Co(Hapda)_2]xH_2O$ oplossing. Die gevolgtrekking is dat die spesie wat teenwoordig is by ‘n pH van 5.5 die $[Co(apda)_2]^{3-}$ kompleks is en dat die $[Co(Hapda)(apda)]^{2-}$ en $[Co(Hapda)_2]^-$ komplekse vorm met die addisie van H^+ by hierdie oplossing. Die twee suur-basis ewewig konstantes, pK_{a1}’ and pK_{a2}’, is spektrofotometries as 2.6(1) en 2.8(1) bepaal.

Die verskeie Co(III)-apda komplekse wat geïsoleer en gekarakteriseer is in hierdie studie kan suksesvol as biologiese modelkomplekse gebruik word in toekomstige studies. Hierdie komplekse kan byvoorbeeld gebruik word om die binding van ‘n metaal aan ‘n funksionele groep van wol na te boots of kan gebruik word as modelkomplekse in farmakologie.

Sleutelwoorde: cobalt(III), N-(2-karboksieetiel)iminodiasynsuur, ionisasie ewewig konstantes, substitusiereaksies, X-straal kristalstruktuurbepaling.